SNC·LAVALIN

nalcor energy

Lower Churchill Project

ENGINEERING REPORT
North Spur Stabilization Works
Progressive Failure Study

SLI Document No. 505573-3281-4GER-0001-01

Nalcor Reference No. MFA-SN-CD-2800-GT-RP-0001 Rev. B2

Date: 21-Dec-2015

Prepared by: Régis Bouchard for
Denise Leahy
Geotechnical Engineer

Verified by: Régis Bouchard
Regis Bouchard
Lead Engineer-Geotechnical

Approved by: Greg Snyder
Greg Snyder
Engineering Manager

REVISION INDEX

Revision					
N°	By	Verif.	Appr.	Date	Remarks
B2	DL	RB	GS	21-Dec-2015	Issued for use.
B1	DL	RB	GS	05-Oct-2015	Issued for use.

NOTICE TO READER

This document contains the expression of the professional opinion of SNC-Lavalin Inc. ("SLI") as to the matters set out herein, using its professional judgment and reasonable care. It is to be read in the context of the agreement dated 09-January-2015 (the "Agreement") between SLI and Nalcor Energy (the "Client") and the methodology, procedures and techniques used, SLI's assumptions, and the circumstances and constraints under which its mandate was performed. This document is written solely for the purpose stated in the Agreement, and for the sole and exclusive benefit of the Client, whose remedies are limited to those set out in the Agreement. This document is meant to be read as a whole, and sections or parts thereof should thus not be read or relied upon out of context.

SLI has, in preparing estimates, as the case may be, followed accepted methodology and procedures, and exercised due care consistent with the intended level of accuracy, using its professional judgment and reasonable care, and is thus of the opinion that there is a high probability that actual values will be consistent with the estimate(s). Unless expressly stated otherwise, assumptions, data and information supplied by, or gathered from other sources (including the Client, other consultants, testing laboratories and equipment suppliers, etc.) upon which SLI's opinion as set out herein are based have not been verified by SLI; SLI makes no representation as to its accuracy and disclaims all liability with respect thereto.

To the extent permitted by law, SLI disclaims any liability to the Client and to third parties in respect of the publication, reference, quoting, or distribution of this report or any of its contents to and reliance thereon by any third party.

TABLE OF CONTENTS

Page No.

LIST OF FIGURES

LIST OF TABLES

LIST OF APPENDICES

1 CONTEXT OF THE STUDY

Forming part of the Lower Churchill Project (LCP) in Newfoundland and Labrador, Canada, the Muskrat Falls Hydroelectric Development is located on the Churchill River, about 291 km downstream of the Churchill Falls Hydroelectric Development which was developed in the early 1970's. The installed capacity of the Muskrat Falls facility will be 824 MW (4 units of 206 MW each).

The North Spur is a deposit of marine and estuarine sediments which naturally provides a partial closure of the Churchill River valley at the Muskrat Falls site. This natural closure is one of the economically attractive features of this site and needs to be maintained for the life of the project.

The North Spur is about one kilometre long between the rock knoll in the south and the Kettle Lakes in the north which represent natural boundaries to the North Spur, in terms of both seepage and stability (Figure 1-1).

The early (1965) studies for the Muskrat Falls site recognized the importance of the North Spur as part of the reservoir retention works. A major slide on the downstream face of the Spur, in November 1978 (Figure 1-1), revealed the fragility of this natural deposit and its susceptibility to toe erosion and ice accumulation in the bay downstream. Maintaining the integrity of the Spur is fundamental to the viability of the project and this fact has been understood from the outset.

The raising of the headpond and the change in the downstream flow regime for the Muskrat Falls hydro-electric project could adversely affect the stability and integrity of the North Spur. Stabilization works to address this have been considered from 1965 to date and the design has been modified and adapted over the decades to arrive at the current 2015 design.

Figure 1-1 : Aerial photo of the North Spur (1988)

1.1 PROGRESSIVE FAILURE STUDY

In the process of assessing the stability of the North Spur before and after stabilization works, LCP performed a specific 2D finite element model study to complete stability analyses done with the Limit Equilibrium Method (LEM).

The lower Churchill River valley shows numerous landslides scarps on each river bank, upstream and downstream from Muskrat Falls site. Most of these landslides show characteristics of flowslide, which is the more frequent landslide type in Eastern Canada.

There is no approved and accepted method to estimate in advance a safety factor before a progressive failure landslide occurs. The cases presented in the literature are always related with a landslide that has already occurred and so all cases presented are examined through a back calculation analysis. After the fact, the safety factor (SF) is known to be 1.0 or slightly below (0,999) and back calculation analysis methods use this fact and assume an unstable conditions immediately before the landslide.

In the predictive approach, for most of slope stability analyses (rotational and regressive) stabilization works try to reduce the occurrence of the first failure. LEM calculations developed early in the past century are used to calculate the SF. This method has its limitations (Krahn, J. 2003), but it has been used with success to predict first failure on a retrogressive landslide. Although the method uses some approximate hypotheses, years of use has shown that method works well when adequately calibrated.

More recently, some researchers tried to better understand the triggering mechanism for "Spreads", a type of progressive failure landslides (Locat et al., 2011). In that landslide mechanism, a failure develops on a pre-sheared plane after a trigger occurs (most often, toe erosion), and the rupture progresses on that plane. The progression is usually from downhill to uphill in eastern Canada clay (Demers et al, 2013). Bernander (2000) shows some examples in Sweden and Norway, where the failure progressed from uphill to downhill, most of the time because of a human trigger. For such cases, the LEM cannot be used: the trigger is uphill and the failure progresses downward, and so the LEM is not applicable. For all cases of downward progressive failure, the landslide topography before movement showed a gentle inclination toward the landslide movement.

The stability of the North Spur is a concern for the Muskrat Falls Project team. Since 1965, stabilization works have been planned to maintain the integrity of this natural dam. Knowledge in geotechnical engineering science has improved over the years and these improvements increase our understanding of soils stratigraphy and properties. Investigation methods and calculation tools are also more powerful and accordingly, the design of stabilization works has been revisited and updated over this time period.

To address the potential for occurrence of progressive failure landslides (both downward and upward), the LCP team has analyzed these potential failure modes. A stress distribution analysis approach was selected and will be presented in the following sections.

1.2 METHODOLOGY SELECTION

A methodology for the numerical analysis of progressive failures has been developed by Locat et al (2007, 2011, 2014) and tested on different landslide events. For analysing the pre-failure conditions, they compare the initial shear stress along a potential horizontal failure surface with the shear strength of the clay. The present study uses this approach at selected locations around the North Spur.

A worst case scenario is assumed in which the mobilized strength under the steeper slopes of the North Spur is conservatively assumed to be the maximum strength available to insure stability of the slopes against progressive failure. The results of the calculations made for the projected conditions after stabilization for the various locations around the Spur are compared to this maximum strength to evaluate the safety margin available against a potential progressive failure.

1.3 SCOPE OF THE PROGRESSIVE FAILURE STUDY

A progressive failure study, complementary to the LEM analysis of failures, was conducted considering the following steps:

1. Base the analyses on soil properties and stratigraphy.
2. Selection and analysis of a section representing the most critical conditions on the North Spur (Section B-B, Fig B-1, Appendices B, north section). Using a 2D finite element model, and evaluate the stress distribution at various levels and compare with soil strength parameters. This condition will be a reference to evaluate the strength mobilization after the stabilization works.
3. Selection and analysis of other sections, representing the actual (Before stabilization, BS) and stabilized conditions (after stabilization, AS) for the southern part of the Spur (Section A-A, D-D, C-C, Fig B-1 Appendix B). Undertake a 2D modeling of the stress distribution on these sections before and after stabilization.
4. Comparison of the estimated mobilized strength before and after stabilization with the present conditions on the reference critical north section.
5. Analysis of the effect of the reservoir impoundment on the southern sections.

2 GEOLOGY

The Muskrat Falls site is underlain by Precambrian granitic and amphibolites gneiss with occasional pegmatite stringers. Outcrops occur along the right bank of the river in addition to the rock knoll.

The present river channel has eroded a bedrock based channel, south around the rock knoll and about one km south of a buried preglacial valley which underlies the northern part of the spur. In the spur about 140 m of glacial sands, gravels and boulders infill the lower part of the preglacial buried valley. Following deglaciation, sea level rose and submerged the Churchill River valley up to about elevation 80 m; abundant sediments carried into this estuary resulted in the deposition of thick marine clay and estuarine silty sand deposits at the Muskrat Falls site. Isostatic rebound following deglaciation caused gradual recession of the sea and resulted in the deposition of fine sand deposits over the underlying marine clay sediments (SLI-AGRA, 1998).

2.1 SEDIMENTATION PROCESS IN THE LOWER CHURCHILL VALLEY

Most of the current knowledge of the Spur stratigraphy and the soil characteristics are derived from the outcomes of the investigation campaigns within the last 50 years which were carried out mainly in 1979 and 2013. The boreholes and in-situ tests performed are shown on Figure A-1 of Appendix A. The hydro-geological information has been obtained from the pumping tests, piezometer readings, in-situ permeability tests and CPT dissipation tests.

The geological features including the stratigraphy and material properties of different layers of overburden, the ground water regime within the Spur, and the effects of existing dewatering system are part of the evolution of the site conditions for the North Spur.

2.2 PLEISTOCENE GEOLOGY

The recent history for the North Spur sedimentation process starts after deglaciation. Observed soil sequence and stratigraphy process are typical of East Canadian valley. The Pleistocene stratigraphic process is very similar to the Saguenay valley in Québec province (Bouchard et al, 1983). The stratigraphic sequence is as follows.

First, over the rock, glacier placed a till deposit of variable thickness. This till deposit is not always present in the stratigraphic sequence.

With the progressive ice melt, fluvio-glacial deposit and ice water contact deposit were placed. In the Churchill River valley, these fluvio-glacial deposits are encountered in the deep buried valley and sometimes on the margin of the valley. Sand, gravel and cobbles particles are common in that generally pervious material. In the deep Churchill River buried valley (under the Spur of land), this deposit can have a thickness up to 160 m. The ice in the valley continued to melt but on the highland, sediment transportation progress and river energy brought material in the valley (depression) or along the contact between the valley wall and the glacial ice (Kame Terrace formation).

From a certain point in geological time, sea water filled the lowered valley and fine sediments (clay and silt deposit) covered the underlying sand and gravel layer (under the North Spur, this strata is called Lower Clay deposit). The deep water fine material, (Lower Clay) reached a thickness of about 50 m in the vicinity of the Spur.

Isostatic rebound of the land led to a decrease of the water thickness. Therefore, the water energy for the main and lateral water courses (Churchill River, Lower Brook, Upper Brook, etc.) increased and the deposition changed from clayey silt (during the period of less energy) to sandy silt to silty sand (during the period of more energy). This stratified deposit is called Stratified Drift.

The last strata in the Churchill River is a deltaic sand (beach sand). It is a shallow water deposit. The top of the sand deposit was remolded by wind forming sand dunes (very evident in the northern part of the Spur).

After and during the final deposition steps with the rebound progress, water courses started to erode the deposits, digging the actual Churchill Valley. At Muskrat Falls, the level of the river is vertically controlled by the upper falls but the lateral erosion process continues and causes landslides on both side of the river. This phenomenon is also acting on the downstream side of Muskrat Falls.

2.3 STRATIGRAPHY

2.3.1 STRATIGRAPHIC CROSS SECTIONS

The interpreted stratigraphy of the overburden layers, from ground surface to the bedrock level, was based on available data from geotechnical investigation campaigns. The stratigraphy model has evolved with time; continuous logs obtained from CPTs and sonic drillings during 2013 investigations along with conventional boreholes drilled during various investigations provided the data to study the stratified nature of the soil.

The simplified 2014 interpretation is illustrated on Figure 2-1; the major soil layers encountered are summarized as:

- Upper sand, generally from elevation 60 m to elevation 45 m to 50 m;
- Stratified drift, including two major deposits of silty sand/sandy silt and silty clay material, generally from elevation 45 m to 50 m to elevation 5 m to 15 m.
- Lower marine clay, generally from elevation 5 m to 15 m to elevation -70 m
- Lower aquifer (pervious sand and gravel layer), generally from elevation -70 m to bedrock.

The nature and the physical and mechanical properties of each soil unit are summarized in the following sections. Stratigraphy is heterogeneous on the North Spur and can change locally.

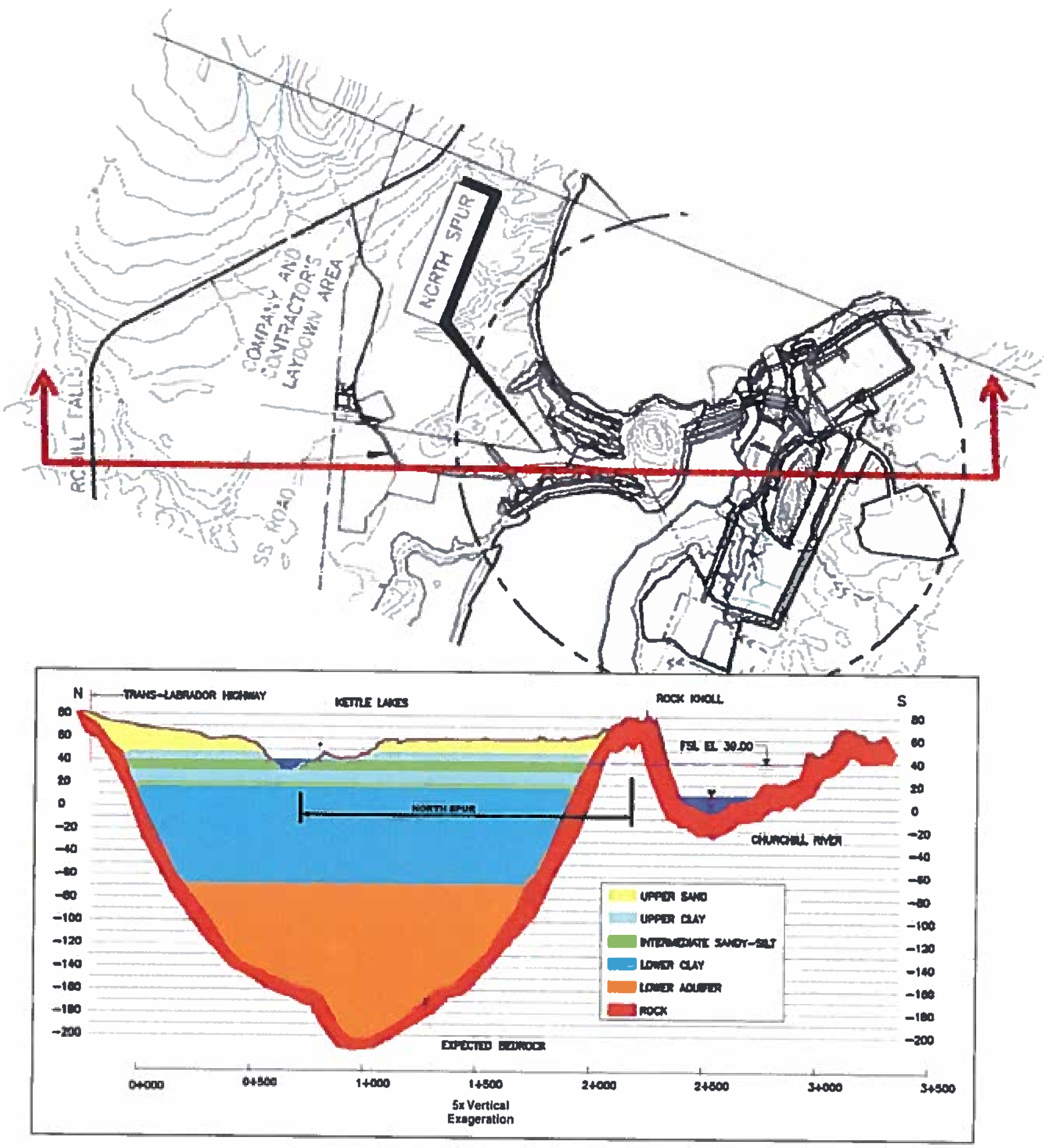

Figure 2-1 : North Spur Schematic Stratigraphy for North-South Cross-Section

2.3.2 Upper Sand Layer

The upper sand layer covers the surface on the North Spur. This layer mainly consists of compact to very dense, grey fine to medium sand with low fines content.

This layer is mostly dry and well drained except for a perched water table observed above the underlying clay or silty clay layer. No permeability tests were performed in this layer. Using grain size distribution curves and empirical relationships, a value of 1×10^{-4} m/s was estimated as the hydraulic conductivity for this layer.

2.3.3 Stratified Drift

The stratified drift is a heterogeneous mix of clays, silts and sands with sub-horizontal layering from the marine and estuarine deposition. This unit consists of alternating layers of silty clay of low to medium plasticity which is referred to as "upper silty clay", and silty sand or sandy silt which is called "silty sand/sandy silt".

2.3.3.1 Upper Silty Clay Layer

A low to medium plastic, sensitive, stiff to very stiff silty clay to clayey silt material has been observed within the stratified drift. A summary of material properties for this upper clay layer is presented in Table 2-1. The Liquidity Index values are above unity. The in-situ undrained shear strength obtained by Vane shear tests ranged from 35 to 135 kPa which indicates clay material of firm to very stiff consistency in an intact condition. The average shear strength parameters of ϕ'=31° and c'=6 kPa were interpreted from the triaxial and Direct Shear Test (DST) test results.

Table 2-1 : Summary of Material Properties for Upper Silty Clay Layer

Property	General Range	Average	Number of tests
Percent finer than 2 microns	35 – 45	–	19
Water content, w %	17 – 43	31	199
Liquid limit, LL %	17 – 43	30	168
Plastic limit, PL %	13 – 32	19	168
Plasticity Index, PI %	2 – 22	11	168
Liquidity Index, LI	0.6 – 2.8	1.3	168
Intact Undrained shear strength, S_u kPa	35 – 135	–	–
Remoulded Undrained shear strength, S_u kPa	60 – 2	–	–
Sensitivity, in-situ, S_t	1 – 36	10	43
Large strain friction angle, ϕ'_{cv} º	30 – 32	–	–
Effective cohesion, c', kPa	0 – 10	–	–
Unit weight, γ kN/m^3	18.4 – 19.7	–	11
Initial void ratio, e_0	0.93 – 1.06	–	–
Compression index, c_c	0.32 – 0.5	–	–
Recompression index, c_r	0.03 – 0.06	–	–
Hydraulic Conductivity, k, m/s	$10^{-7} – 10^{-9}$	–	–
Salt content, g/l	0.8 – 1.5	–	–

2.3.3.2 *Intermediate Silty Sand/Sandy Silt Layers*

The results of sieve analyses on samples recovered from the intermediate silty sand/sandy silt layers indicated a generally fine silty sand material with an average of 27% fines content (passing sieve # 200). The standard penetration tests carried out in this layer resulted in N values generally higher than 50 which indicate the layers are in a dense to very dense compacted condition. Three consolidated undrained triaxial tests were conducted on samples from Silty Sand/Sandy Silt layers, during the 1979 investigations, which resulted in an average effective friction angle of 35° to 37° and effective cohesion of 0 kPa under large strain conditions. Two direct shear tests were completed on silty sand and sandy silt samples from borehole NS-1-13, between elevations 28 to 38 m, which resulted in average values of $\phi'=35°$ and $c'=0$.

The presence of silty clay or clayey silt strata interbedded within the intermediate silty sand layer influences permeability test results with values from 10^{-7} to 10^{-9} m/s.

2.3.4 Lower Marine Clay Unit

The lower clay layer is located below the stratified drift and above the lower aquifer (lower sand and gravel layer). This layer consists of clay of low to medium plasticity which exhibits lower values of liquidity index than the upper clay layer and can be classified as slightly sensitive.

The consistency of clay is stiff to very stiff with in-situ undrained shear strength of 53 to 200 kPa. A summary of material properties for the lower clay layer is presented in Table 2-2.

As will be discussed below, based on CPT and vane data, the undrained shear strength at a given elevation is generally similar throughout the North Spur with the Over-Consolidation Ratio (OCR) at about 1.0 below the crest and between 3 and 15 below the upstream and downstream toe. It should be noted that some of the material at shallow depth below the toe in areas subjected to previous slides can be remoulded.

Table 2-2: Summary of Material Properties for Lower Clay Layer (1979 Investigations)

Property	General Range	Average	Number of tests
Percent finer than 2 microns	15 – 35		
Water content, w %	17 – 45	29	201
Liquid limit, LL %	22 – 48	37	123
Plastic limit, PL %	13 – 27	21	123
Plasticity Index, PI %	7 – 25	16	123
Liquidity Index, LI	0.1 – 2	0.6	123
Intact Undrained shear strength, S_u, kPa	53 – 200	–	–
Remoulded Undrained shear strength, S_u, kPa	8 – 96	–	–
Sensitivity in-situ, s_t	2 – 11	4	35
Large strain friction angle, ϕ'_{cv} º	33	–	–
Effective cohesion, c', kPa	6	–	–
Salt content, g/l	8 – 22	–	8
Unit weight, γ , kN/m^3	19.2 – 19.5	–	3
Hydraulic Conductivity, k, m/s	$10^{-7} – 10^{-9}$	–	–

2.3.5 Lower Sand and Gravel Unit (Lower Aquifer)

The lower aquifer layer is located below the lower clay layer and above the bedrock. It consists of sand and gravel with some cobbles and boulders with a fines content (silt and clay) between 5 and 40%.

Some samples from this layer were found to contain a high proportion (75%) of fines but pumping tests indicated an average coefficient of permeability of 10^{-4} m/s and consequently this unit is expected to have on average a relatively low fines content.

2.3.6 Bedrock

The type of bedrock is generally granite gneiss with pegmatite intrusions. Its depth is very variable across the North Spur as can be observed on Figure 2-1 and on the section views of Appendix A.

2.4 HYDROGEOLOGY

Interpretation of the different stratigraphic and hydrogeological data permitted to identify three different aquifers in the North Spur. In the surficial upper sand layer unit overlying the stratified drift, a perched aquifer exists below the ground surface. A second aquifer, labelled as "intermediate aquifer", was identified inside the stratified drift unit. Finally, overlying the bedrock and limited in the upper part by the lower marine clay unit, the "lower aquifer" was identified during the works.

A 3D hydrogeological model of the North Spur was prepared based on the regional geology information and the piezometric data available. Findings and conclusions of these works are presented in details in the Hatch (2015) report. Relevant results for present conditions and for conditions after reservoir impoundment are discussed in this section.

2.4.1 Existing Conditions

A perched water table was observed in the upper sand layer in some boreholes. This water table is mainly recharged by precipitation and water infiltration from top of the Spur. Due to higher permeability of this layer the ground water easily drains through the upstream, downstream and kettle lakes slopes at elevations 40 to 45 m.

An intermediate aquifer is observed in the stratified drift and the average piezometric contours are shown in Figure 2-2 indicating water equivalent levels of 30 to 35 m in the center of the North Spur.

Due to a significant vertical gradient, a downward ground water flow, from perched aquifer to intermediate aquifer and to lower aquifer, was identified.

A lower aquifer was identified in the lower granular layer (generally below elevation -70 m). The piezometric levels in this aquifer were measured during investigations to change from 15 m and 13.5 m on the upstream side to 4.3 m on the downstream side of the North Spur.

The river bathymetry shows that a deep depression, with a minimum elevation at about – 60 m, exists in the bay downstream of the Spur. Considering the top elevation of the lower aquifer, it is expected that the lower aquifer is connected to the downstream side of the river in this area. This is illustrated on Figure 2-3 showing the piezometric contours estimated for the lower aquifer unit.

Figures 2-2 and 2-3 were prepared by SNC-Lavalin NL (1980) based on piezometric data measured before the installation of the dewatering system to reduce the water level in the Intermediate Aquifer. These pumps had a significant effect in the southern and central part of the downstream side of the North Spur but only a negligible effect in the northern part.

2.4.2 Reservoir Impoundment

In the 3D hydrogeological study of the North Spur (Hatch, 2015), the Lower and Intermediate aquifers were modeled for various hydrogeological scenarios to assess their response during reservoir impoundment. Two separate models were developed for these aquifers since the lower marine clay unit acts as a boundary region between them. These models were calibrated for the existing conditions with a river elevation at 17 m on the upstream side and at 3 m on the downstream side.

The study concluded that after the projected full reservoir impoundment (elevation 39 m), the piezometric level in the Lower Aquifer would raise from elevation 4.1 to 6.9 m below the downstream toe of the North Spur and from 6.9 to 14.4 m below the upstream toe as illustrated on Figure 2-4.

For the Intermediate Aquifer, the model illustrates the effect of the stabilization works on the seepage conditions. Figure 2-5 shows that due to the installation of cut-off walls, till blanket and finger drains, the normal water level below the crest on the upstream side of the Spur is expected to drop from the FSL of 39 m to a water level of 25 m at a distance of 20 m from the crest.

Figure 2-2 : Intermediate Aquifer – Piezometric Contours (SNC-LAVALIN NL, 1980)

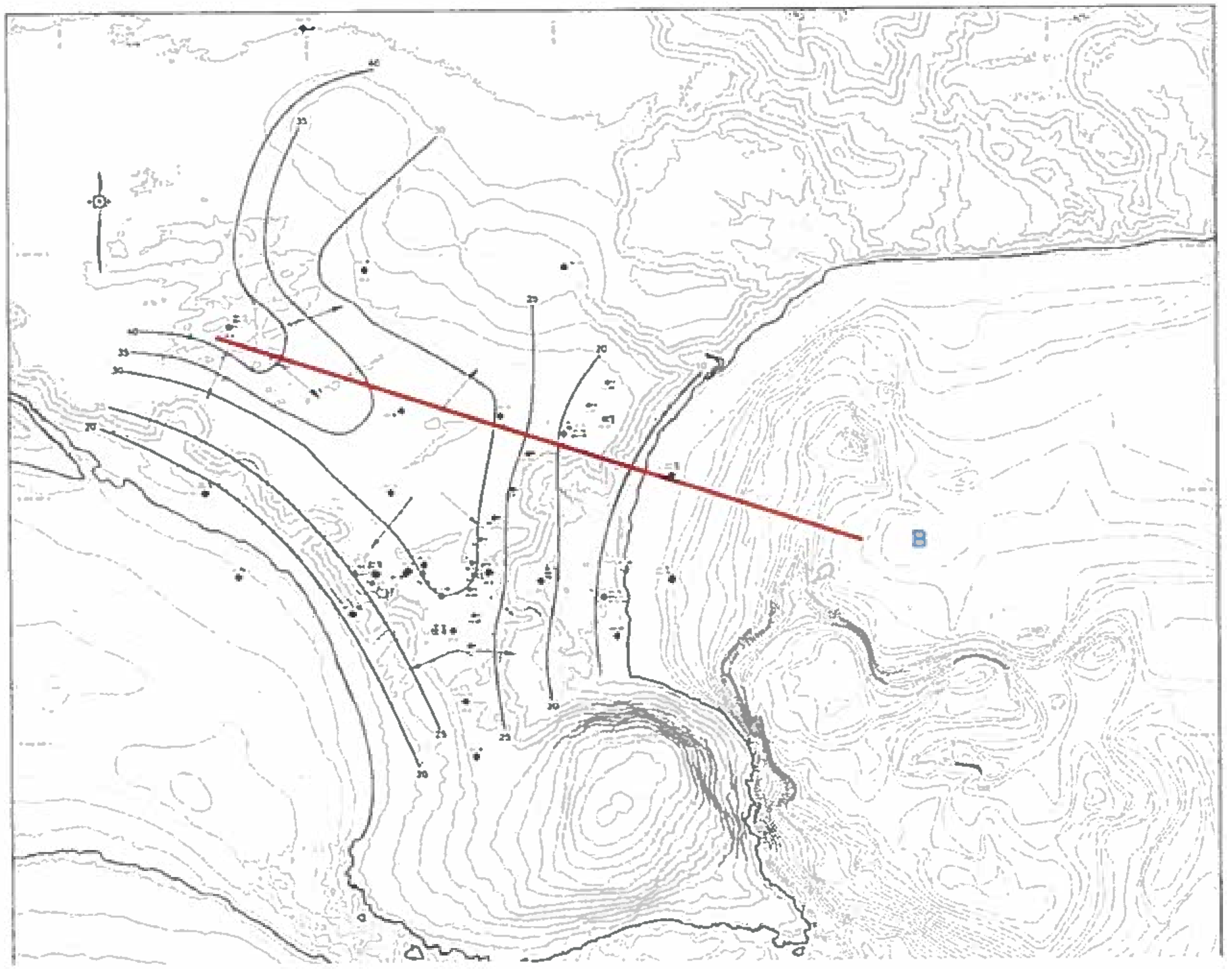

Figure 2-3 : Lower Aquifer – Piezometric Contours (SNC-LAVALIN NL, 1980)

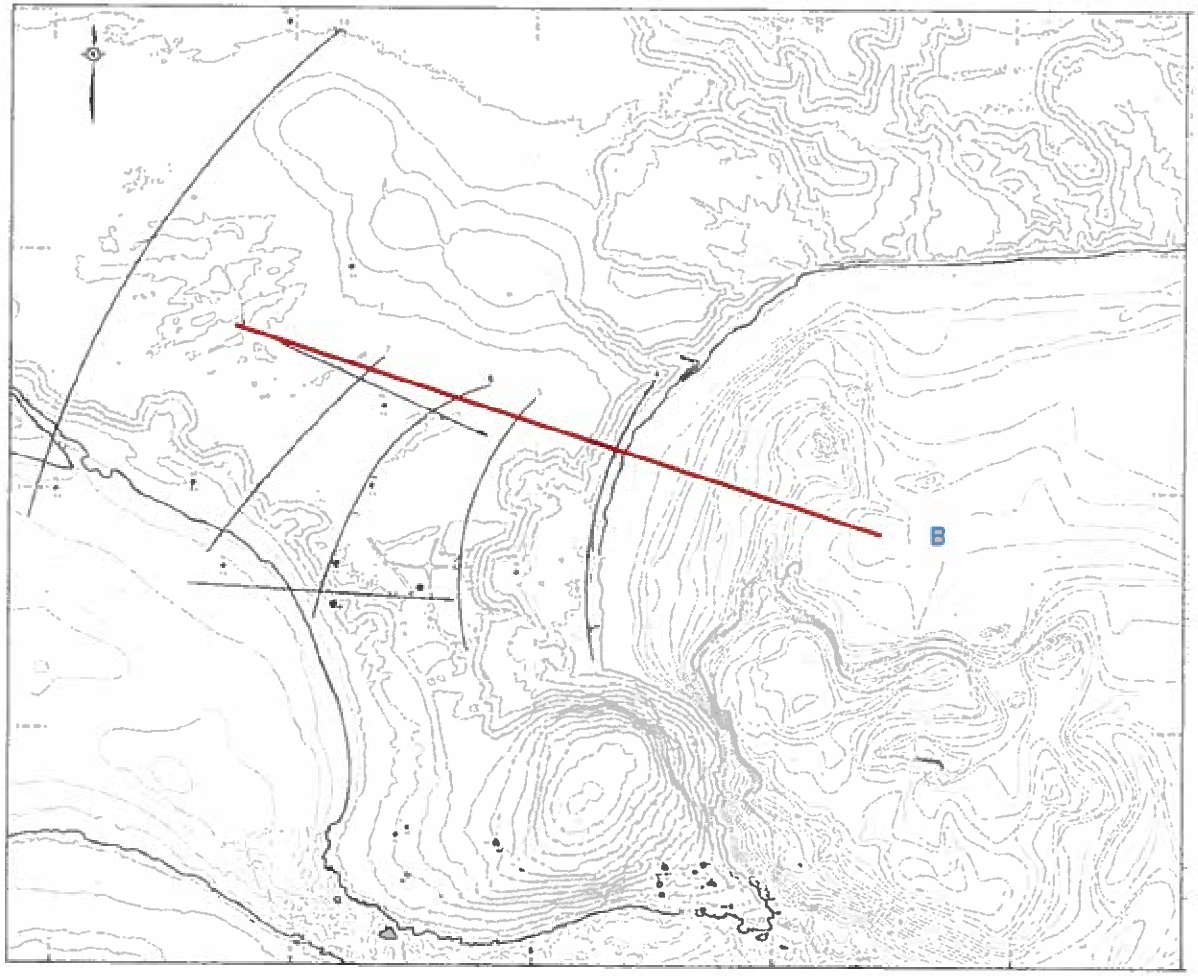

Figure 2-4 : Lower Aquifer – Effect of Full Reservoir Impoundment at Elevation 39 m

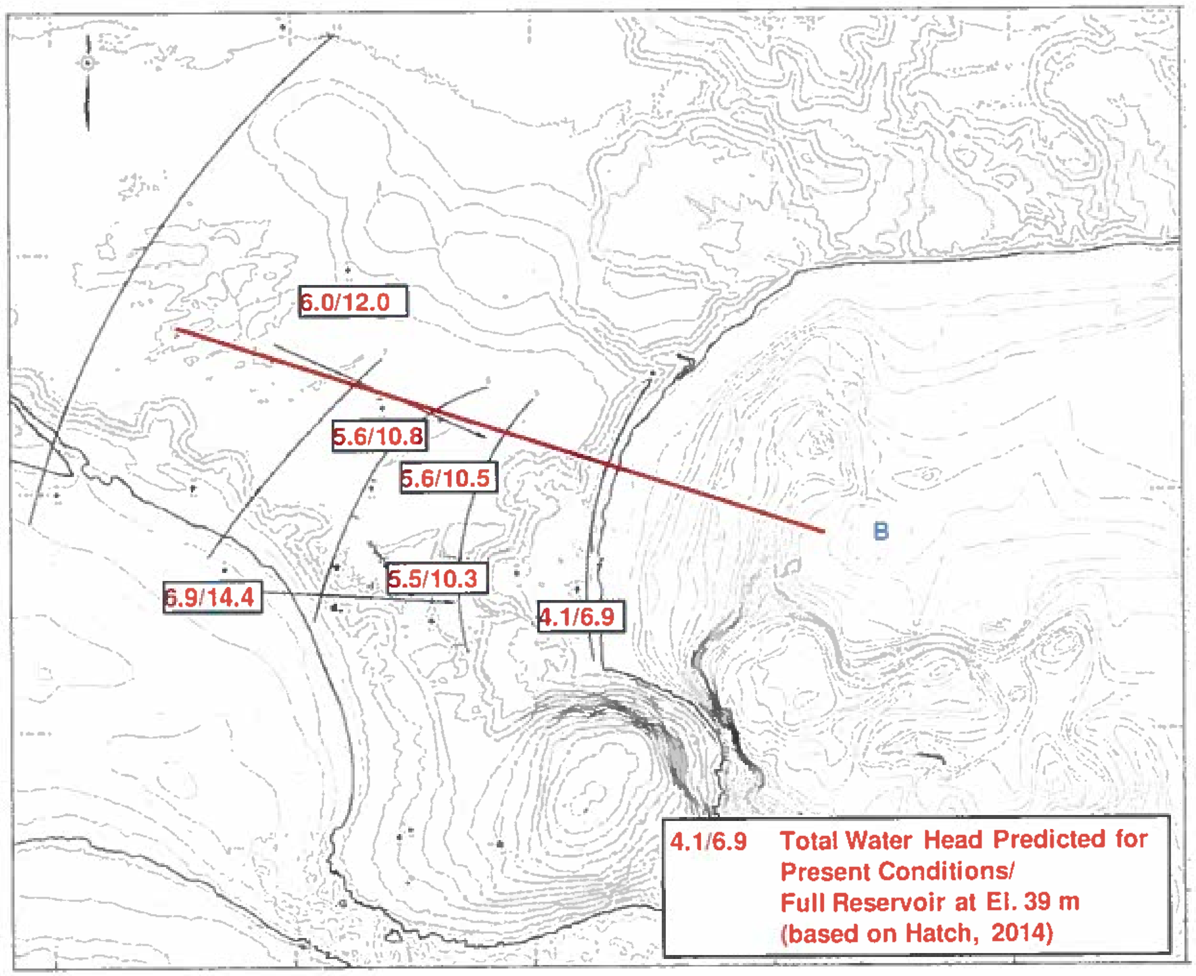

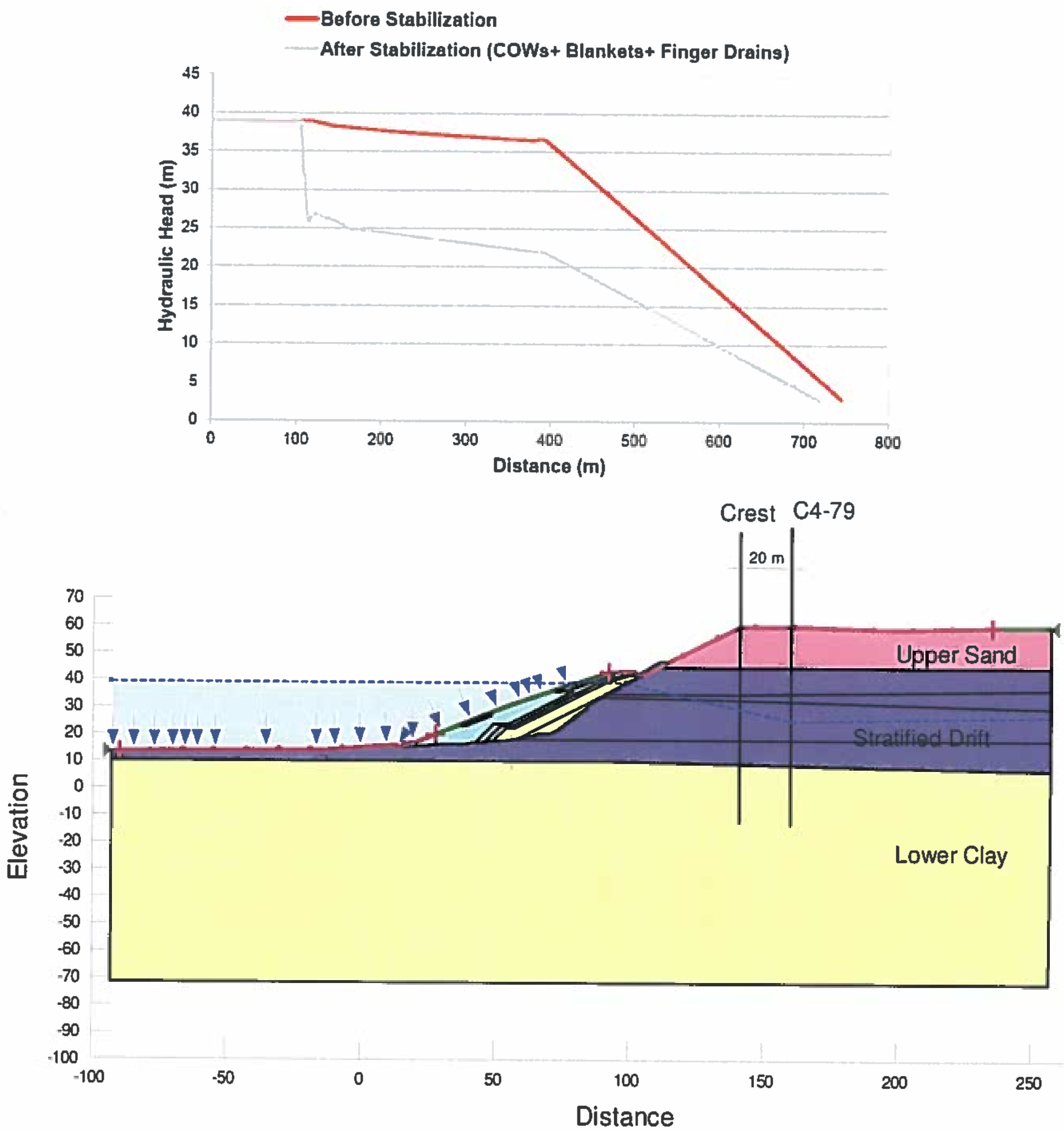

Figure 2-5 : 3D Hydrogeological Study (Hatch, 2015) Results for Full Reservoir Impoundment

3 LANDSLIDES HAZARDS

3.1 LANDSLIDES IN SENSITIVE CLAYS

There are hundreds of landslides in sensitive clays every year in Eastern Canada. Most of them are single rotational landslides of limited size but there are also large landslides (> 1 ha) that are classified as flowslides and spreads. According to Demers et al. (2013), in the Province of Quebec, 58% of the large landslides are flowslides, 37% are spreads and the remaining 5% are of another type or intermediate.

Progressive Failure

Sensitive clays from Eastern Canada show a strain-softening behaviour in undrained conditions and may therefore be susceptible to progressive failure (Locat, 2013). Locat (2011) reports the description of the concept of progressive failure by Terzaghi and Peck (1948) and Skempton (1964). Considering the strain-softening behaviour of clays, Skempton (1964) described the failure mode occurring during progressive failure with the following statement: "[…] if for any reason a clay is forced to pass the peak at some particular point within its mass, the strength at that point will decrease. This action will throw additional stress on to the clay at some other point, causing the peak to be passed at that point also. In this way a progressive failure can be initiated and, in the limit, the strength along the entire length of a slip surface will fall to the residual value." Figure 3-1 illustrates how the shear strength along a potential failure surface may vary from peak shear strength to large-deformation shear strength. The soil in the potential sliding mass is therefore subjected to local failure when it reaches its peak shear strength (points 1 to 3 along the potential failure surface in Fig. 3-1), prior to global failure taking place when the entire failure surface is formed (Locat et al, 2011).

3.1.1 Single Rotational Landslides

Rotational landslides can be single or can be the initial instability leading to flow slides. The single rotational landslide is characterised by the fact that a significant portion of the material displaced by the failure stays at the toe of the slope and stabilizes the slope, thereby preventing further instabilities.

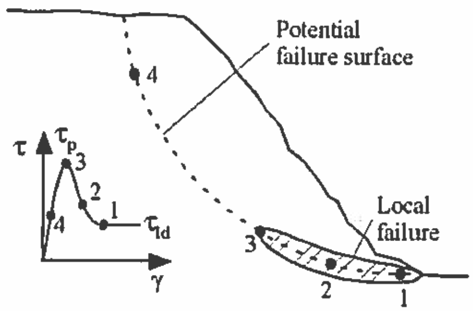

Figure 3-1 : Progressive failure along a circular failure surface (from Locat et al, 2011)

The stability of rotational landslides for natural slopes is determined through limit equilibrium stability analyses in terms of effective stresses (Lefebvre, 1981; Tavenas & Leroueil, 1981). A conservative estimate of the effective strength parameters and of the fluctuations of piezometric conditions are essential.

3.1.2 Flowslides

As indicated in Figure 3-2, flowslides in sensitive clays result from a succession of slides. There must be an initial slide (failure (1) in Figure 3-2). If the potential energy due to the slump is large enough to remould the clay, that latter becomes remoulded and flows out of the crater if the liquidity index is large enough or the remoulded shear strength small enough. The backscarp thus stands there without being supported by debris. If this backscarp is unstable either in undrained or partly drained conditions, there will be another failure (failure (2) in Figure 3-2), instantaneously or after some time that can be minutes, hours or days (Demers et al., 2013). And the process may go on and on. To get a flowslide in sensitive clays, there are thus four requirements (Tavenas, 1984; Leroueil et al., 1996):

- There must be an initial slope failure.
- There must be enough potential energy for remoulding the clay. Experience shows that to reach this condition in Eastern Canada clays the stability factor $N_s = \gamma H/S_u$, in which N_s must be larger than about 3 in clays with a plasticity index of 10 or less, increasing to about 7 or 8 in a clay with a plasticity index of 40.

- Once remoulded, the clay must be able to flow out of the crater. This is possible when remoulded shear strength S_{ur} < 1.0 kPa or a liquidity index I_L > 1.2. (Lebuis et al., 1983).
- There must be a topography which permits the evacuation of the liquefied debris.

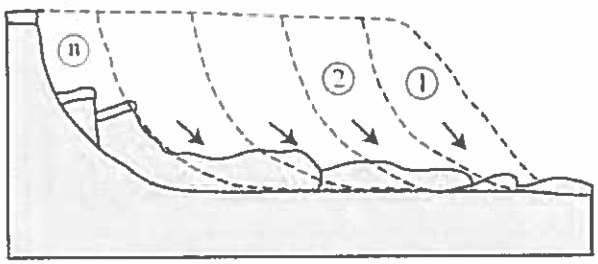

Figure 3-2 : Flowslide in sensitive clay (Locat et al, 2011)

3.1.3 Progressive Failure

Experience shows that spreads in sensitive clays generally start from a disturbance such as erosion or a small landslide at the toe of the slope and that progressive failure develops along a quasi-horizontal shear surface or shear zone and that finally the soil above the shear surface dislocates into horsts and grabens. The development of spreads, or upward progressive failure, in sensitive clays has been described by Locat et al. (2011, 2013 and 2014). If there is a slope as that shown with the dashed line in Figure 3-3a, the shear stress along a potential horizontal surface can be as τ_{0x}, dashed line in Figure 3-3b. The undrained peak shear strength τ_p and the large deformation strength τ_{ld} can be as shown in Figure 3-3b. If there is erosion or a small landslide at the toe of the slope, the shear stress will locally increase (τ_{1x} in Figure 3-3b) and possibly locally reach the undrained shear strength τ_p of the clay. If this happens, progressive failure develops upwards from A towards B (τ_{2x}, τ_{3x}, ... in Figure 3-3b). Then the soil above the shear surface, which is on a layer of more or less remoulded soil will dislocate in horsts and grabens.

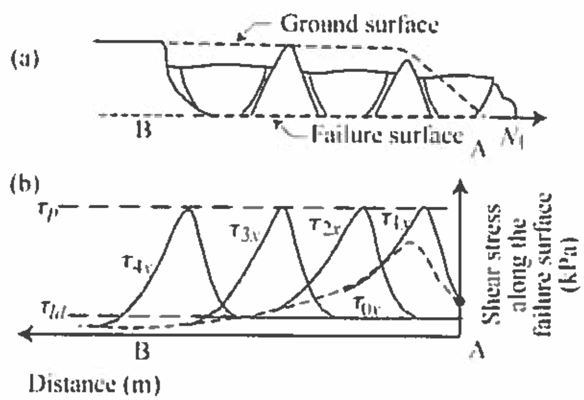

Figure 3-3 : Spread Landslide resulting from progressive failure in sensitive clay (Locat et al, 2011)

Progressive failure may also develop as a result of loading or piling in the slope or beyond the crest of the slope, as at the level of point B in Figure 3-3. If loading or piling generates a shear stress that locally exceeds the undrained shear strength (e.g. τ_{4x} in Figure 3-3b), failure may progress downward towards the toe of the slope (Point A in Figure 3-3) and generate a global failure. It is the explanation given by Bernander (2000) and Locat et al. (2011) to the Surte landslide that occurred in 1950 in Sweden as a consequence of piling in the slope. It is also thought that the Rigaud landslide that occurred in the Province of Quebec in 1978 (Carson, 1979) because of piling may resulted from downward progressive failure. Whatever the progression direction of failure, to have progressive failure, it is necessary for the shear stress to locally reach the undrained shear strength of the clay.

3.2 LANDSLIDES HAZARD IN THE CONTEXT OF THE NORTH SPUR

Based on observations and past investigations, it is recognised that single rotational landslides and flowslides have occurred along the Churchill River but no clear evidence of spreads or other progressive failures. Given the presence of sensitive clays, the conditions for the different types of landslides were examined.

3.2.1 Conditions for Single or First-time Rotational Slides

Minimum effective strength parameters for a first-time failure can be established based on the stability conditions of the steep slopes on the Spur. For the design, it must be insured that all slopes will be stable.

Limit equilibrium stability analyses were performed in terms of effective stresses on the basis of an effective friction angle and an effective cohesion for the slopes of the North Spur. The effective strength parameters considered have been verified by the stability analysis of the steepest slope as described in SLI (2015a). The stabilization works for all the slopes have been designed so that the calculated factor of safety is at least 1.5. Also, measures have been taken so that there will be no future erosion at the toe of the slopes.

3.2.2 Conditions for Flowslides

As stated above, there are necessary conditions to have a flowslide: a first-time failure; sufficient energy to remould the clay ($\gamma H/S_u > 3$ or 4 for the clays at the North Spur); and remoulded shear strength $S_{ur} < 1.0$ kPa or a liquidity index $I_L > 1.2$.

For the Upper Clay layer 1, typical characteristics are: S_u about 45 kPa; $\gamma H/S_u$ about 7; and I_L about 1.4 For the Upper Clay layer 2, typical characteristics are: S_u about 60 kPa; $\gamma H/S_u$ about 10; and I_L average 1.4 (greater than 1.0). So, if a first-time failure occurred, there could be retrogression and flowslide; the 1978 landslide confirms that possibility. However, as indicated in Section 3.2.1, the slopes will be stabilized so that a first-time failure will not occur.

The Lower Clay layer is found at elevations below 15 m and has a typical liquidity index of 0.6. Consequently, even if there would be a first-time failure in this unit, there would not be retrogression and flowslide.

3.2.3 Conditions for Spreads

The possibility of a spread or of other types of progressive failure on the North Spur exists because the clays are sensitive. However, conventional limit equilibrium methods, applied to progressive landslides, generally give factors of safety for spreads well above unity and therefore cannot explain observed ground movements (Locat, 2014). To have such progressive failure, there must be a disturbance, such as a movement at the bottom of a slope caused by erosion (this could be the case in the Churchill River Valley). Such a disturbance could cause the shear stress on a horizontal plane will reach the undrained shear strength of the clay. Such possibility is to be avoided by protecting the toe of slope to prevent erosion. At the North Spur, the stabilization works address the erosion protection at the toe of the slopes specifically to avoid the first movement or disturbance at that place. The horizontal shear stress is also reduced with the addition of a protective berm. With these measures of protection, the first movement will not appear so regressive or progressive landslide will not occur. Other protective methods put in place to avoid triggering a progressive failure include no fill near the crest of slopes, no driving piles, and no increase to groundwater pressure

3.2.4 Interpretation of 1978 Landslide

The most recent large deep seated landslide at the North Spur occurred in November 1978 on the downstream side and removed about 1 million m^3 of soil. The maximum distance of the retrogression from the original slope was less than 200 m. The slide involved a block movement triggered by weak layers within the stratified drift, followed by retrogressive flow slides, conditions where shearing resistance first increases and then decreases with increasing strain, and, as result, the peak shear strengths of the material at all points along a slip surface cannot be mobilized simultaneously.

This slide is a confirmation that the slopes of the North Spur could be subject to retrogressive slides.

4 DESCRIPTION OF STABILIZATION MEASURES

Projected stabilization works of the North Spur are described in the Design Report (SLI, 2015a) and Technical Specifications (SLI, 2015b). This design calls for 1) a control of the groundwater in the North Spur, 2) an erosion protection on both sides, upstream and downstream, of the Spur and 3) local unloading of the upper part of the Spur.

4.1 GROUNDWATER CONTROL

Groundwater control on the North Spur will be assured by the following measures:

- Upstream cut-off wall:
  construction of a cement bentonite cut-off wall and till blanket barrier;
- Northwest cut-off wall:
  construction of a cement bentonite cut-off wall in the northwest area of the Spur;
- Finger drains:
  construction of finger drains and inverted drains in the downstream area;
- Improvement of drainage of the Kettle Lakes;
- Installation of relief wells in the lower aquifer (if needed).

4.2 EROSION PROTECTION AND SLOPE UNLOADING

Based on stability analyses of the slopes of the Spur in their present condition, the stability could be marginal locally and the main triggering factor of instability has been identified to be toe erosion due to water and ice level fluctuations. Therefore, construction of a berm and of rock embankments to protect the upstream and downstream slopes against erosion and local excavations of the upper layers to unload the slopes has been planned as part of the stabilization works.

5 PROGRESSIVE FAILURE POTENTIAL

As mentioned above, to prevent progressive failures in sensitive clays, the possibility of a disturbance somewhere such that the shear stress on a horizontal plane would reach the undrained shear strength of the clay should be avoided. A method has been developed by Locat et al (2013) for the back analysis of progressive failure. The first part of this method will be used for North Spur to assess the present stability (regarding the progressive failure mechanism) of the North Spur slopes.

5.1 METHODOLOGY

The methodology proposed by Locat et al (2013) for the analysis of progressive failure defines two important points:

1) <u>The initial shear stress:</u>

   The initial shear stress along a potential failure surface, most of the time close to the horizontal reaches its maximum about under the crest of the slope.

   As shown in Section 5-4, planned stabilization works will increase the slope stability (safety factor increases) and thus reduce the initial shear stress that will become smaller compared to the soil shear resistance.

2) <u>Disturbance:</u>

   If a significant disturbance occurs which increases the shear stress at a specific location up to the soil shear resistance, then progressive failure can start and possibly continue, leading to a global failure. This disturbance can come from downhill or uphill.

   In the eastern sensitive clay, this disturbance is more often the result of erosion or after a small slide at the foot of the slope. However, the disturbance could also come from uphill, such as pile driving or other human trigger, and therefore, precautions will be taken to prevent any disturbance upslope and on the crest as well.

In summary, if improvements are made to stability, the probability of having a progressive failure can be decreased compared to what it was before. If, in addition, significant disturbance is prevented, then progressive failure cannot occur. This approach was applied by the design team to prepare the stabilization works for the North Spur site.

Numerical Finite element analyses have been performed on representative cross-sections to study the shear stresses along various horizontal surfaces passing through two Upper Clay Layers and through the Lower Clay. These analyses have considered four stages: before river erosion, before stabilization works, after stabilization works and after reservoir infilling.

5.2 TYPE OF ANALYSES

As described above, the first part of the method developed by Locat et al (2013) for the back analysis of progressive failures was used to estimate the stress distribution for various conditions. The process was to prepare a 2D stress distribution numerical model and to recreate the stress conditions in the clay layers for a reference case representing the most severe existing conditions on the North Spur slopes. Then, the projected conditions after the stabilization works were modeled and the predicted stress distribution was compared with that of the reference case.

Three types of analyses were performed using the software and soil models described in Section 5.3:

- Seepage analyses to estimate the water pressure distribution in the soil units forming the Spur and to calibrate the model against the observed piezometric conditions;
- Slope Stability analyses to estimate the effect of a surcharge at the crest of the Spur using the Limit Equilibrium Method (LEM)
- Stress Distribution analyses to estimate the stress distribution in the Spur assuming an elastic-plastic behavior model.

5.3 SOFTWARE AND SOIL MODEL

5.3.1 Seepage Analyses

The seepage analyses were performed using the Seep/W module of the GeoStudio Suite version 8.14.1.10087 developed by GeoSlope International (1991-2014). This 2D program can simulate various infiltration and seepage situations including saturated and unsaturated flow, for both steady state and transient conditions. In this study, steady state analyses were performed using for unsaturated materials some hydraulic conductivity functions typical for the kind of material forming the North Spur.

5.3.2 Slope Stability Analyses

The slope stability analyses were performed using the Slope/W module of the GeoStudio Suite version 8.14.1.10087 developed by GeoSlope International (1991-2014). This 2D program can analyze the stability of slopes and dams using the LEM. In this study, static effective stress analyses (Morgenstern-Price method) were performed using for all materials a shear strength defined by the cohesion, c', and the friction angle, φ'.

5.3.3 Stress Distribution Analyses

The stress distribution analyses were performed using the Sigma/W module of the GeoStudio Suite version 8.14.1.10087 developed by GeoSlope International (1991-2014). This 2D program can simulate the stress distribution and the load/deformation changes for a wide range of soil conditions and models. The analyses can be coupled with the seepage analyses. In this study, only the elastic and elastic-plastic models will be used in uncoupled analyses but using the results of the seepage analyses to estimate the water pressure distribution in the spur.

The elastic model is a linear model for which stresses are directly proportional to the strains. The proportionality constants are Young's Modulus, E, and Poisson's Ratio, ν.

The elastic-plastic model in Sigma/W describes an elastic, perfectly-plastic relationship. Stresses are directly proportional to strains until the yield point is reached. The parameters in the elastic domain are the same as for the elastic model. Beyond the yield point, the stress-strain curve is perfectly horizontal. Sigma/W uses the Mohr-Coulomb yield criterion as the yield function. The Mohr-Coulomb yield criterion is defined by the cohesion, c', and the friction angle, φ'.

5.4 SELECTION OF REPRESENTATIVE SECTIONS

5.4.1 Reference North Section B-B

Based on topographic and stratigraphic information, the most critical slope of the North Spur has been identified on the downstream side of the spur, on Section B-B, about 200 m south-west of Kettle Lakes outlet, where the steep slope is still intact as shown on Figure 5-1. Short-term stability analyses for the static conditions performed in the SLI (2015a) study have shown that the present factor of safety would be about 1.0 as illustrated on Figure 5-2-a, i.e. the current stability of this slope would be only marginal. After proposed re-grading and stabilization works (see Figure 5-2-b), the factor of safety is expected to be about 1.6.

Section B-B will be analysed with the latest interpreted stratigraphy, as illustrated on Figure 5-3 and on Figure A-3 of Appendix A; this stratigraphy is similar to the stratigraphy assumed in the stability analyses of Figure 5-2.

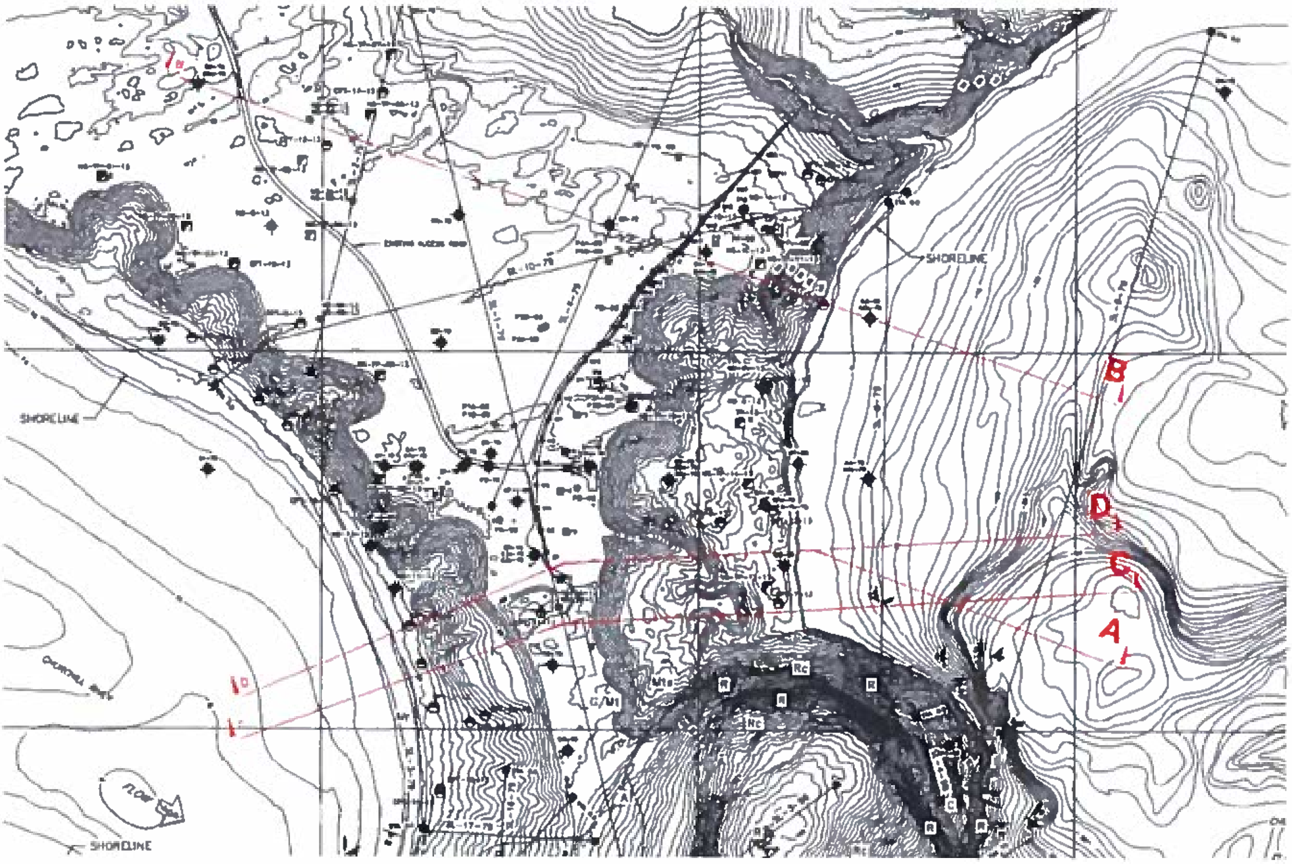

Figure 5-1 : Representative Sections - Location Plan

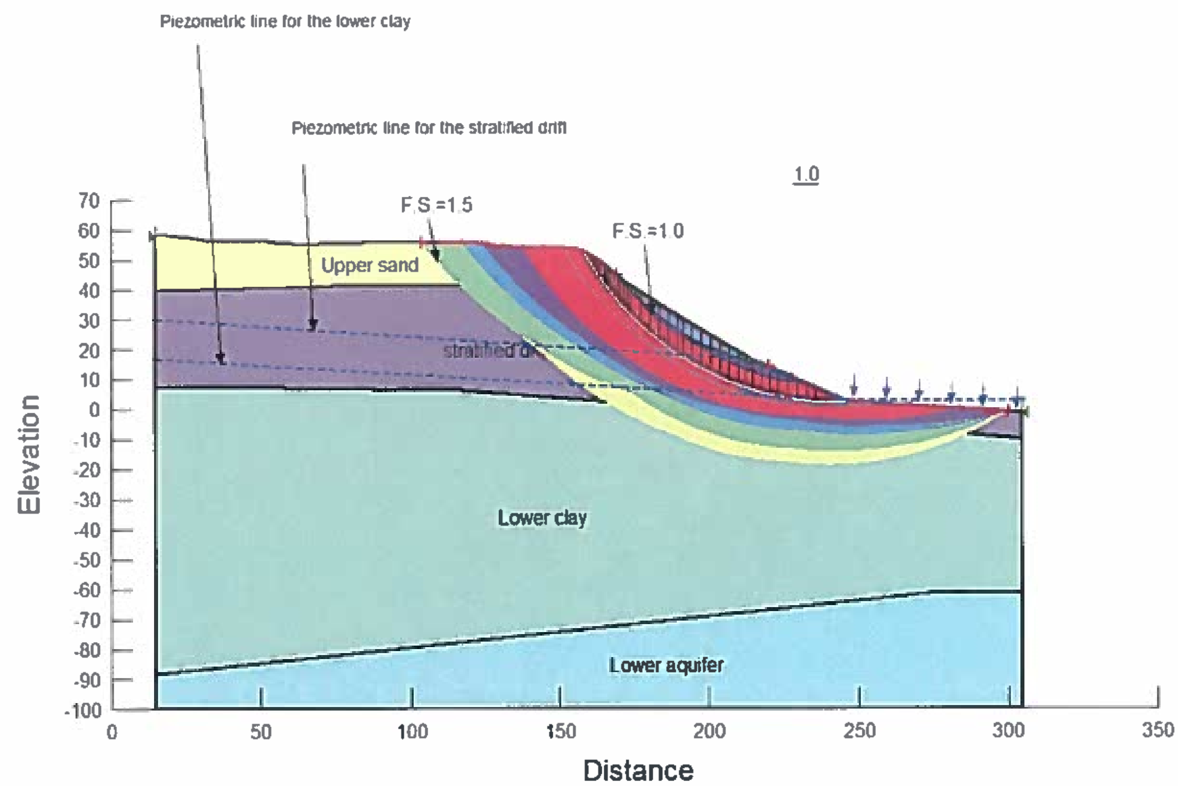

a) Section B-B - Before Stabilization Works

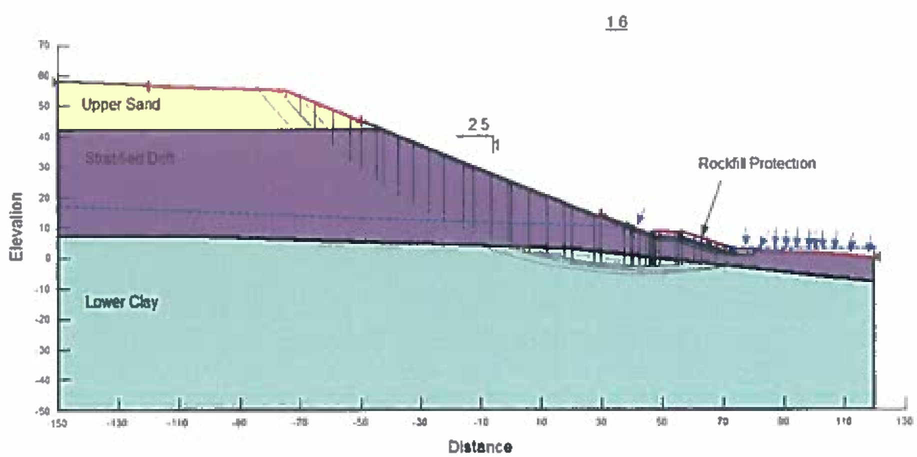

b) Section B-B - After Stabilization Works

Figure 5-2 : Stability Analyses of Downstream Section (SLI, 2015) a) Before and b) After Stabilization Works

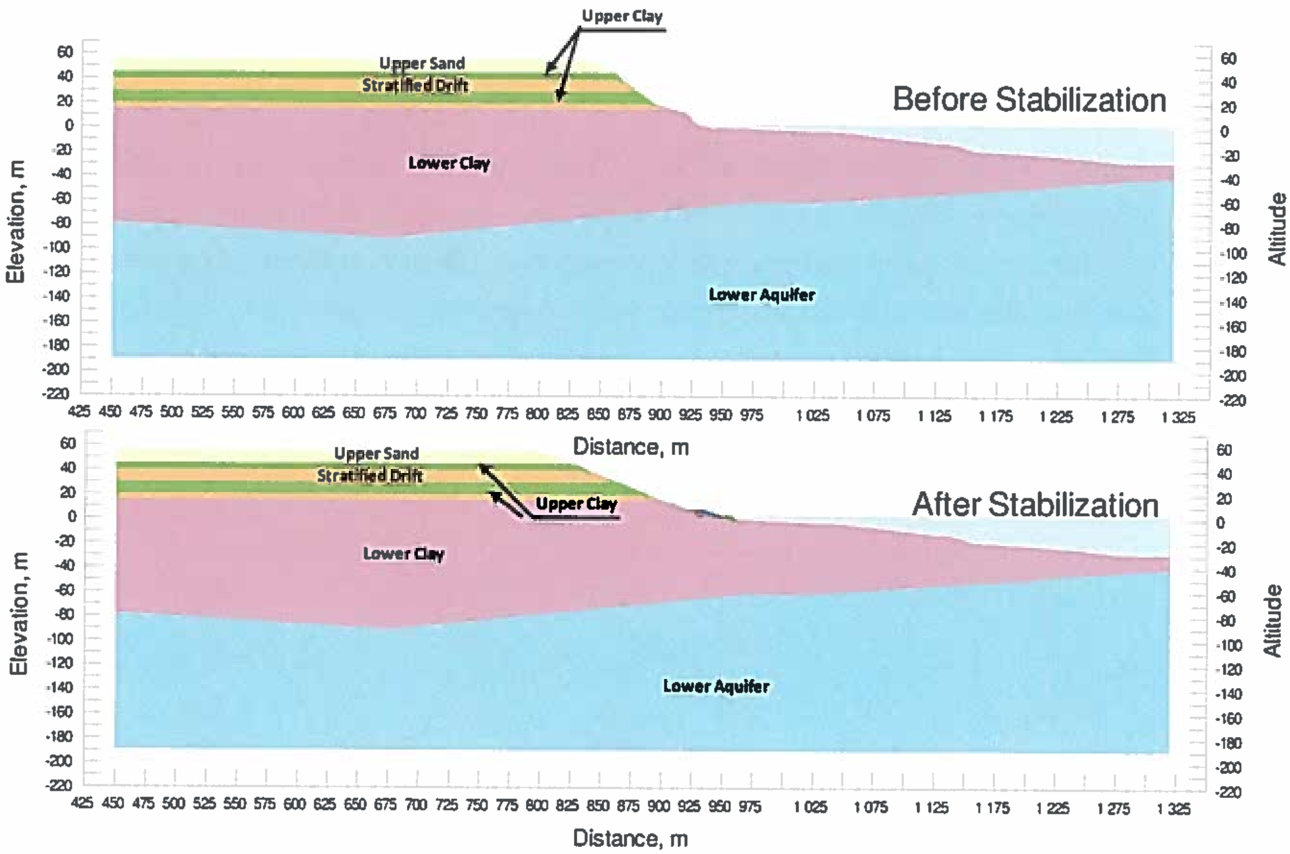

Figure 5-3 : Section B-B - Stratigraphy

5.4.2 Narrow South Sections

Three cross-sections were selected in the southern portion of the Spur where the crest is already narrow due to past landslides. These sections are located in plan on Figures 5-1 (present conditions) and 5-4 (stabilized conditions) and are shown on the figures of Appendix A:

- Section D-D (Figure A-4) was selected to represent the narrow portion of the Spur with the steepest stabilized slope;
- Section A-A (Figure A-3) is a version of Section D-D modified to examine the stability of the downstream submarine depression located near the rock knoll;

- Section C-C shown on Figure 5-4 was also analyzed but not retained because it was judged less representative than Section D-D.

On the downstream side of these sections where landslides have already occurred (see Figure 1-1 and 3-1), the slope is gentler and the presence of slide debris in the toe area has a stabilizing effect. On the upstream side of the spur, the height of the slope relative to the toe elevation is lower and the presence of the reservoir will have a stabilizing effect. Based on previous seepage analyses, after the completion of the stabilization works, the normal water level below the crest is expected to be at an elevation of 25 m at a distance of 20 m from the crest as illustrated on Figure 2-5; a conservative water table elevation of 30 m was assumed in the analyses.

Figure 5-4 : Localization of Sections Analysed for Stabilized Conditions

6 SEEPAGE ANALYSES

As described in Section 2.4, the seepage conditions at the North Spur are highly three dimensional. The objective of the seepage analyses on Reference Section B-B was to obtain a pore water distribution similar to what has been interpreted based on piezometric data available. Only the main findings will be presented in the following sections. Detailed figures can be found in Appendix C.

6.1 MATERIAL PROPERTIES

The material properties used in the seepage analyses are presented in Table 6-1. The values were selected based on the 3D Hatch (2015) Hydrogeology study. A best fit process was applied to have a good behavior between the two models.

Table 6-1 : Seepage Analyses - Material Properties

Material	Porosity n	Hydraulic k (m/s)
Upper Sand	0.36	1.00E-04
Upper Clay	0.48	1.00E-07
Silty Sand/Sandy Silt	0.41	8.00E-06
Lower Clay	0.48	1.00E-08
Lower Acquifer	0.36	1.40E-04

6.2 BOUNDARY CONDITIONS AND RESULTS

Two seepage models were retained, one for the Upper Clay layers and one for the Lower Clay unit. The results were used in the stress distribution analyses.

6.2.1 Lower Clay Model

The seepage analyses will be illustrated with the analyses performed for reference Section B-B. The boundary conditions were selected based on the results of the 3D hydrology study (see Figures 2-3 and 2-4) in the intermediate and lower aquifer units as illustrated on Figure 6-1. Then, the boundary conditions were adjusted to fit the piezometric data: a small amount of infiltration was added at the Spur surface and the water level at the upstream boundary of the Upper Clay-1 layer was raised to an elevation of 45 m. Figure 6-2 shows the water pressure contours predicted by this adjusted model. They reasonably match the piezometric data in the Lower clay as can be seen on Figure C-5 of Appendix C.

6.2.2 Upper Clay Model

However, for the Upper clay layers, given some local higher piezometric level (see Figure C-7 of Appendix C) and given the reported local perched water table at the boundary between Upper Clay-1 and the Upper Sand unit, it was decided to assume for the Upper Clay layers a hydrostatic water table at the surface of Upper Clay-1, at an elevation of 45 m, as illustrated on Figure 6-3. These assumptions are on the safe side.

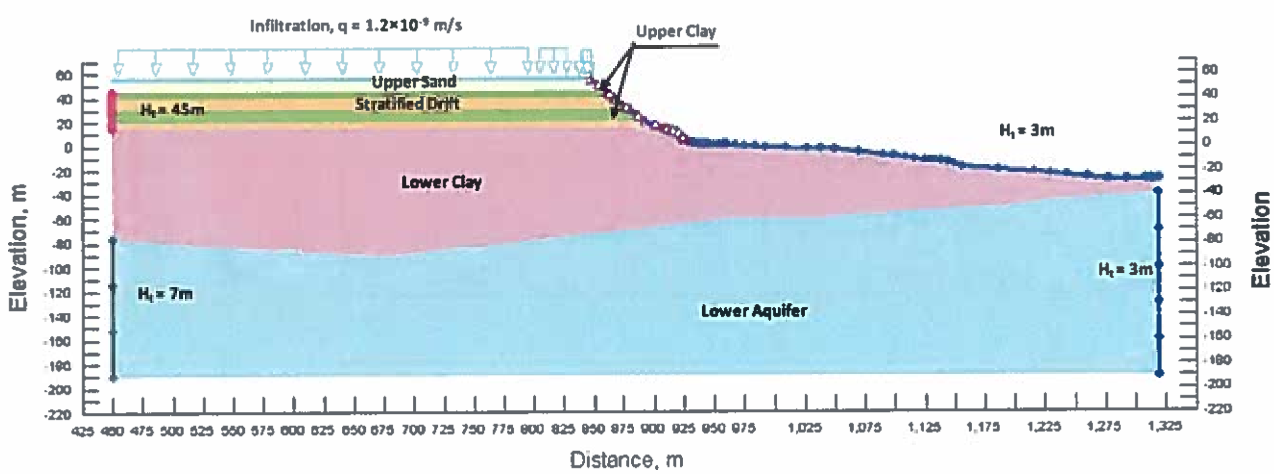

Figure 6-1 : Section B-B - Seepage Model to Simulate Piezometric Conditions in Lower Clay - Boundary conditions

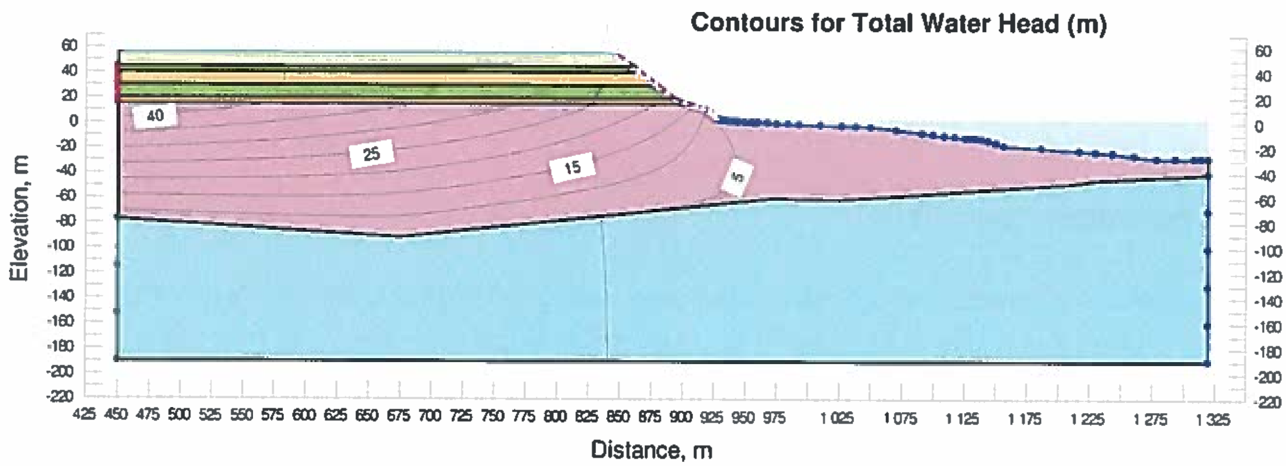

Figure 6-2 : Section B-B - Seepage Model to Simulate Piezometric Conditions in Lower Clay – Total Water Head Isocontours

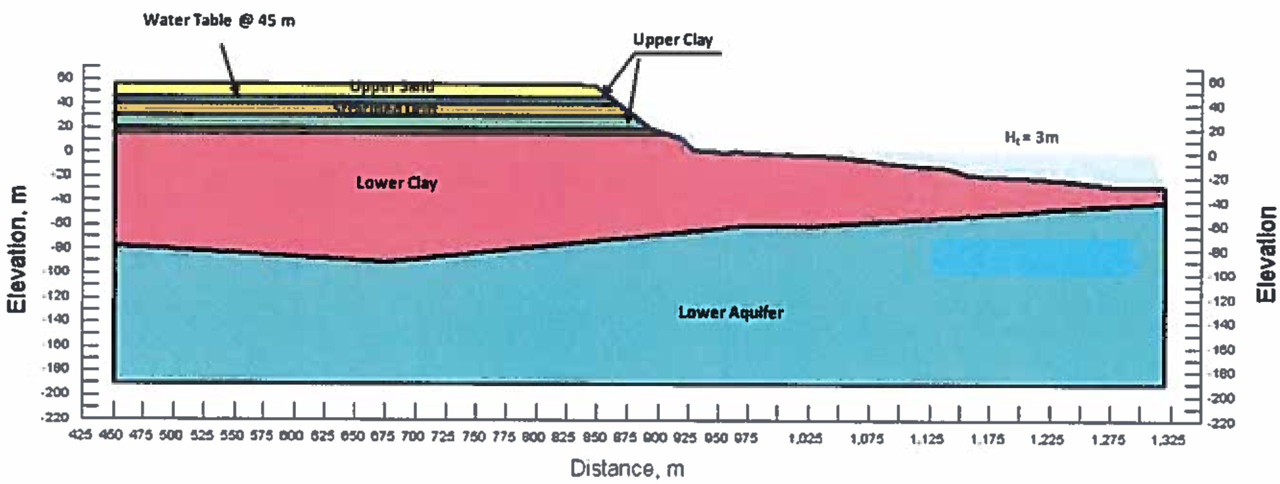

Figure 6-3 : Section B-B - Seepage Model to Simulate Piezometric Conditions in Upper Clay Layers

7 STRESS DISTRIBUTION ANALYSES

The stress distribution analyses performed are described in the following sections and on the figures of Appendix C.

7.1 CONDITIONS SIMULATED

For each section, two models were analysed: one for the Upper Clay layers (above 20 m) with a hydrostatic water table at elevation 45 m; and one for the Lower Clay unit (below 15 m) using the results of the seepage analyses described above. In each case, the phases presented in Table 7-1 were simulated.

For simplicity, the unloading from the "Flat Ground" condition to the "Before Stabilization" present condition was performed in one single step using the elastic model and then, the elastic-plastic model was introduced via the "Stress Redistribution" type of analysis proposed by Sigma/W.

The "After Stabilization" phase is simulated first for the present upstream river elevation at 17 m and then for the reservoir at FSL (Full Supply Level) elevation of 39 m.

Table 7-1 : Stress Distribution - Simulation Phases

Phase	Piezometric Conditions	Constitutive Model for Clay Layers	Type of Analyses[1]
Flat Ground Horizontal normally consolidated soil deposit as it was before erosion by the Churchill River			
1 - End of sedimentation	Water Table at Ground Surface	Elastic	in-situ
2 –Continental rise	Water Table at Elev. 45 m		
Upper Clay Model			
3 – River Erosion	Water Table at Elev. 45 m	Elastic	Load-deformation
4 – Before Stabilization	Water Table at Elev. 45 m	Elastic-Plastic	Stress Redistribution
5 – After Stabilization	Water Table at Elev. 45 m	Elastic-Plastic	Load-deformation
6 – Reservoir Impoundment at Elev. 39 m	Water Table at Elev. 45 m	Elastic-Plastic	Load-deformation
Lower Clay Model			
3 – River Erosion	From Seepage Analysis	Elastic	Load-deformation
4 – Before Stabilization	From Seepage Analysis	Elastic-Plastic	Stress Redistribution
5 – After Stabilization	From Seepage Analysis	Elastic-Plastic	Load-deformation
6 – Reservoir Impoundment at Elev. 39 m	From Seepage Analysis	Elastic-Plastic	Load-deformation

Note 1: Types of analyses proposed by Sigma/W:

- In-situ : analysis formulated specifically for establishing the initial stresses as a result of gravity
- Load-deformation : analysis used to apply loads and find the resulting stress changes
- Stress-redistribution : analysis used to re-distribute stresses when some part of the model is overstressed

7.2 MATERIAL PROPERTIES

The material properties used in the stress distribution analyses are presented in Table 7-2. These properties are similar to what has been used in previous studies and are based on the investigation data presented above, or otherwise on typical values for these kinds of materials. The shear modulus, G, was selected mainly based on the shear wave velocity, Vs, measured in seismo-piezocone tests performed on the North Spur. For the clay layers, the Poisson's ratio for the initial flat ground conditions was selected to produce a stress ratio, K_0 equal to $(1 - \sin \varphi')$ typical of normally-consolidated conditions. This is also used for the stress increase due to the lowering of the water table in Phase 2. For Phases 3 and following, the Poisson's ratio is reduced to 0.25, a value proposed by Locat et al (2014) for unloading.

Table 7-2 : Stress Distribution Analyses - Material Properties

Material	Total Unit Weight	Porosity	Cohesion	Internal Friction Angle	Poisson's Ratio	Young Modulus
	γ_{Total}	n	c'	ϕ'	ν	E
	(kN/m³)		(kPa)	(°)		kPa
Upper Sand	19	0.36	0	35	0.334	400,000
Sandy Silt/Silty Sand	19.5	0.41	0	35	0.334	600,000
Upper Clay	18.5	0.48	6	31	0.334 (0.25)[1]	300,000
Lower Clay	18.5	0.48	6	31	0.334 (0.25)[1]	500,000
Lower Aquifer	20	0.36	0	35	0.334	1,500,000

Note 1: in parenthesis, value of Poisson's ratio for unloading.

7.3 SHEAR STRENGTH OF THE CLAY

Undrained shear strength data from CPT and Vane tests performed at the North Spur have be compiled and are presented on the figures of Appendix B. As can be seen on Figure 7-1, based on CPT (Nkt of 15) and Vane data, the undrained shear strength (Cu) at a given elevation is generally similar throughout the North Spur. It should be noted that some lower strength were measured below the slide debris at the toe of the southern downstream slope (CPT-07-13 and CPT-23-13 on Figure 7-1). They are interpreted as an indication of local remolding due to unloading and plastification of the material below the toe in areas subjected to previous slides.

Based on correlations presented by Leroueil et al (1983), for normally consolidated conditions and for a plasticity index of 10, the shear strength would be expected to be about 0.22 σ'_v. The measured strength data of Figure 7-1 appear to be equal or somewhat lower than 0.20 σ'_v estimated with the lower clay seepage model.

The same information is presented on Figure 7-2 in terms of the preconsolidation pressure, σ'_p, based on CPT (σ'_p is estimated using $N\sigma$ of 15) and Vane data (σ'_p is estimated as Cu/0.20). The σ'_p profiles are compared with the effective vertical stress (σ'_v) profiles indicating generally normally consolidated conditions (OCR near 1.0) under the crest of the Spur and an OCR of about 3 – 5 at the toe of the slope. OCR is defined as the ratio between σ'_p and σ'_v.

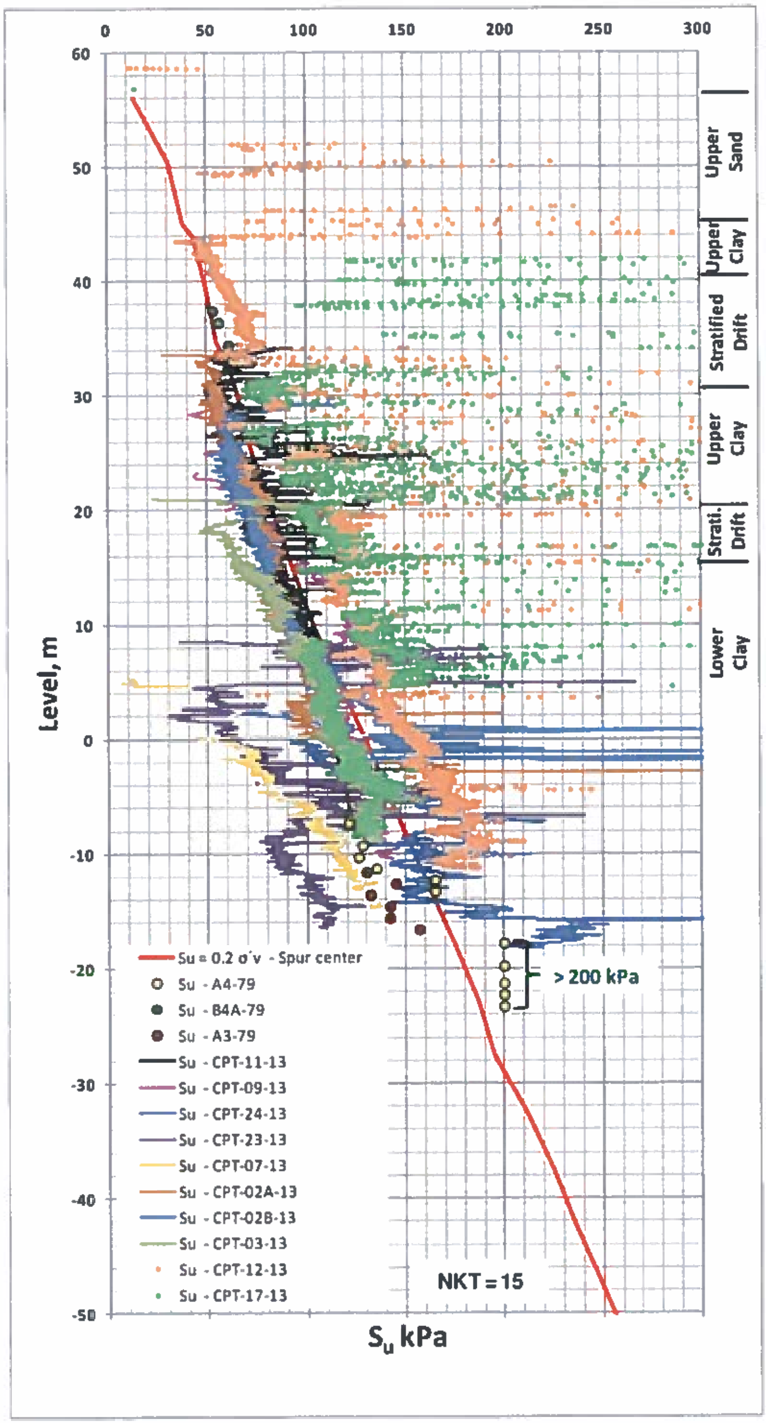

Figure 7-1 : Shear Strength of Clay

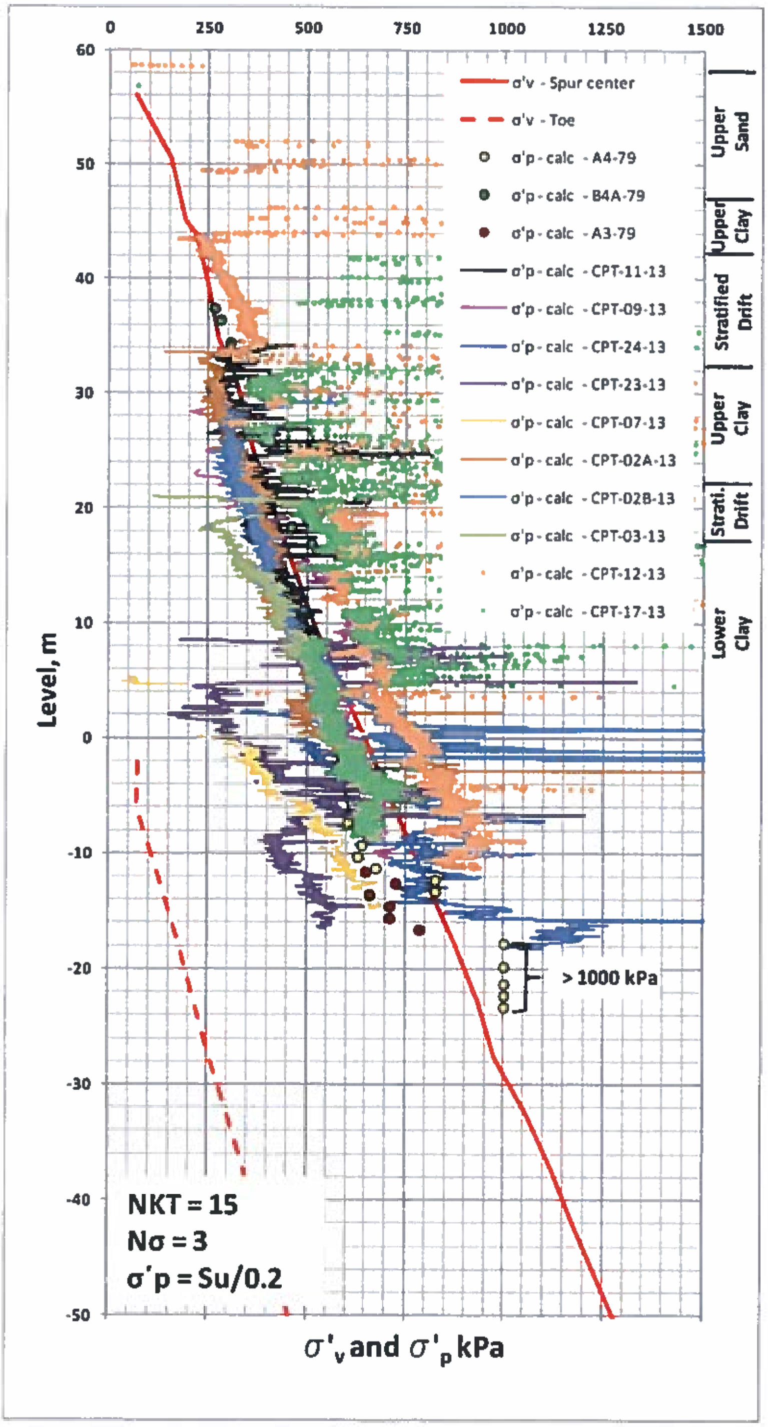

Figure 7-2 : Effective Vertical Stresses

7.4 VERTICAL AND HORIZONTAL PROFILES FOR PRESENTATION OF RESULTS

All sections have been analysed using the methodology described above. In accordance with the method proposed by Locat (2007) and Leroueil (2015), the results are presented below in terms of shear stress on a horizontal plane (τ_{xy}). They will be shown as isocontours on a section view. Various horizontal planes will be studied in more detail as illustrated on Figure 7-3 at elevation 40 m and 20 m for the Upper Clay model and at elevations 5 m, -10 m, -18 m and -28 m for the Lower Clay model. Only graphs related to elevation 20 m and -10 m will be presented in the following sections but all graphs can be found on the figures of Appendix C.

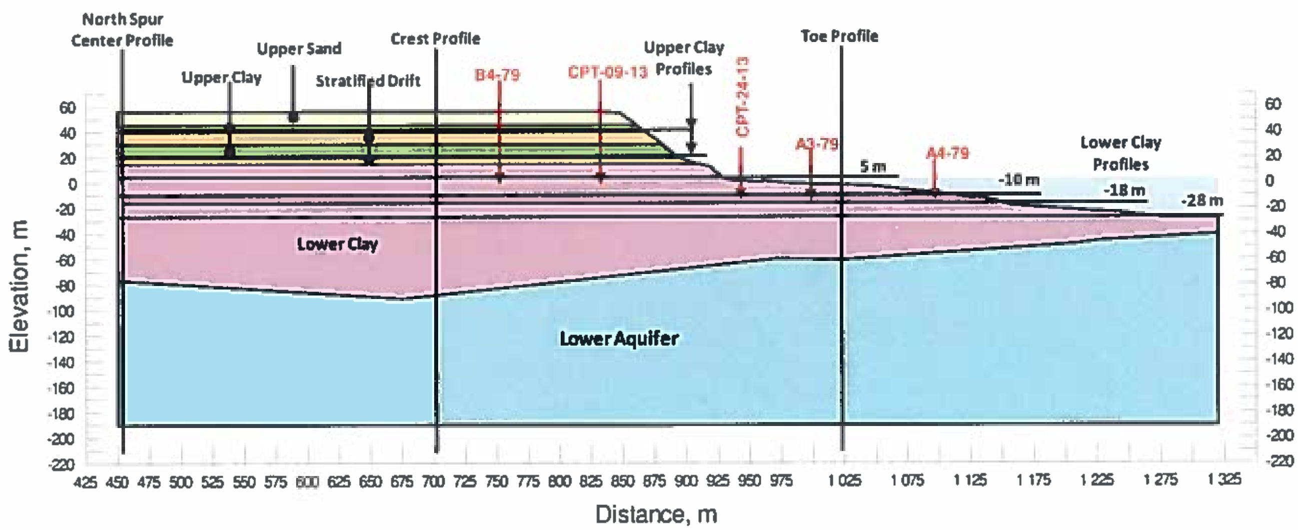

Figure 7-3 : Section B-B - Vertical Stress Profiles and Horizontal Plans

7.5 REFERENCE SECTION B-B

As noted above, two seepage models were considered, one for the Upper Clay layers and one for the Lower Clay unit. They will be presented below.

The results for the present conditions at reference Section B-B (the steep section located on the downstream side of the northern part of the Spur) are presented on the top part of

Figure 7-4 as isocontours of shear stress on horizontal surfaces for the Lower Clay seepage conditions.

The same analyses were performed for the Upper Clay seepage conditions (for a hydrostatic water table at elevation 45 m) and, in both cases, for the projected conditions after the implementation of the proposed stabilization measures. Typical results are presented on Figure 7-4 at elevation 20 m in the Upper Clay and at elevation -10 in the Lower Clay. (Please note that due to the sign convention in Sigma/W, τ_{xy} is negative below the downstream slope (as shown on isocontours) but that absolute values are shown for the horizontal plane profiles.)

For example, on the horizontal plane at elevation -10 m, it can be observed that the maximum shear stress along that plane is about 190 kPa and is observed below the lower part of the slope. It can be observed that this 190 kPa stress is greater than the 140 kPa undrained shear strength estimated based on the CPT and Vane tests. Similarly, the maximum shear stress of about 165 kPa predicted by the model along the 20m Upper Clay plane is greater than 80 kPa CPT/Vane undrained shear strength.

The undrained shear strength measured in vane tests or in CPT tests calibrated with vane tests is thus lower than the predicted mobilized shear strength for the present conditions. This indicates that this type of stress distribution analysis underestimates the stability of Section B-B for the present stable conditions.

For the conditions after stabilization, the analyses generally indicate a significant reduction of the predicted maximum value of the shear stress on horizontal plane (τ_{xy}) as illustrated on Figure 7-4 with a reduction of 45% on the 20 m Upper Clay line and of 25% on the -10 m Lower Clay line. Between chainage 800 m and 850 m, the shear stress may appear to increase but Figure 7-5 illustrates that this is a reduction in function of the distance from crest (chainage 850 m before stabilization and chainage 800 m after stabilization).

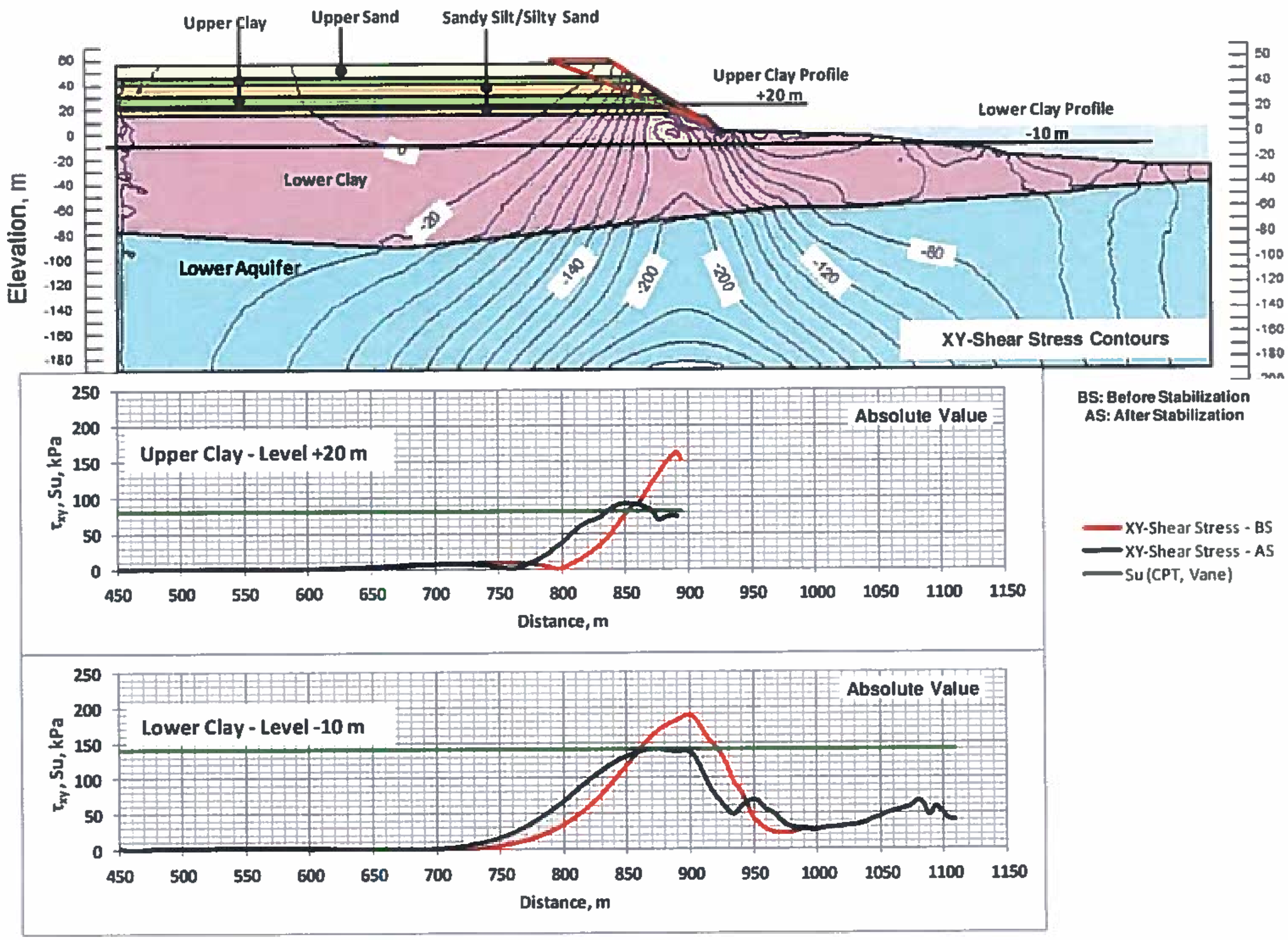

Figure 7-4 : Section B-B - Shear Stresses and Shear Strength on Lines +20m and -10m

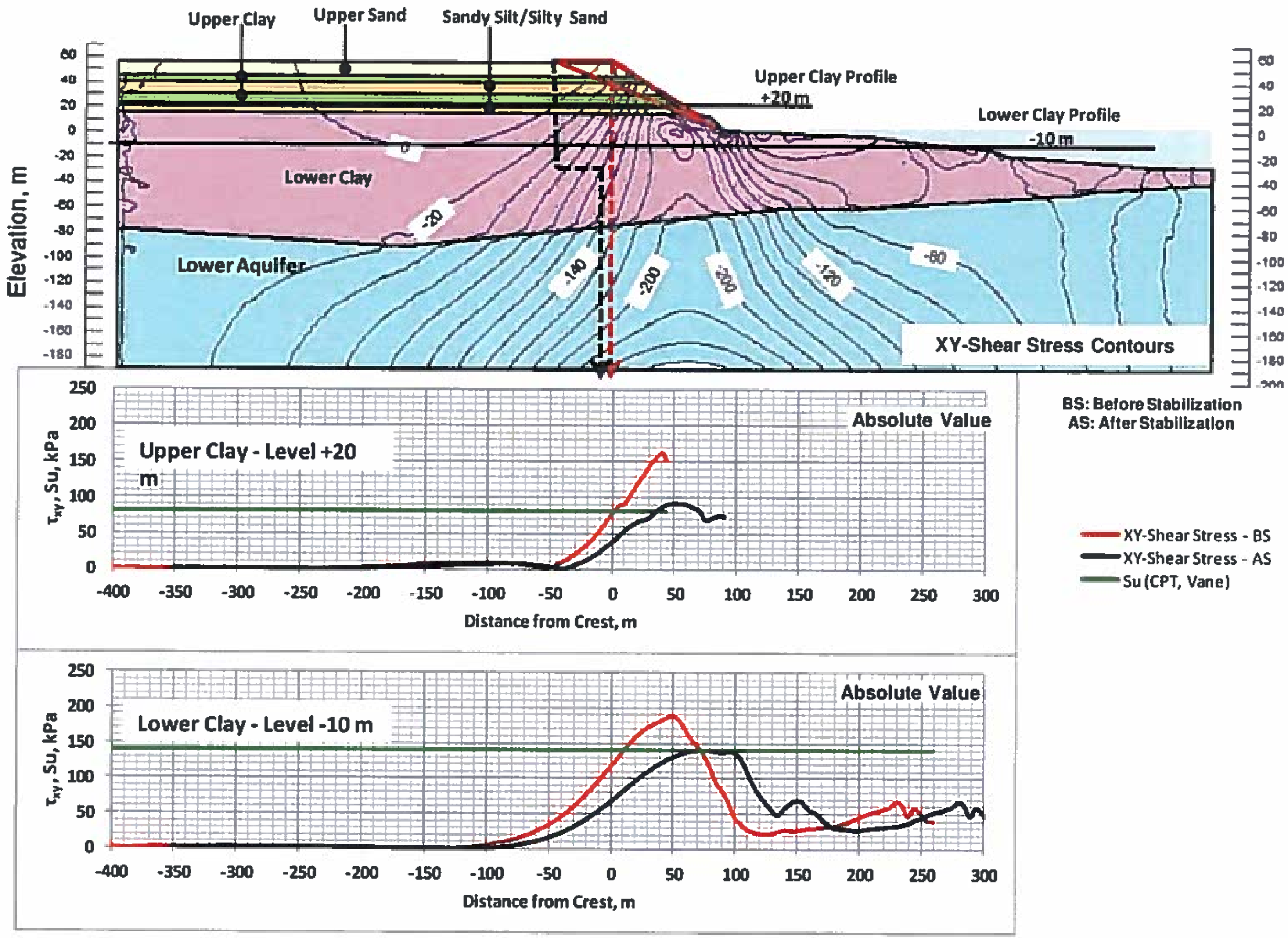

Figure 7-5 : Section B-B - Shear Stresses and Shear Strength on Lines +20m and -10m Relative to Crest

7.5.1 Validation Analyses and Plots

Although the model is fully convergent, the isocontours on Figure 7-4 present some signs of perturbation near the ground surface in the toe area. These are due to boundary effects of the numerical model. Verification analyses were performed and have shown that these boundary perturbations have no significant effect on the general profile of shear stress on a horizontal plane (τ_{xy}) and no effect on the predicted maximum value of τ_{xy}.

7.5.2 Effective Stresses Representation

The results of Figure 7-4 are also presented on Figures 7-6 and 7-7 in terms of effective stresses using the Mohr circle representation; the following three points were selected along the horizontal plane at Elevation -10 m: points A (Uphill), B (Slope) and C (Toe).

Figure 7-6 is showing the effective stresses (principal, horizontal and vertical) at point B for the initial "Flat Ground" conditions, the present "Before Stabilization" conditions and the projected "After Stabilization" conditions. The principal stresses (σ'_1 and σ'_3) are defined as the intercepts of the Mohr Circle with the t = 0 axis. On each circle, a circle indicates the point (σ'_h , τ_{xy}) and a triangle the point (σ'_v , τ_{xy}). Note that the Mohr circles for points on horizontal line -18 m were also prepared and are shown on Figures C-28 to C-35 of Appendix C.

Figure 7-7 is presenting the same information for the projected "After Stabilization" conditions, comparing the stresses at points A (Uphill), B (Slope) and C (Toe).

This information indicates that the strength of the clay layers of the North Spur is generally not fully mobilized and especially at point B corresponding to the point of maximum value of the shear stress on the horizontal plane at elevation -10 m (τ_{xy}) (see Figure 7-4).

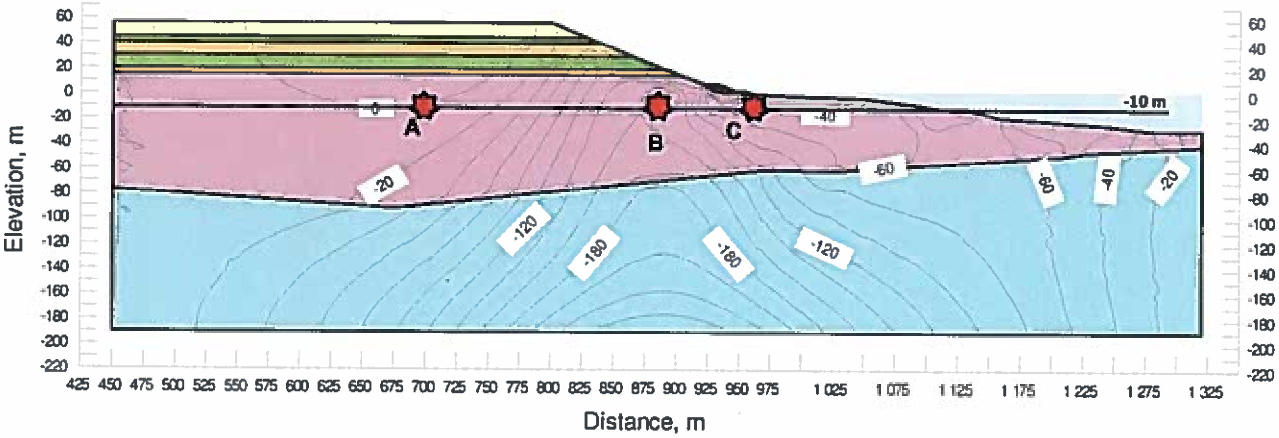

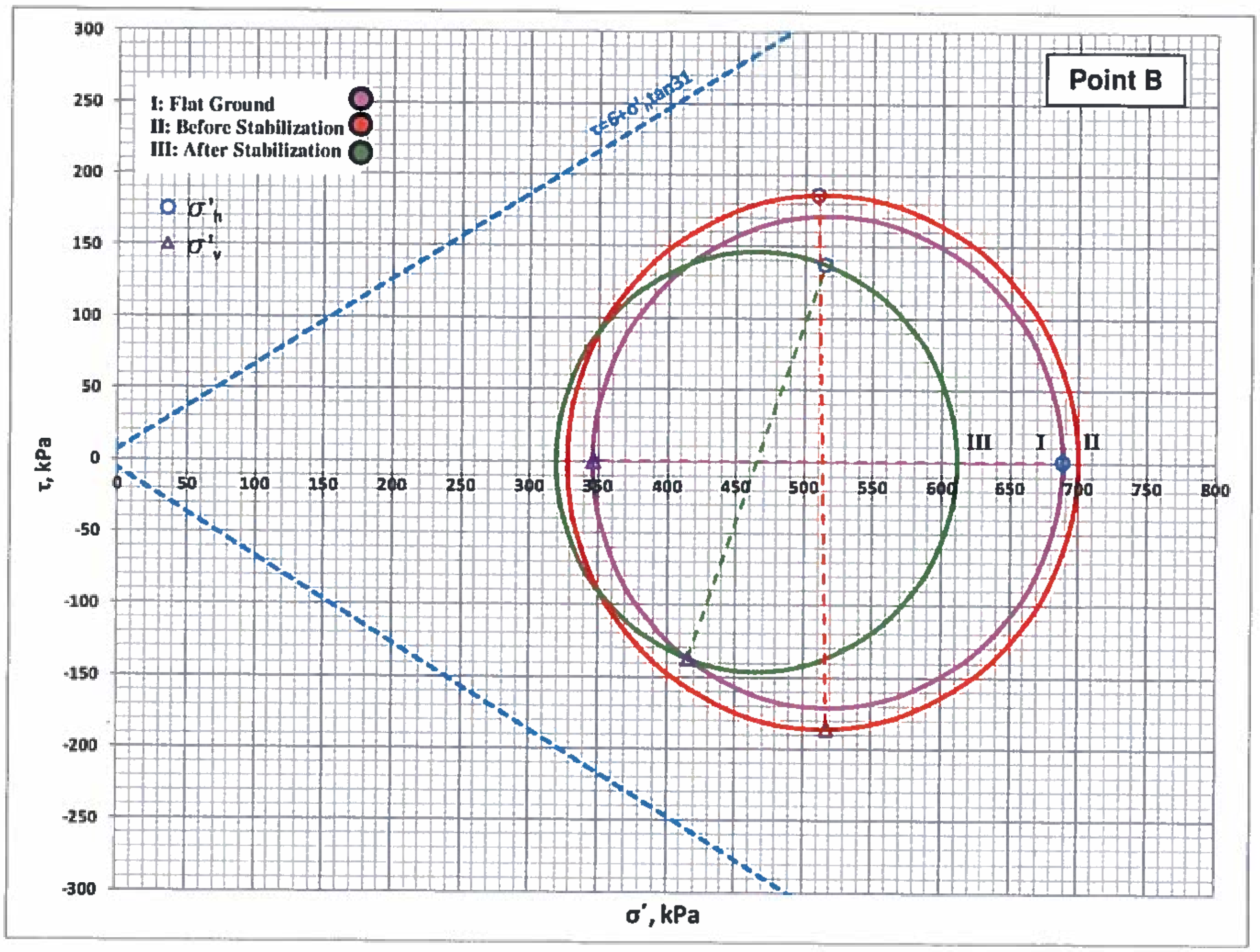

Figure 7-6 : Section B-B – Effective Stresses for Point B on Line -10m

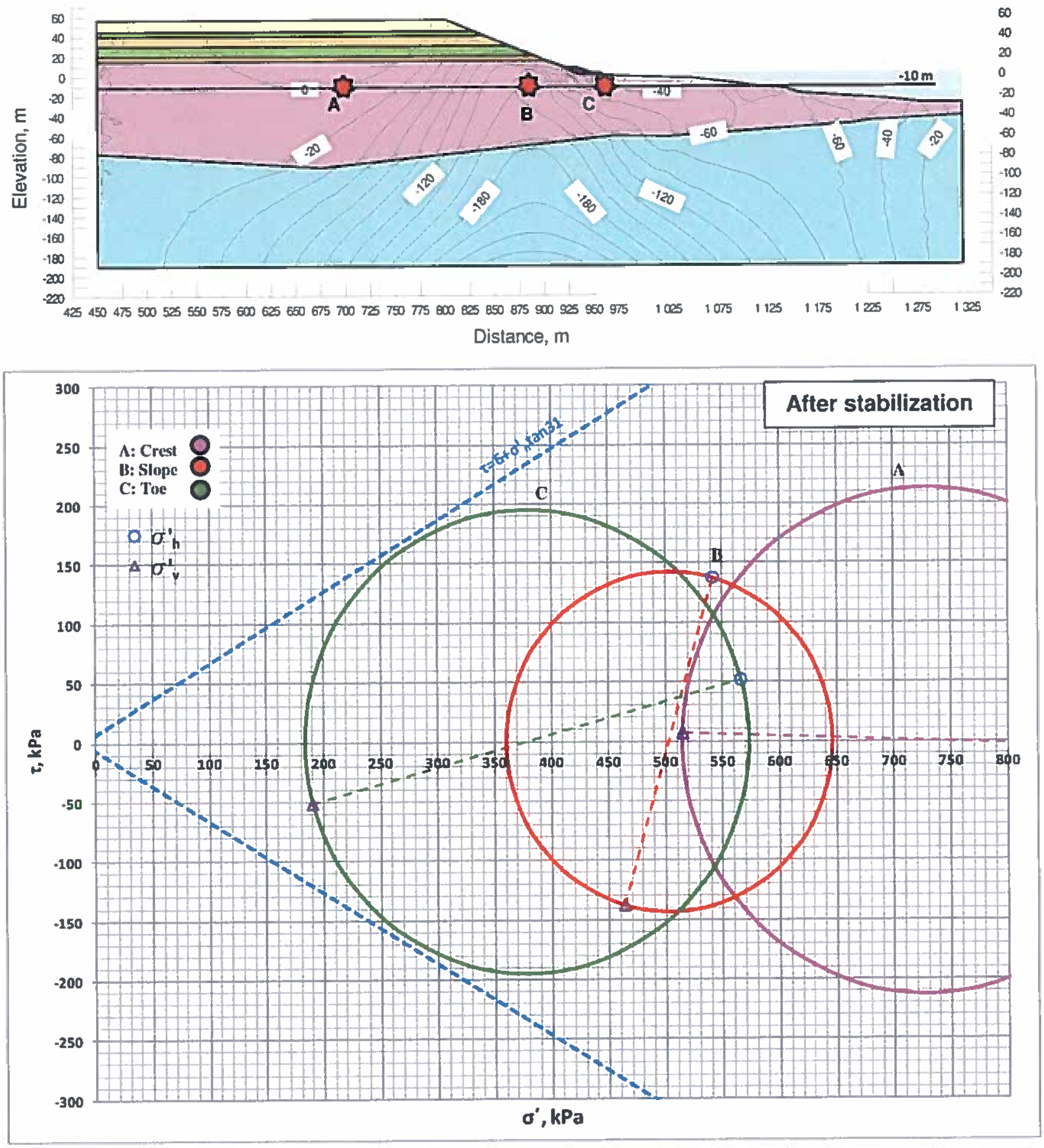

Figure 7-7 : Section B-B – Effective Stresses for Points A, B and C on Line -10m – After Stabilization

7.6 Effect of a Surcharge

The preceding analyses have considered the potential for the development of spreads, or upward progressive failure, initiated by a disturbance such as erosion at the toe Section B-B. As described above, progressive failure may also develop downward as a result of loading or piling on the slope or beyond the crest of the slope that would locally exceed the undrained shear strength.

Additional stress distribution analyses were performed on reference section B-B to evaluate the effect of a loading at or beyond the crest. For this purpose, a 5 m high and 100 m wide fill with a unit weight of 20 kN/m^3 has been considered at various distances from the crest of the slope of Section BB. The results for horizontal planes at elevation 20 m in the Upper Clay and at elevation -10 in the Lower Clay are summarized on Figure 7-8. They indicate that beyond a distance of about 100 m, the presence of the fill has a negligible effect on the maximum undrained shear stress below the crest on such horizontal planes.

The effect of a surcharge was also analysed by effective stress LEM stability analyses as illustrated on Figure 7-9: they indicate that the surcharge has no effect on the minimum factor of safety which is controlled by the inclination of the slope.

During construction, the contractor will not be allowed to stockpile materials within 100 m of the crest and all excavated materials from the slope stabilization work will be hauled to designated disposal site well away from the crest. Following construction, the North Spur will be treated as a dam, and be subject to normal dam safety protocol which does not allow construction, excavation, surcharging or other such activities on the crest, slopes or toe of the North Spur without careful review and approval..

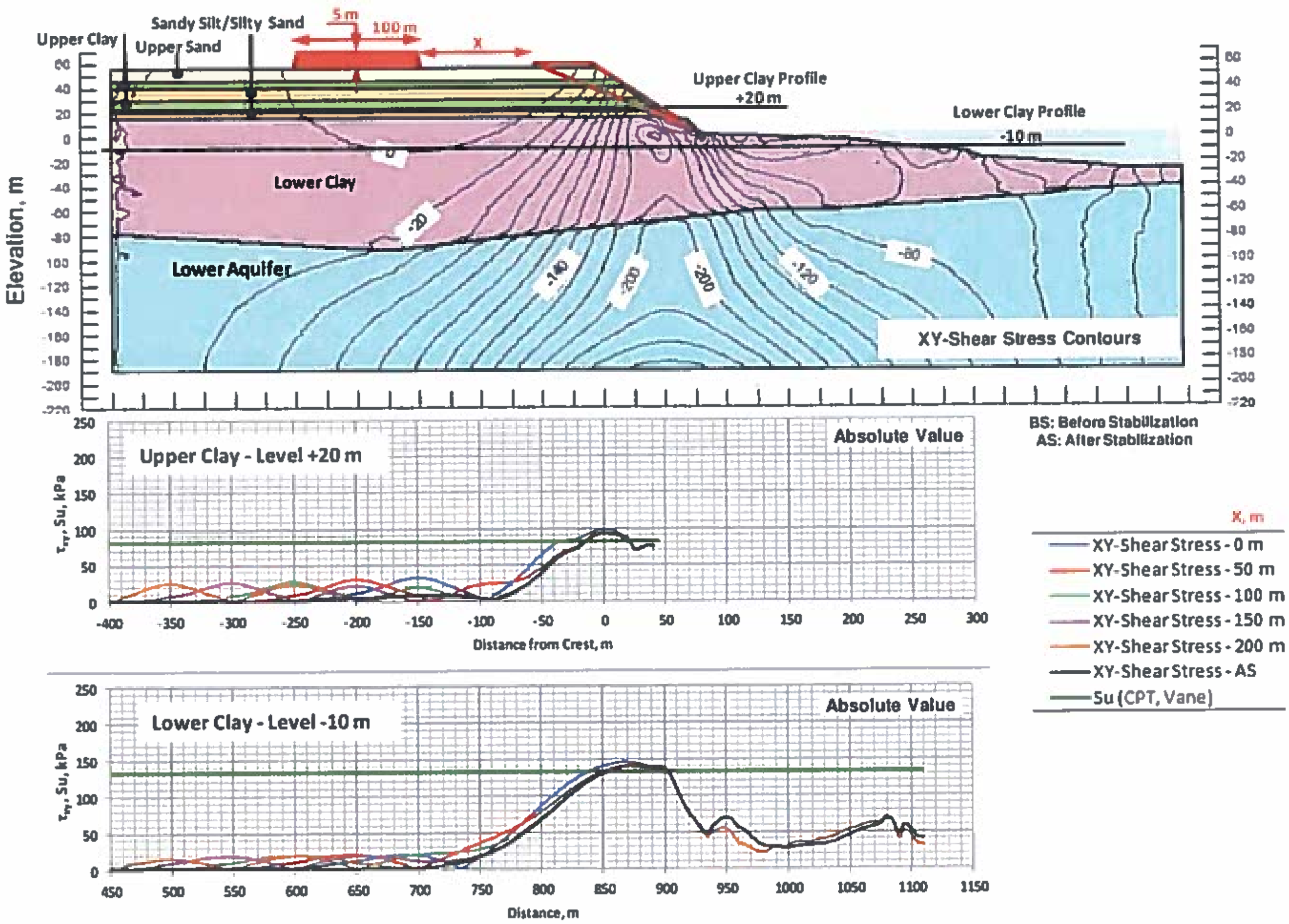

Figure 7-8 : Section B-B - Effect of a Surcharge – Stress Distribution Analyses

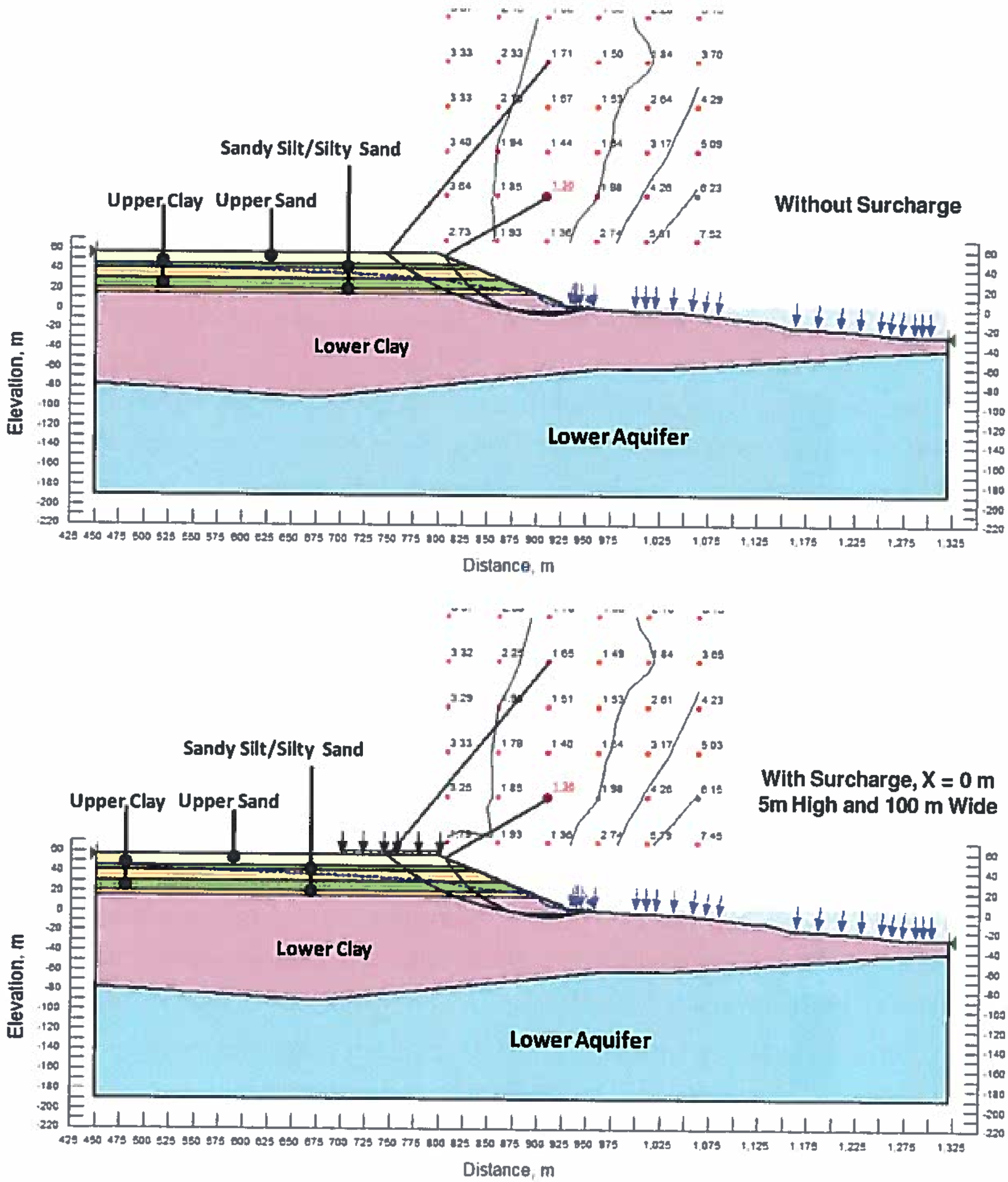

Figure 7-9 : Section B-B - Effect of a Surcharge – Slope Stability Analyses

7.7 Narrow Section D-D

The narrow sections illustrated on Figure 5-4 were analysed using the same methodology and the results are illustrated on the figures of Appendix C. Section D-D was selected as representative of the narrow part of the Spur with the steepest stabilized slope (see localisation on Figure 5-4). The results of analyses for Section D-D are presented on Figure 7-10. Three conditions were analysed: before stabilization, after stabilization and after reservoir impoundment at elevation 39 m. The model predicts that the stabilization works will produce no significant reduction of the shear stresses on the upstream side of the Spur but a 25% reduction on horizontal plane -10 m in the Lower Clay on the downstream side. This reduction is relative to the conditions before stabilization for which the maximum horizontal shear stresses are already more than 20% below the undrained shear strength measured in CPT and Vane tests.

For the conditions after reservoir impoundment, a source of concern could be the effect of the reservoir horizontal water pressure on the lateral stability of the Spur. As shown on Figure 7-11, the model predicts a reduction of the shear stress on the upstream side and no effect in the center and the downstream side of the Spur. And indeed, the lateral unit force due to the reservoir water pressure above elevation 20 m is estimated to be 1 700 kN/m for the maximum reservoir elevation at 39 m. This force is significantly lower than the integrated resistance of the clay required to support the upstream slope before the reservoir impoundment; this resistance is predicted by the model to be about 7 500 kN/m in the Upper Clay at elevation 20 m (See Figure 7-7).

On Figure 7-12, the shear stresses mobilized on Section D-D after stabilization are compared with the shear stresses presently mobilized on Section B-B. It can be seen that the values of maximum shear stress on a horizontal plane (τ_{xy}) predicted by the model for the conditions on section D-D after the implementation of the proposed stabilization measures are about 50% of the values predicted on Section B-B for the present conditions.

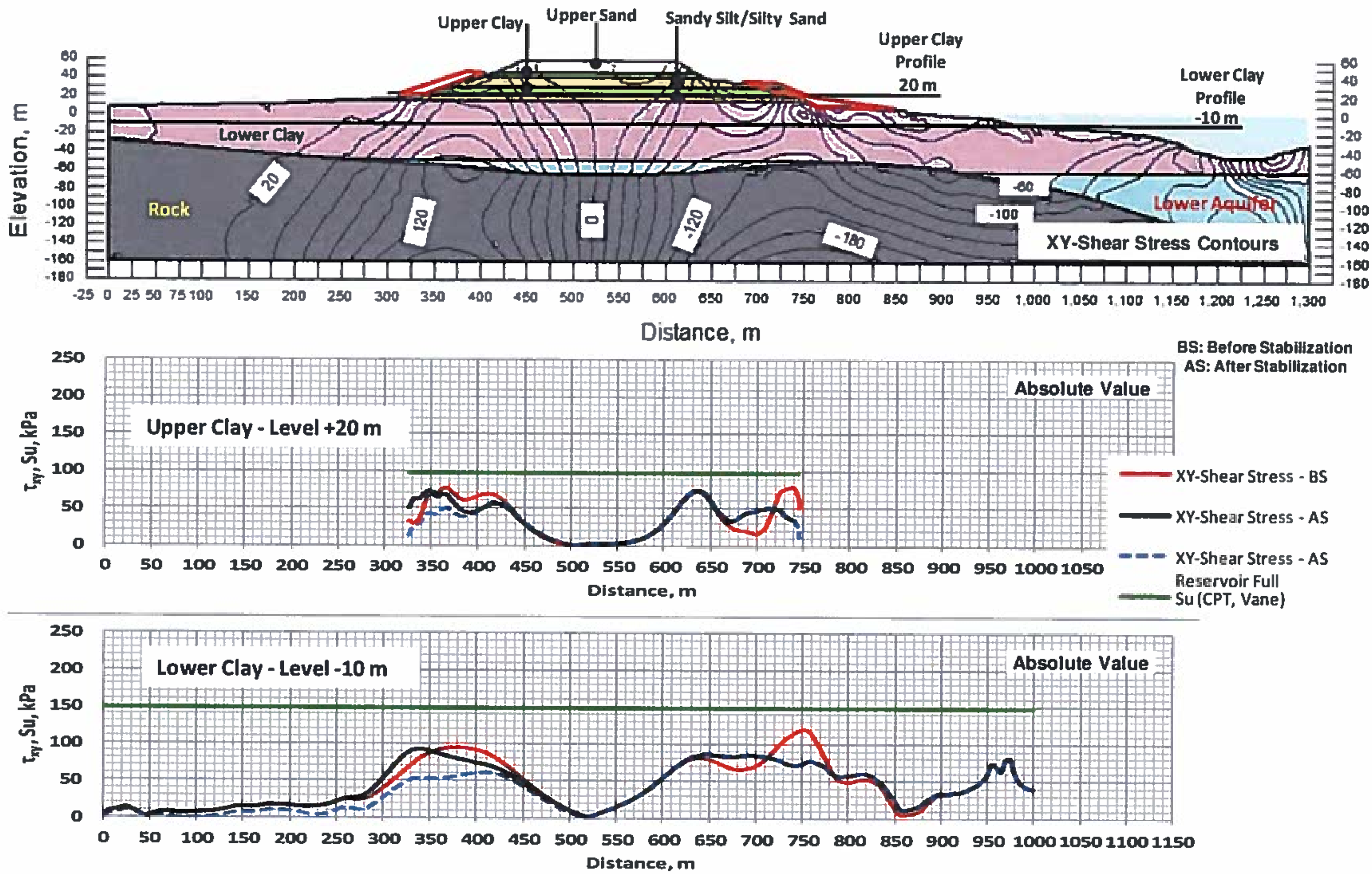

Figure 7-10 : Section D-D - Shear Stresses and Shear Strength on Lines +20m and -10m

SNC·LAVALIN	NORTH SPUR STABILIZATION WORKS – Progressive Failure Study	Revision		Page
	Nalcor Doc. No. MFA-SN-CD-2800-GT-RP-0001	B2	Date	
	SLI Doc. No. 505573-3281-4GER-0001	01	21-Dec-2015	62

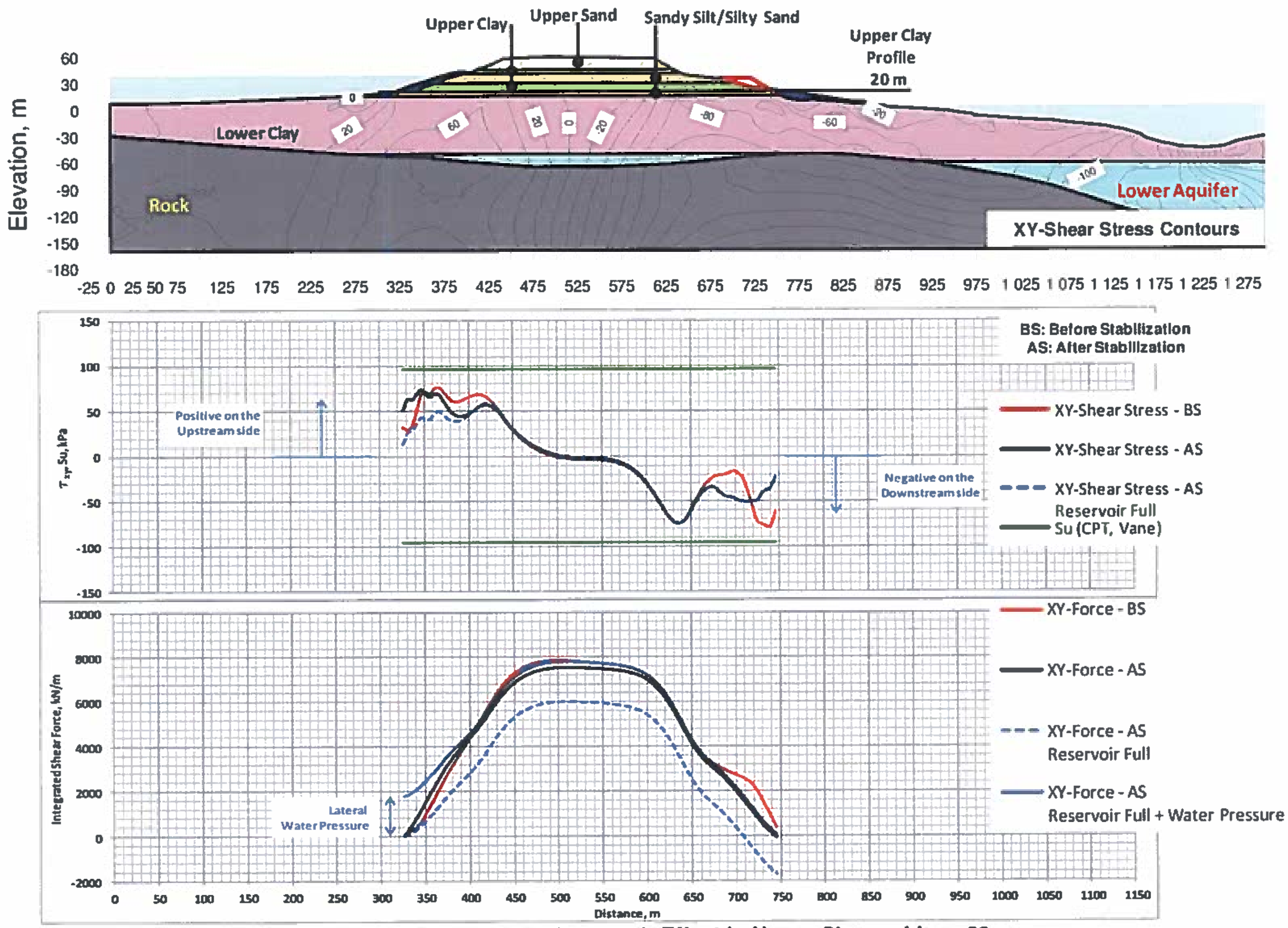

Figure 7-11 : Section D-D - Reservoir Effect in Upper Clay on Line +20 m

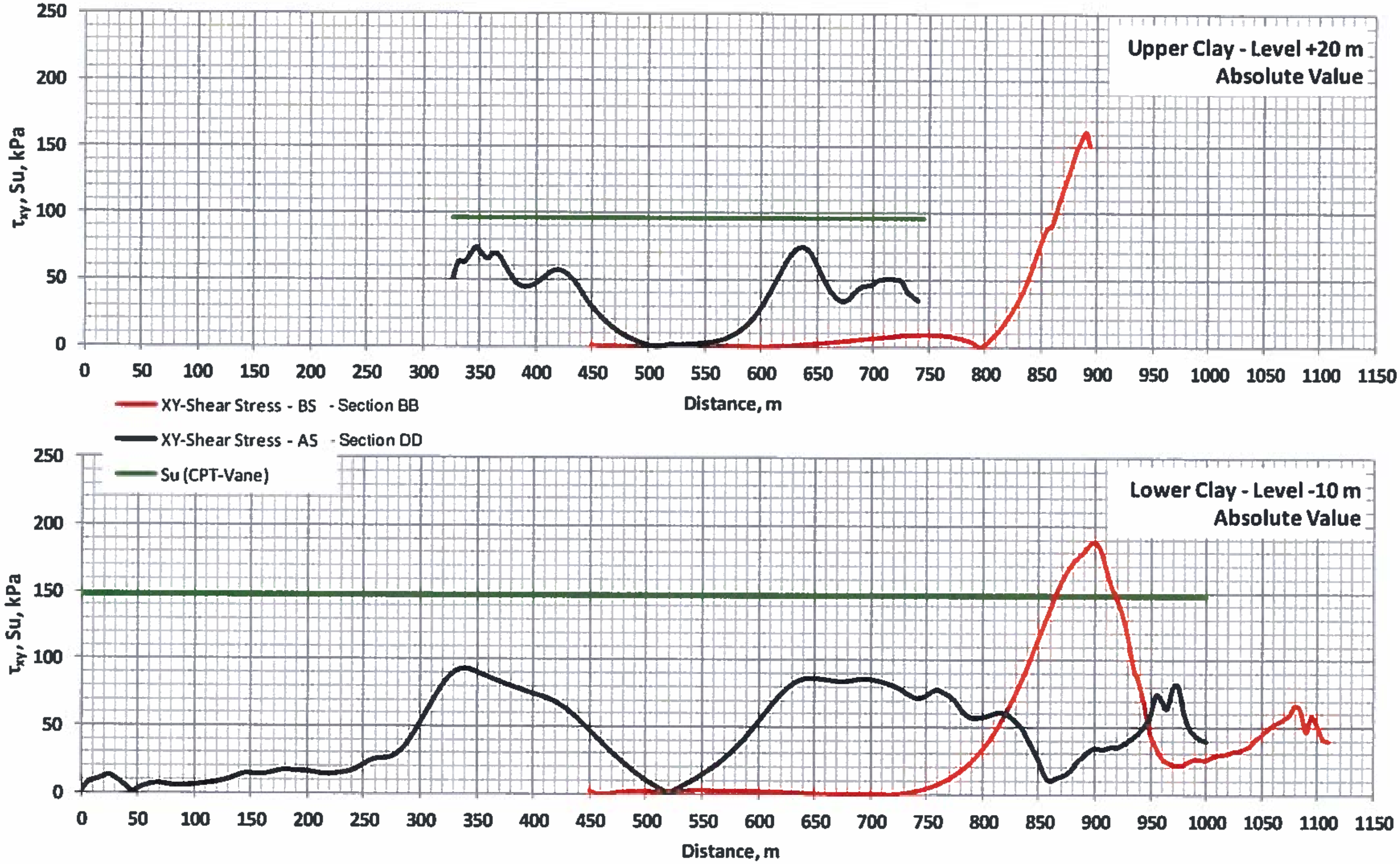

Figure 7-12 : Sections B-B and D-D - Shear Stress Comparison - Lines +20 m and -10 m

7.8 Section A-A for Submarine Downstream Depression

Section A-A, a modified version of Section D-D was prepared to study the stability of the downstream submarine depression located near the rock knoll. The topography of this section is as indicated in plan on Figures 5-1 (present conditions) and 5-4 (stabilized conditions) and in section of Figure 7-13. The boundary between the Lower Clay layer and the Lower Aquifer is assumed to be at Elevation -52 m and the shear stresses were examined on a horizontal plane at Elevation -50 m.

Section A-A was analysed using the same methodology as for sections B-B and D-D. The results are presented on the figures of Appendix C and summarised on Figure 7-13. It can be seen that the model predicts that the stabilization works will produce no significant reduction of the shear stresses in the Lower Clay on horizontal plane -50 m. However, the maximum horizontal shear stresses on this horizontal plane are about 30% lower than the undrained shear strength estimated by extrapolation of the measured strength profile (CPT and Vane tests) of Figure 7-1.

The effect of the Spur on the stresses near the downstream submarine depression was further examined by conducting a sensitivity analysis where the material forming the Spur was removed all together. As indicated on Figure 7-13, the horizontal shear stresses on Elevation -50 m horizontal plane show no change near the submarine depression.

Finally, Figure 7-13 also confirms that the reservoir impoundment at Elevation 39 m has no effect on the shear stresses on the downstream side of the Spur.

The stability of the downstream submarine depression can thus be examined independently of the North Spur and there is no potential for a retrogressive failure for the conditions at the North Spur following completion of the stabilization works.

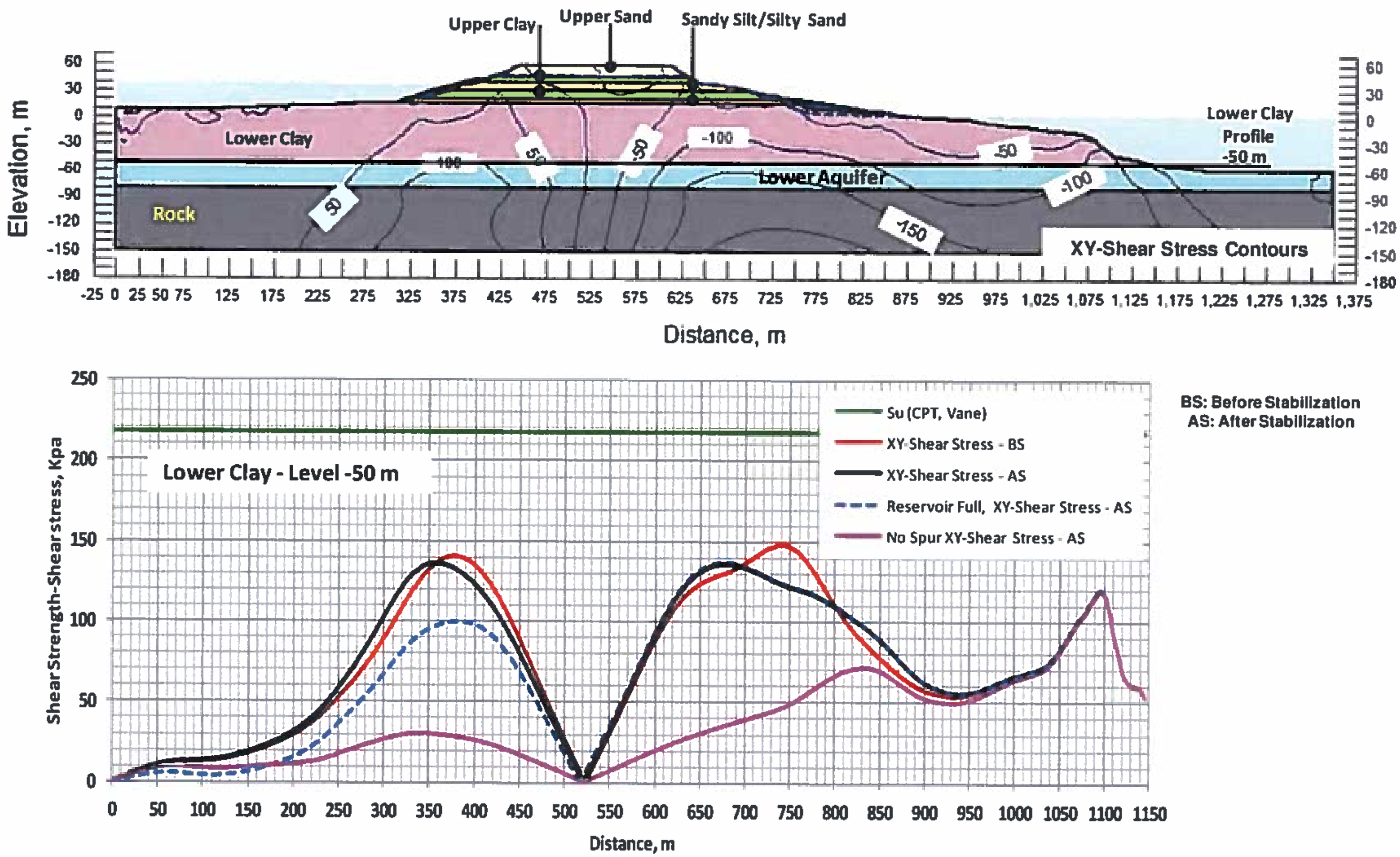

Figure 7-13 : Section A-A – Downstream Submarine Depression - Shear Stresses and Shear Strength on Line -50m

8 DISCUSSION AND CONCLUSION

The North Spur is a natural dam consisting in a succession of soil layers which include layers of sensitive clay (two main layers of Upper Clay in the stratified drift) and a Lower Clay, characterised respectively by an average Liquidity Index (LI) of 1.4 and 0.6.

Based on observations made along the Churchill River and experience in Eastern Canada in general (Demers et al., 2013), there may be three types of landslides in sensitive clays: simple rotational slides, retrogressive slides or flowslides, and spreads (progressive failure). Generally, if stability factor is improved, then the probability of having a failure can be significantly decreased compared to what it was before.

For the North Spur, the stabilization works for all the slopes have been designed so that the calculated factor of safety is at least 1.5. In addition, the stabilization measures ensure that there will be no erosion at the toe of the slopes and therefore avoid any first-time failure or simple rotational slide required to initiate a retrogressive slide and any other type of slide in the first place.

The objective of the present report was to demonstrate that the stabilization works adequately address the stability of the North Spur with regards to potential for occurrence of progressive failure landslides.

8.1 PROGRESSIVE FAILURE

Several 2-D finite-element analyses have been performed on the basis of geometry and soil parameters defined in previous investigations and studies. The aim of these analyses was to evaluate the shear stresses mobilized over horizontal surfaces and the possibility that local failure could trigger progressive failure. The results have been shown in Sections 7.5 to 7.7. The main conclusions will be summarized here below.

8.1.1 Reference Case – Section B-B

The first analysis has been performed for the existing conditions at section (BB) where the slope around the North Spur is the most abrupt but still stable, thus at a factor of safety at least equal to 1.0. This was to define the maximum shear stress mobilized along horizontal shear surfaces on the site. The analysis of the section after stabilization works shows a reduction of this shear stress by 40 – 45% in the Upper Clay and by 20 – 30% in the Lower Clay, thus a significant improvement against the possibility of progressive failure.

8.1.2 Effect of a Surcharge

The influence of a fill that would be put on the northern part of the Spur has been studied. For this purpose a 5 m high and 100 m wide fill were considered at different distances from the crest of the slope of Section BB. The analyses show that such a fill does not influence the shear stresses below the crest when the distance of the fill to the crest greater than 100 m. It is thus recommended crest not be surcharged with fill at distances from the crest less than 100 m.

During construction of the stabilization works, the contractor will not be allowed to stockpile materials within 100 m of the crest and all excavated materials from the slope stabilization work will be hauled to designated disposal site well away from the crest. Following construction, the North Spur will be treated as a dam, and be subject to normal dam safety protocol which does not allow construction, excavation, surcharging or other such activities on the crest, slopes or toe of the North Spur without careful review and approval. Narrow Sector – Section D-D

Analyses have also been performed for southern section (DD). The shear stresses on horizontal surfaces are reduced due to stabilization works to less than 50% of the maximum shear stress mobilized in Section BB, and thus very far from conditions that could trigger progressive failure.

It is worth noting that reservoir impoundment at FSL decreases the shear stresses on the upstream side of the North Spur but does not influence the stress level on the downstream side. It thus cannot be a trigger for downhill progressive failure.

All these analyses show that the stabilized North Spur, before or after impoundment will not be subjected to progressive failure. As indicated above, following construction, the North Spur will be treated as a dam, and be subject to normal dam safety protocol which does not allow construction, excavation, surcharging or other such activities on the crest, slopes or toe of the North Spur without careful review and approval.

The "Downstream Depression"

With its bottom at an approximate elevation of -52 m, the downstream depression is entirely in the Lower Clay layer, mainly below elevation – 12 m. Limit equilibrium analyses have been performed in terms of effective stresses and the calculated factor of safety is equal to 1.5, and this is for shallow slides, indicating that deeper surfaces would correspond to higher SF values. So, there would not be first-time failure there.

If it is assumed that a first-time failure may occur, because the liquidity index in the Lower Clay layer is typically equal to 0.6, no flowslide or retrogression landslide may develop. The landslide would thus be limited to a single rotational slide of limited depth.

Numerical analyses have also been performed and have shown that: (a) the North Spur has no influence on the shear stresses below the slope of the downstream depression; and (b) at the base of the depression, the mobilized shear stress is only about 60 % of the minimum estimated undrained shear strength and, consequently, undrained progressive failure that would require that the shear stress reaches the strength will never be initiated.

8.2 CONCLUSION

The objective of the present report was to evaluate the impacts of the projected stabilization works to insure the stability of the Spur regarding the occurrence of a progressive failure landslide.

The possibility of occurrence of uphill or downhill progressive landslide has been studied and the results show that with the mitigation measures taken, the stability of the North Spur regarding such events is adequate and that a progressive failure landslide will not occur. It is important that once construction of the stabilization measure are complete, that the North Spur area be treated as a dam, and subject to regular inspections and restrictions to activities on the crest, slope and toe that may impact the measure put in place to stabilize this structure.

9 REFERENCES

AMEC Earth & Environmental Ltd. (AMEC, 2008). Bank Stability Study for the Proposed Lower Churchill Hydroelectric Generation Project: Environmental Baseline Report. Prepared for Newfoundland and Labrador Hydro, St. John's, NL.

Bouchard, R., Dion, D.J. and Tavenas, F. (1983) Origine de la consolidation des argiles du Saguenay, Québec. Canadian Geotechnical Journal, 20 (2):315-328.

Demers, D., Robitaille, D., Locat, P. and Potvin, J. (2013) Inventory of large landslides in 749 sensitive clays in the province of Québec, Canada: preliminary analysis. In L'Heureux, 750 J.S. et al. (eds.) Landslides in sensitive clays: From geosciences to risk management, 751 Advances in Natural and Technological Hazards Research 36. Springer. pp. 77-89.Tavenas, 1984.

Hatch (2015) Three Dimensional (3D) Hydrogeological Study for the North Spur - Final Report H346252-0000-00-124-0001, Rev. A, June, 2015

Leroueil, S., Tavenas, F., and Le Bihan, J.-P. (1983): Propriétés caractéristiques des argiles de l'est du Canada, Canadian Geotechnical Journal, vol. 20, n° 4, p. 681-705.

Leroueil S, Vaunat J, Picarelli L, Locat J, Faure R, Lee H (1996) A geotechnical characterisation of slope movements. In: Senneset K (ed) Proceedings of the 7th international symposium on landslides, Trondheim, 1. Balkema, Rotterdam, pp 53–74

Lebuis J, Robert JM, Rissmann P (1983) Regional mapping of landslide hazard in Quebec. In: Proceedings of the symposium on slopes on soft clays. Swedish Geotechnical Institute report no. 17, Linköping, Sweden, pp 205–262

Lefebvre, G. 1981. Fourth Canadian Geotechnical Colloquium: strength and slope stability in Canadian soft clay deposits. Canadian Geotechnical Journal, 18(3): 420-442.

Locat, A., Leroueil, S., Bernander, S., Demers, D., Jostad, H.P., and Ouehb, L. (2011) Progressive failures in eastern Canadian and Scandinavian sensitive clays. Canadian Geotechnical Journal, 48(11) pp. 1696–1712.

Locat, A., Jostad H.P. and Leroueil, S. (2013) Numerical modeling of progressive failure and its implication to spreads in sensitive clays. Canadian Geotechnical Journal, 50(9) pp. 961-978.

Locat A., Leroueil S., Fortin A., Demers D. and Jostad H.P. (2015) The 1994 landslide at Sainte-Monique, Quebec: Geotechnical Investigation and Application of Progressive Failure Analysis. (in preparation)

SNC-Lavalin Newfoundland Ltd (SNC-Lavalin NL, 1980) Engineering Report and 1979 Field Investigation Program. Volumes I to IV, March 1980.

SNC-Lavalin and AGRA Monenco (SLI-AGRA, 1998) Muskrat Falls Hydroelectric Development Final Feasibility Study Report – Volume I – Engineering Report.

SNC-Lavalin (SLI, 2015a) *Lower Churchill Project - Engineering Report - North Spur Stabilization*. Draft Report no 505573-3281-4GER-0001-PA, April 2015.

SNC-Lavalin (SLI, 2015b) Technical Specifications and drawings.

Tavenas F, Leroueil S (1981) Creep and failure in slopes in clays. Can Geotech J 18(1):106–120

Tavenas F (1984) Landslides in Canadian sensitive clays – a state of the art. In: Proceedings of the 4th international symposium on landslides. Canadian Geotechnical Society, vol 1, pp 141–153.

APPENDICES

NOTE:

APPENDICES HAVE NOT CHANGED FROM REVISION A1 (16 JUNE 2015).

- **APPENDIX A - REFERENCE DRAWINGS**
- **APPENDIX B – GEOTECHNICAL INVESTIGATION SHEAR STRENGTH DATA**
- **APPENIX C – SEEPAGE AND STRESS DISTRIBUTION ANALYSES – FIGURES.**

Figure A-1

Figure A-2

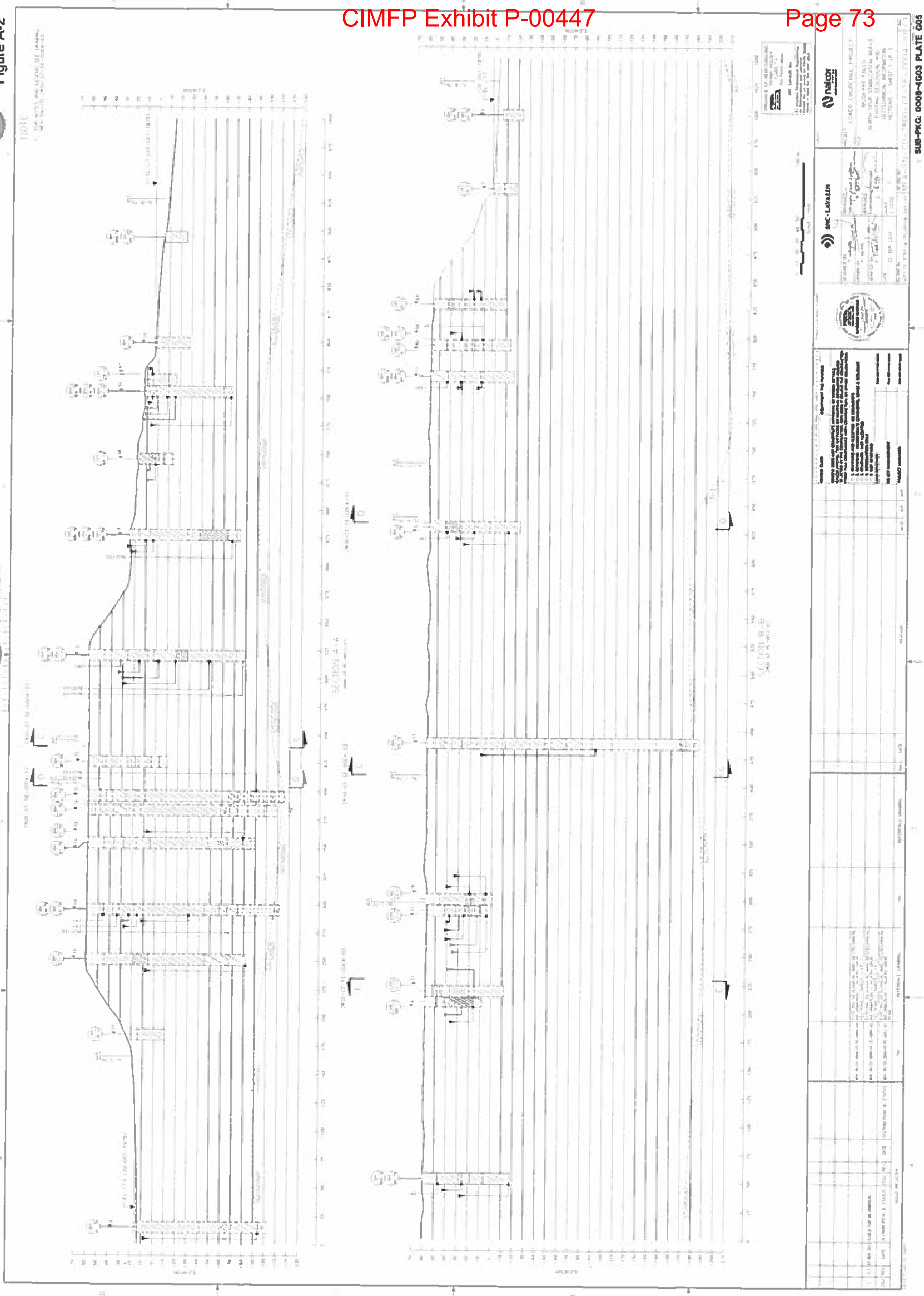

Figure A-3

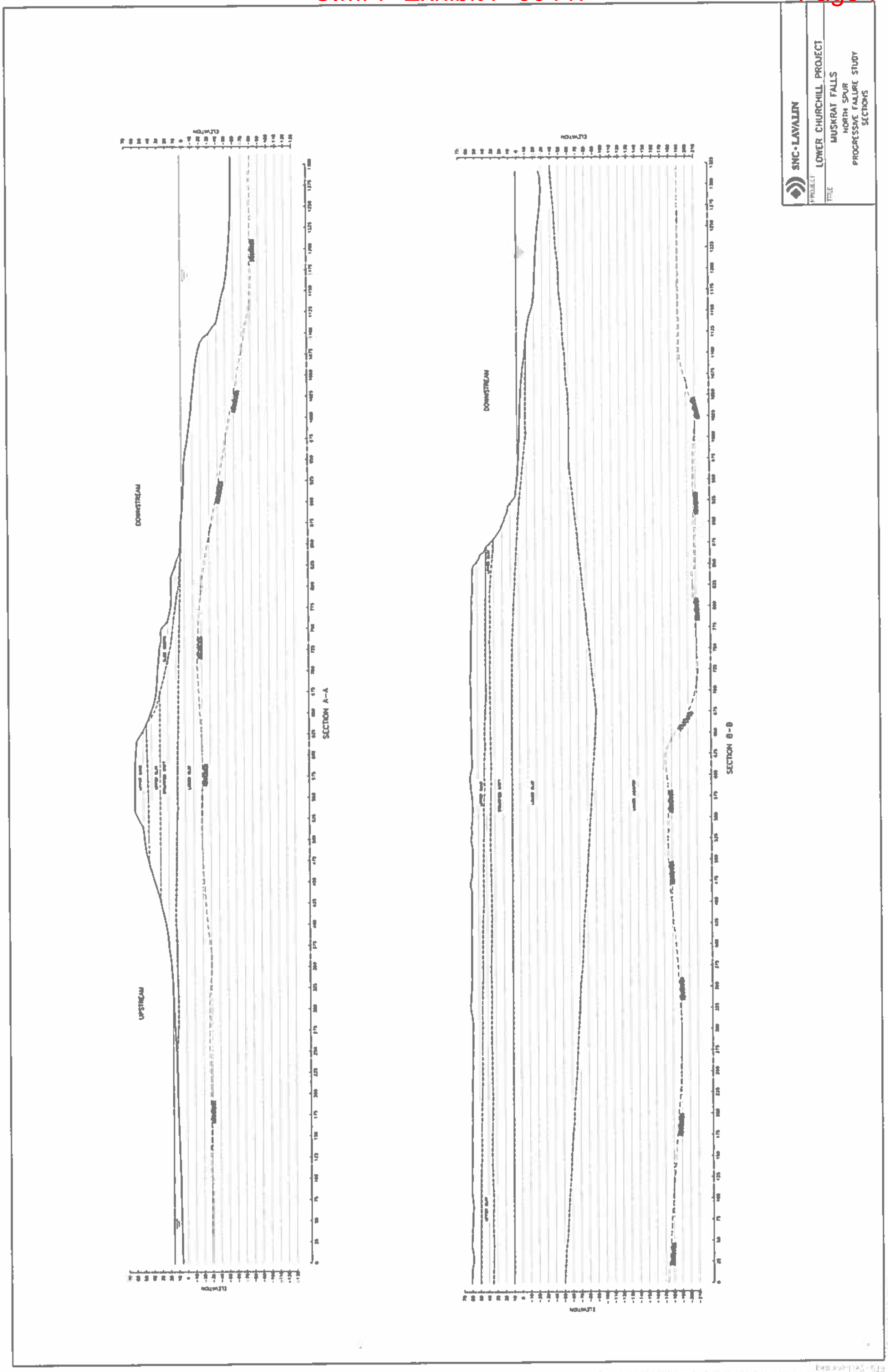
SNC·LAVALIN
LOWER CHURCHILL PROJECT
MUSKRAT FALLS
NORTH SPUR
PROGRESSIVE FAILURE STUDY
SECTIONS
SECTION A-A
UPSTREAM
DOWNSTREAM
ELEVATION
SECTION B-B

Figure A-4

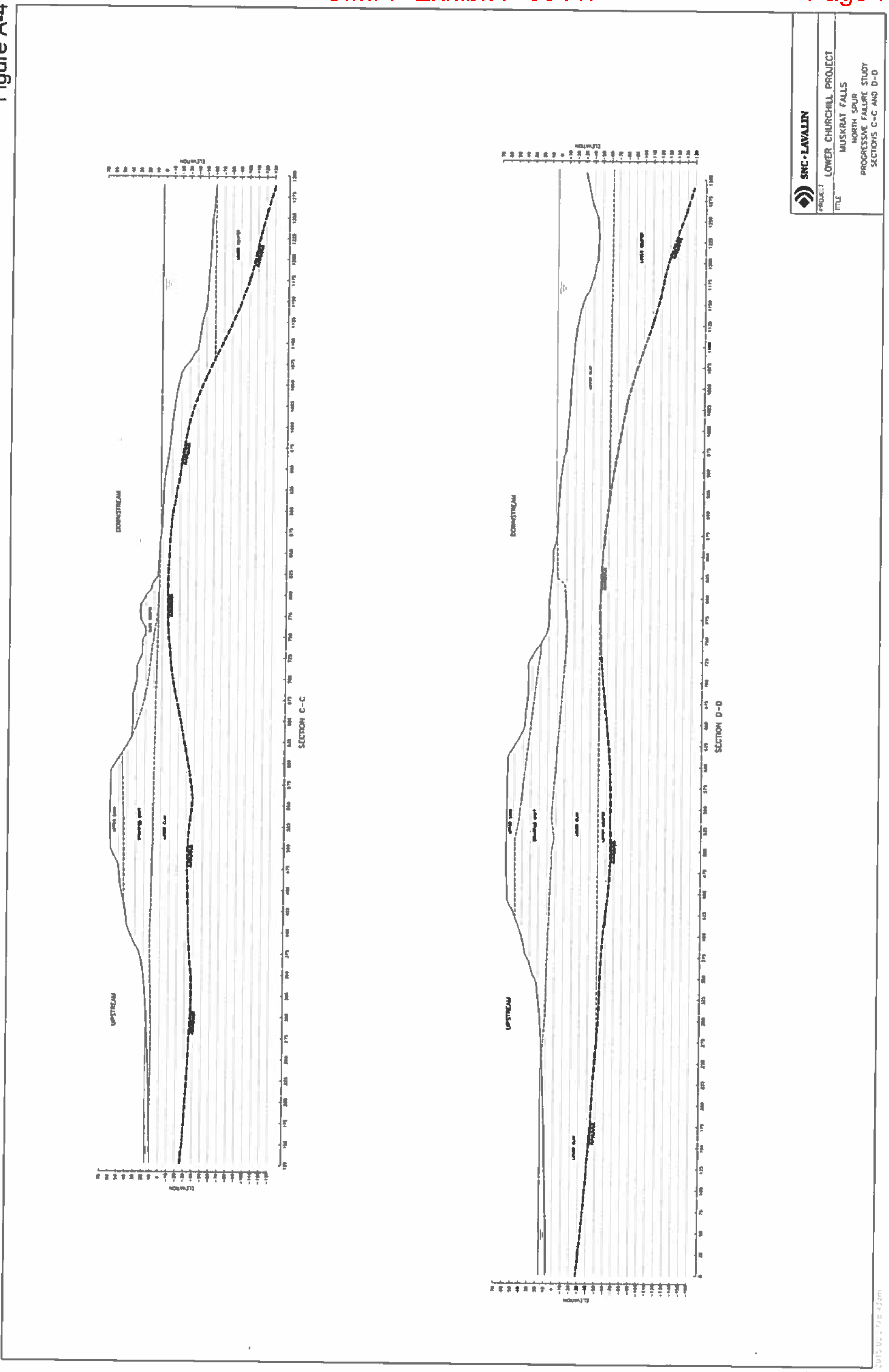
SNC·LAVALIN
LOWER CHURCHILL PROJECT
MUSKRAT FALLS
NORTH SPUR
PROGRESSIVE FAILURE STUDY
SECTIONS C-C AND D-D
UPSTREAM
DOWNSTREAM
SECTION C-C
SECTION D-D
ELEVATION

Figure A-5

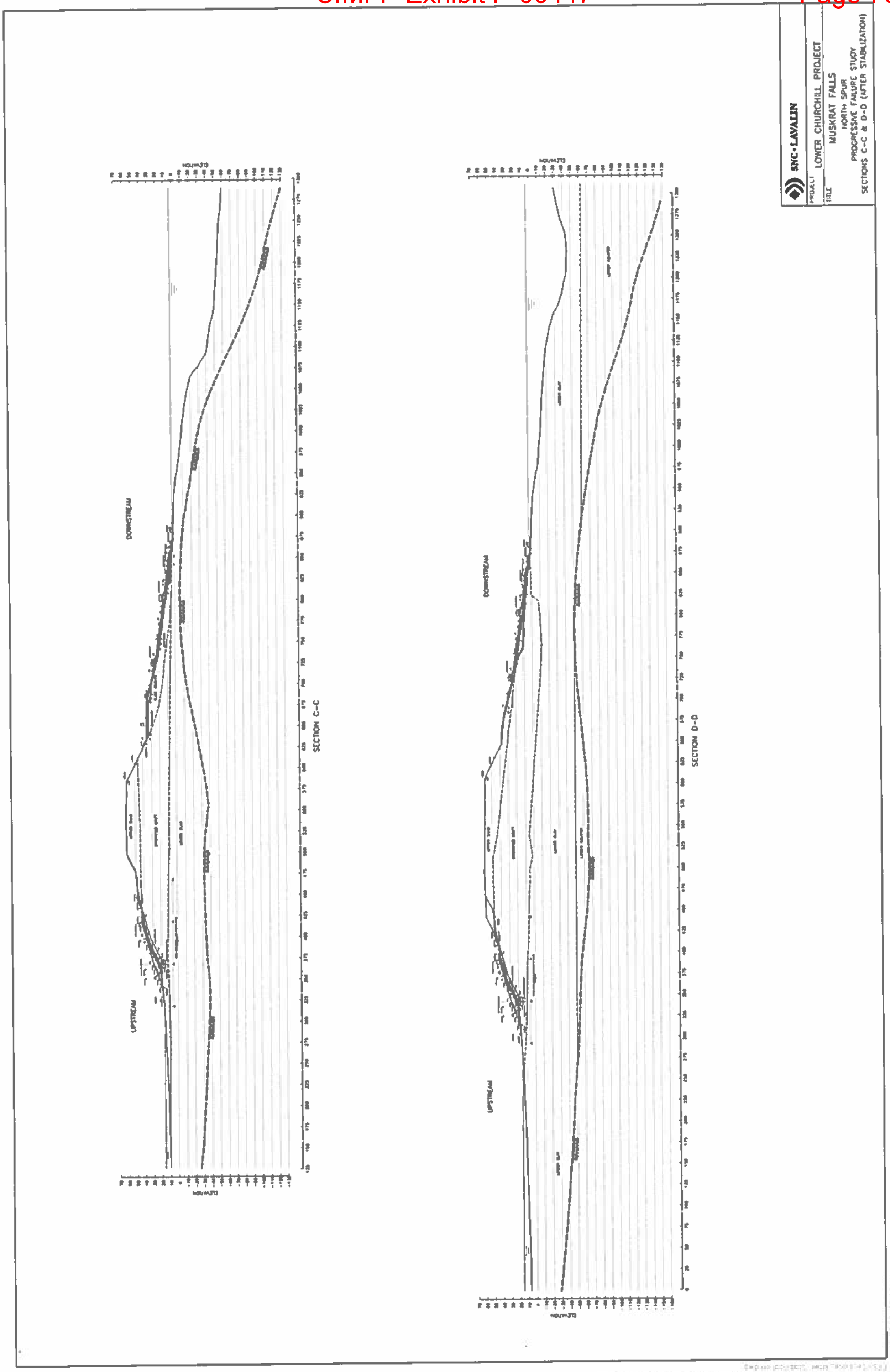
SNC·LAVALIN
PROJECT
LOWER CHURCHILL PROJECT
TITLE
MUSKRAT FALLS
NORTH SPUR
PROGRESSIVE FAILURE STUDY
SECTIONS C-C & D-D (AFTER STABILIZATION)
SECTION C-C
SECTION D-D
UPSTREAM
DOWNSTREAM
ELEVATION

SNC·LAVALIN	NORTH SPUR STABILIZATION WORKS - Progressive Failure Study		Revision
	Nalcor Doc. No. MFA-SN-CD-2800-GT-RP-0001 Rev. A1	SLI Doc. No. 505573-3281-4GER-0001-PB	Date
	Figure B-1	NORTH SPUR – LOCALIZATION OF SECTIONS AND IN SITU TESTS AND BOREHOLES	16-JUN-2015

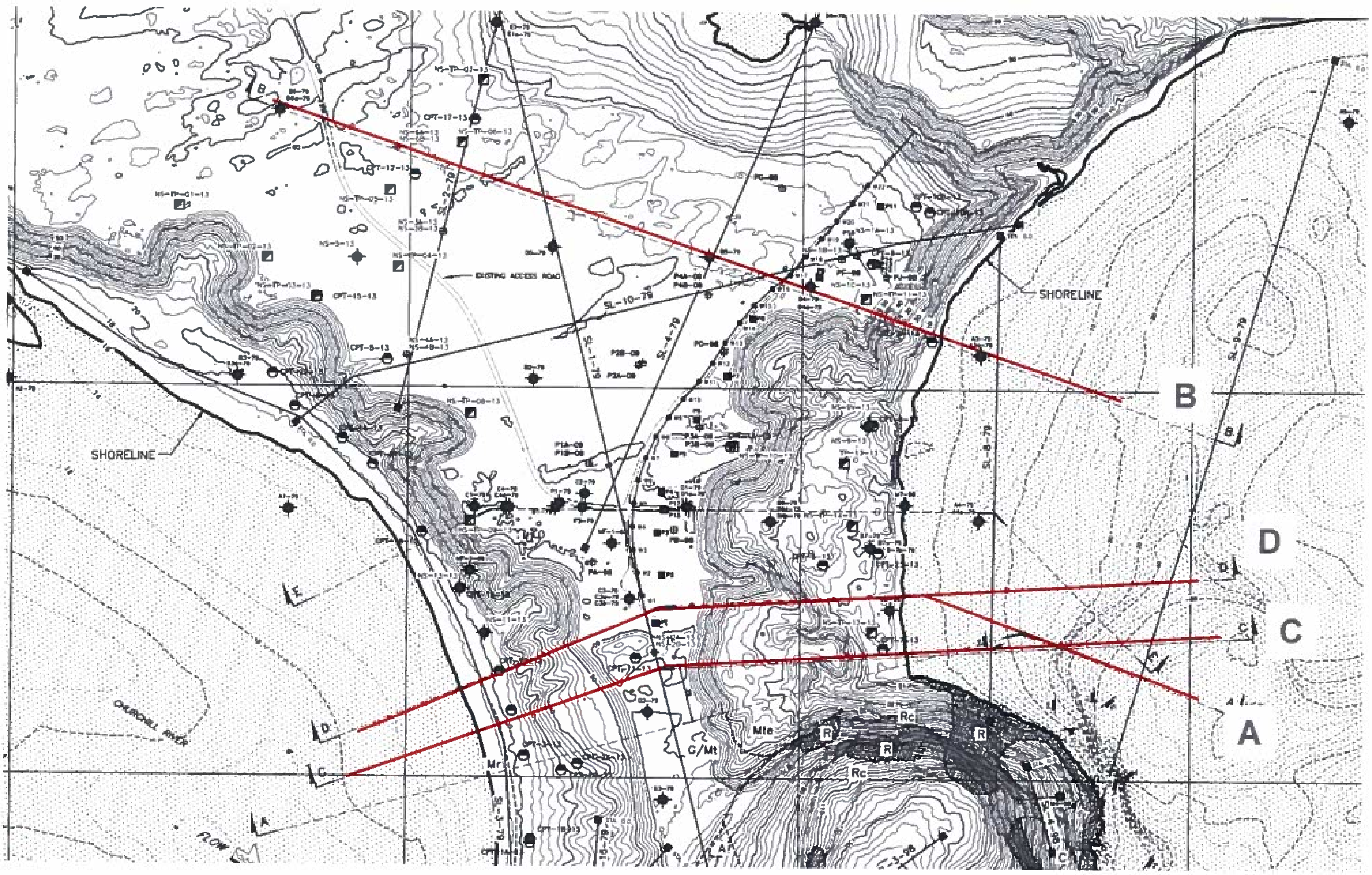

SNC·LAVALIN	NORTH SPUR STABILIZATION WORKS - Progressive Failure Study		Revision
	Nalcor Doc. No. MFA-SN-CD-2800-GT-RP-0001 Rev. A1	SLI Doc. No. 505573-3281-4GER-0001-PB	Date
	Figure B-2	SECTION B–B – CENTER PROFILE - VERTICAL EFFECTIVE STRESS PROFILE AND SHEAR STRENGTH ESTIMATION	16-JUN-2015

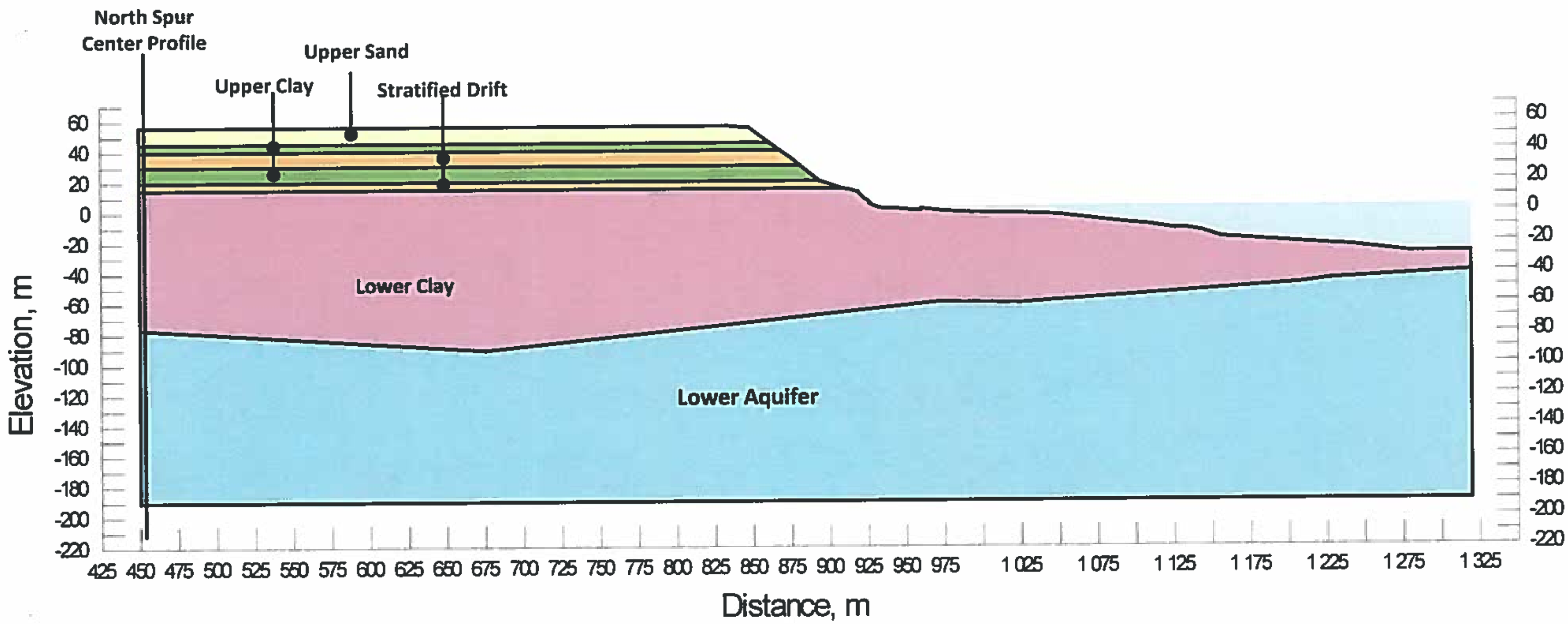

→ **Profile of B-B 0,2 σ'_v shown on figures B-3 to B-5 is based on the vertical effective stress, σ'_v, calculated along the « North Spur Center Profile » indicated on the cross-section above.**

SNC·LAVALIN	NORTH SPUR STABILIZATION WORKS - Progressive Failure Study		Revision
	Nalcor Doc. No. MFA-SN-CD-2800-GT-RP-0001 Rev. A1	SLI Doc. No. 505573-3281-4GER-0001-PB	Date
	Figure B-3	SHEAR STRENGTH OF CLAY – CPTU AND VANE SCISSOMETER TESTS AT NORTH SPUR	16-JUN-2015

CPTU Tests

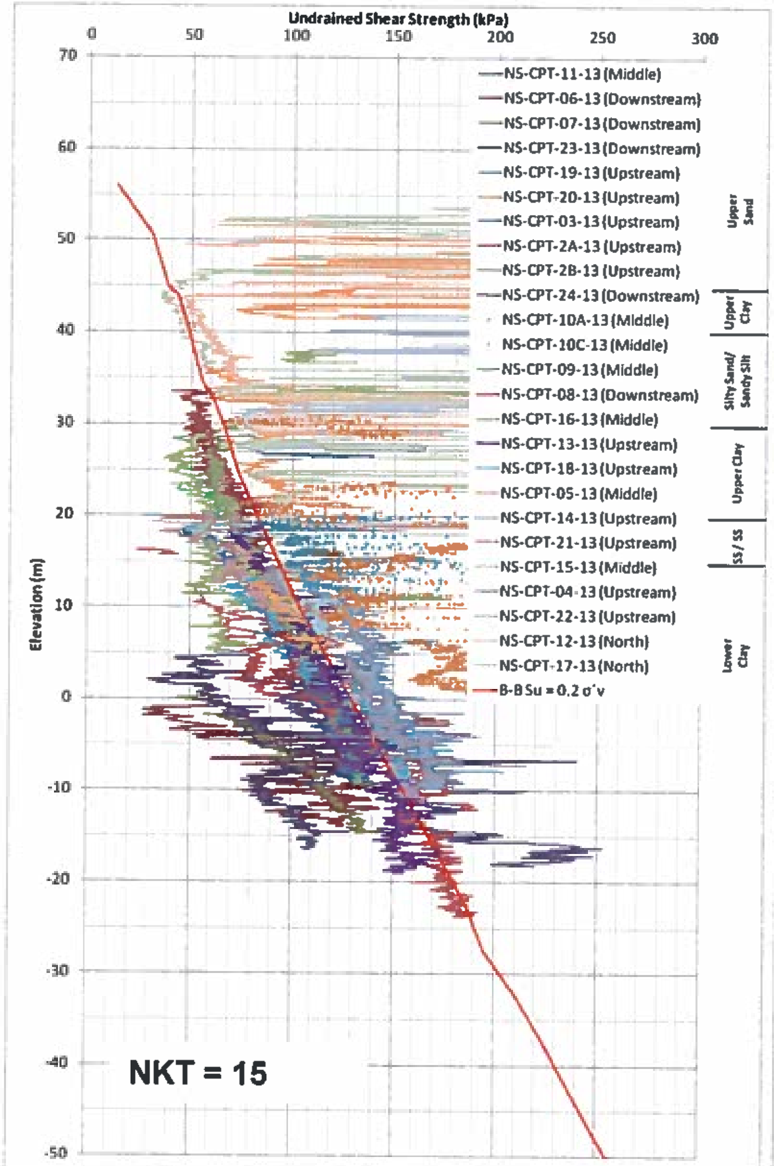

Vane Scissometer Tests

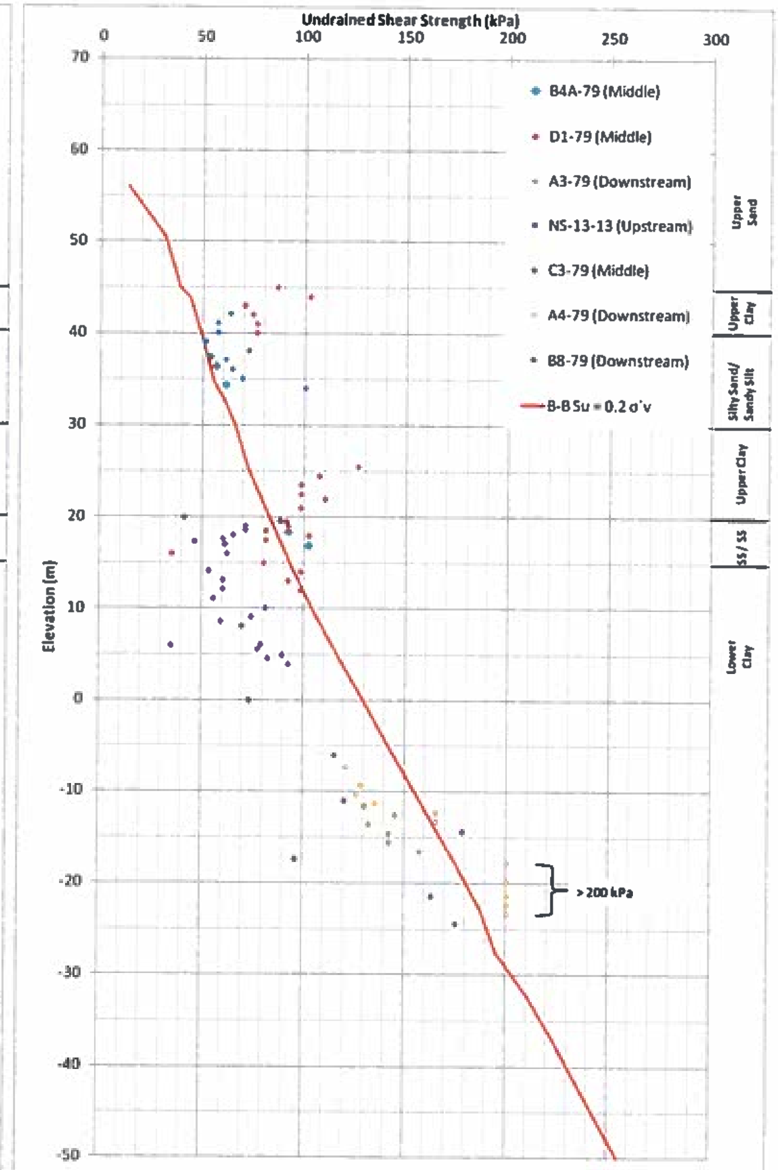

SNC·LAVALIN	NORTH SPUR STABILIZATION WORKS - Progressive Failure Study		Revision
	Nalcor Doc. No. MFA-SN-CD-2800-GT-RP-0001 Rev. A1	SLI Doc. No. 505573-3281-4GER-0001-PB	Date
	Figure B-4	SHEAR STRENGTH OF CLAY – UPSTREAM AND DOWNSTREAM SIDES OF NORTH SPUR	16-JUN-2015

Upstream Side South

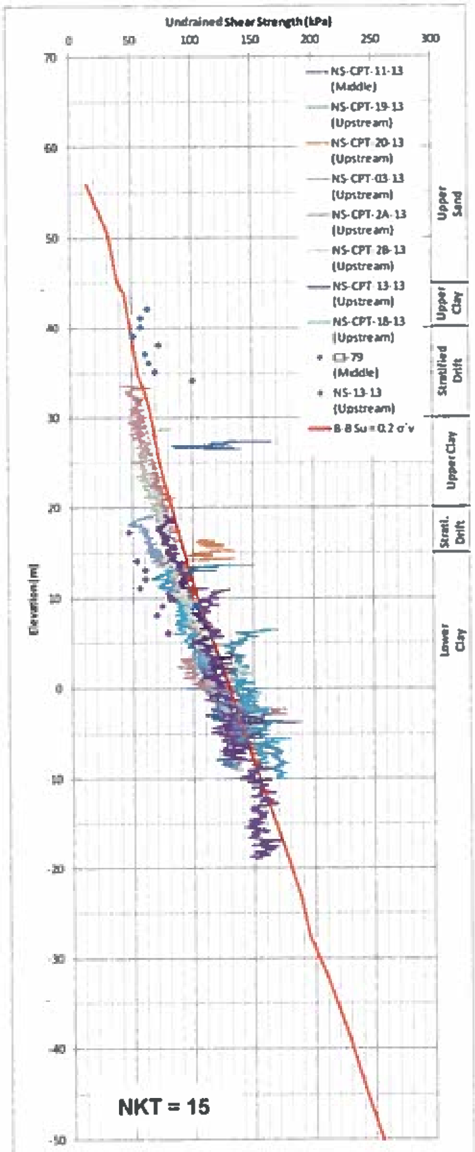

Upstream Side North

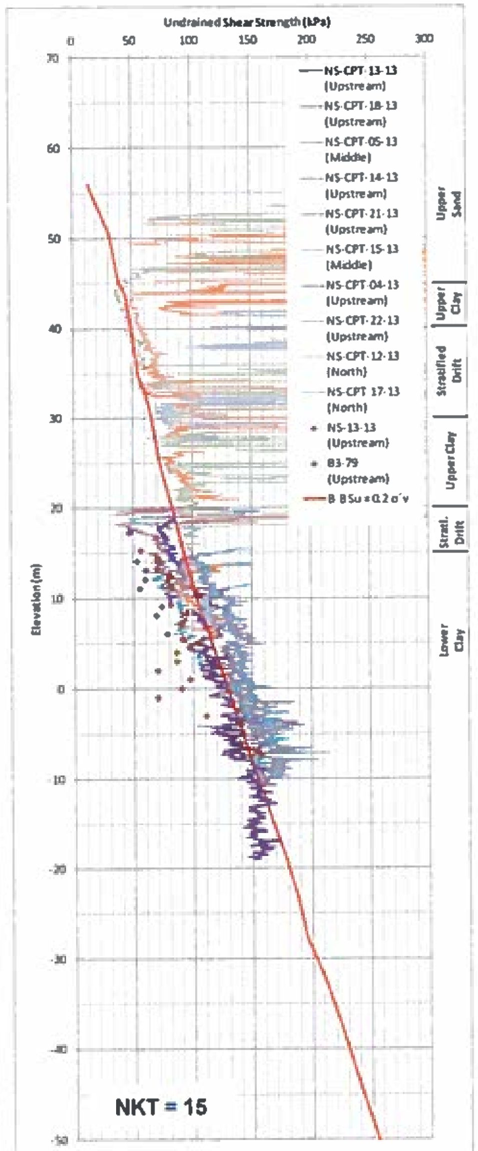

Downstream Side South

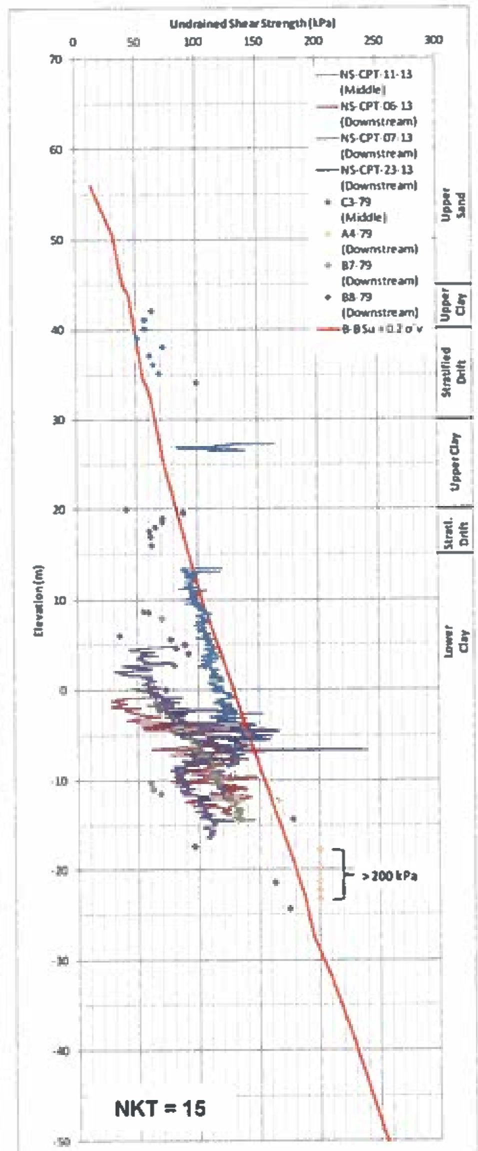

Downstream Side North

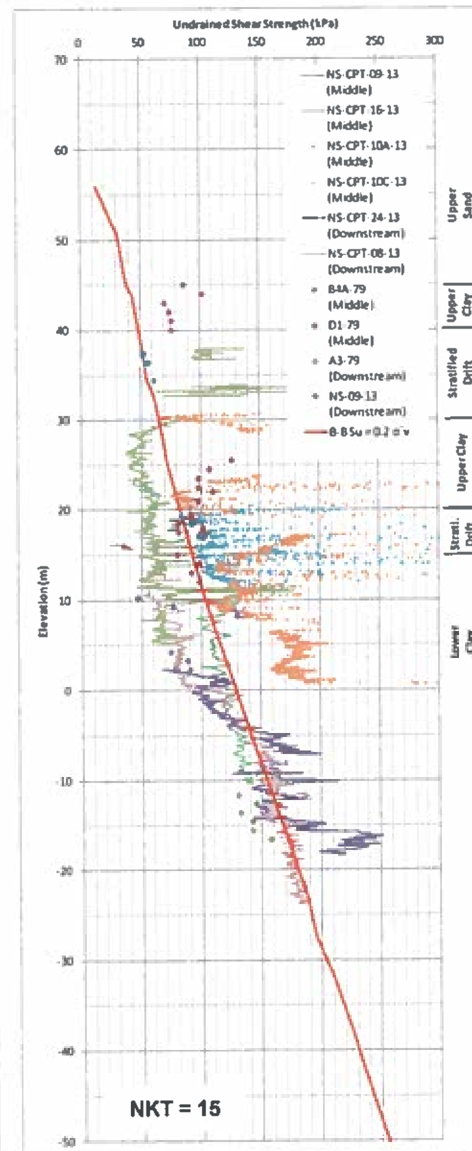

SNC·LAVALIN	NORTH SPUR STABILIZATION WORKS - Progressive Failure Study		Revision
	Nalcor Doc. No. MFA-SN-CD-2800-GT-RP-0001 Rev. A1	SLI Doc. No. 505573-3281-4GER-0001-PB	Date
	Figure B-5	SHEAR STRENGTH OF CLAY – UPSTREAM TOE, MIDDLE CREST AND DOWNSTREAM TOE	16-JUN-2015

Upstream Side Toe Area

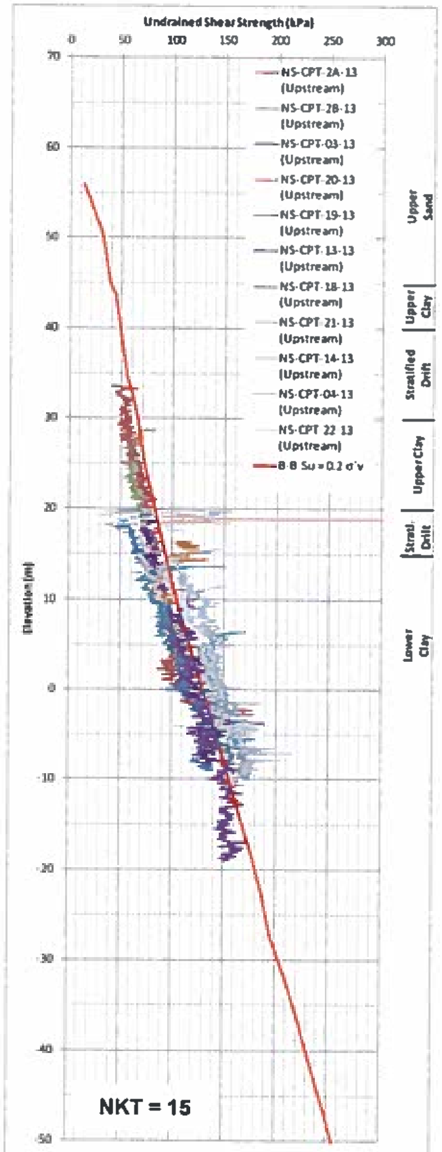

Crest of Spur Uphill Area

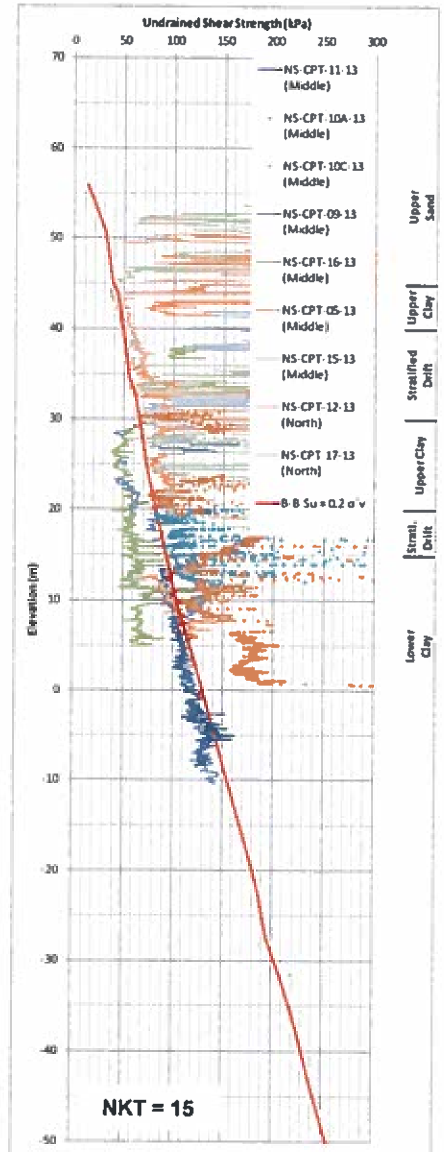

Downstream Side Toe Area

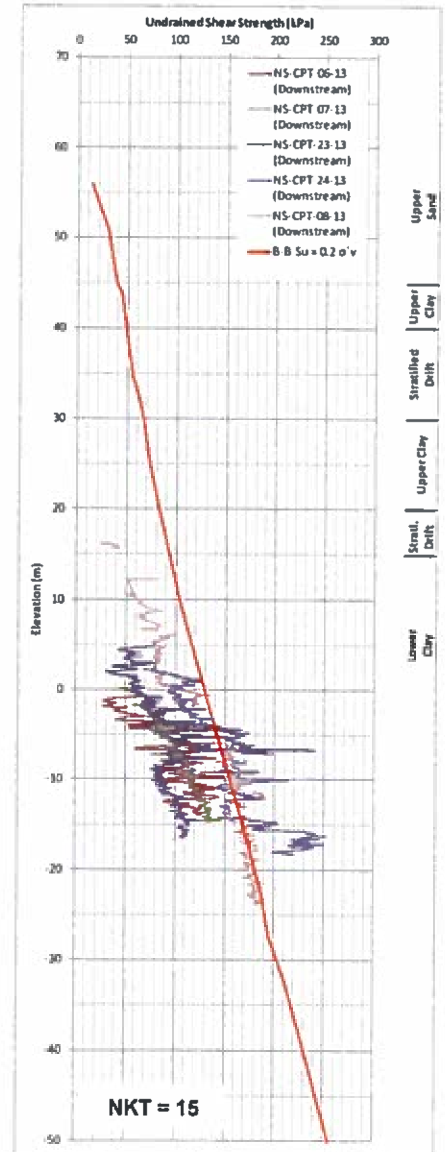

SNC·LAVALIN	NORTH SPUR STABILIZATION WORKS - Progressive Failure Study		Revision
	Nalcor Doc. No. MFA-SN-CD-2800-GT-RP-0001 Rev. A1	SLI Doc. No. 505573-3281-4GER-0001-PB	Date
	Figure C-1	NORTH SPUR – LOCALIZATION OF SECTIONS ON PRESENT TOPOGRAPHY	16-JUN-2015

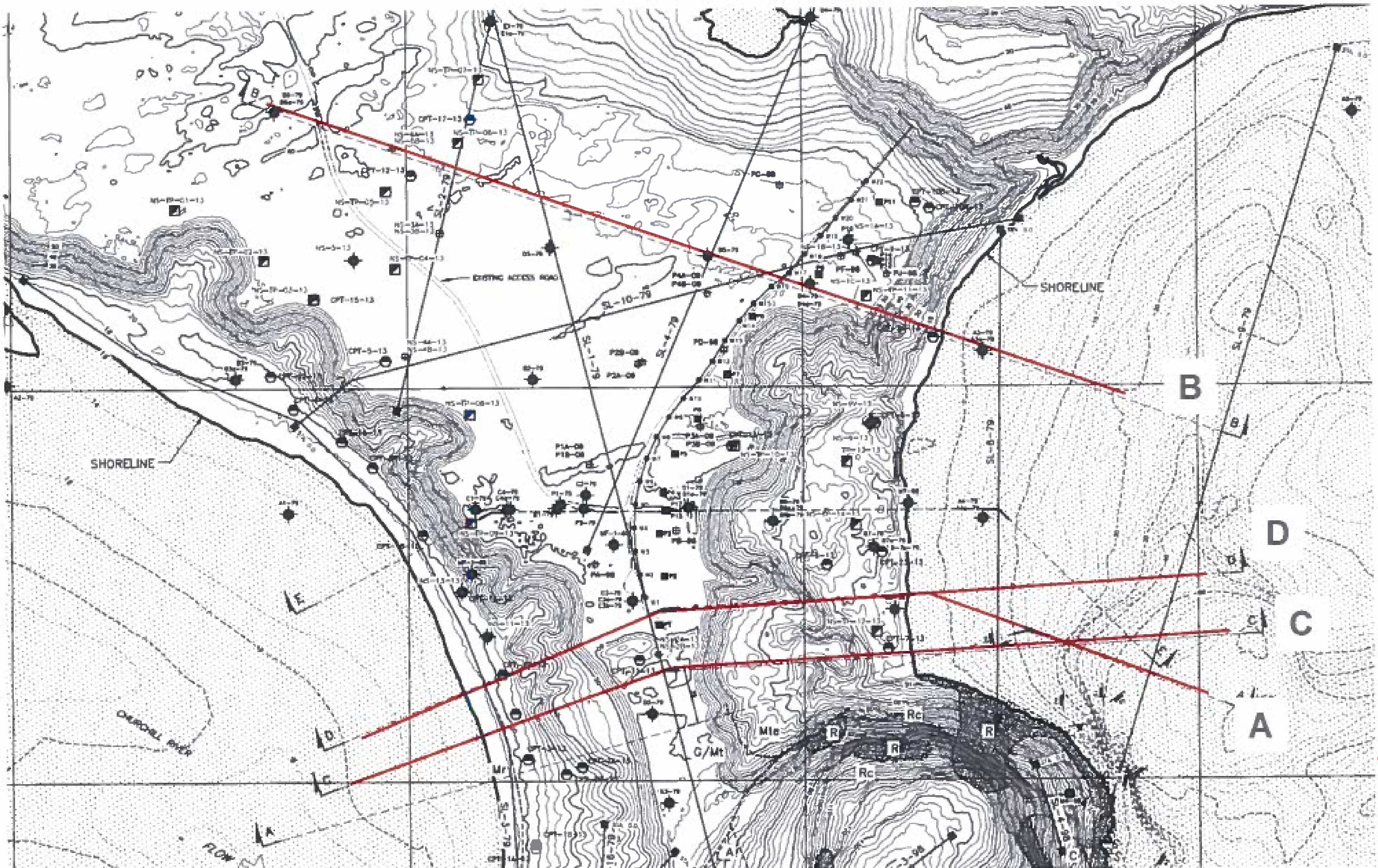

SNC·LAVALIN	NORTH SPUR STABILIZATION WORKS - Progressive Failure Study		Revision
	Nalcor Doc. No. MFA-SN-CD-2800-GT-RP-0001 Rev. A1	SLI Doc. No. 505573-3281-4GER-0001-PB	Date
	Figure C-2	NORTH SPUR – LOCALIZATION OF SECTIONS ON PROJECTED STABILIZED TOPOGRAPHY	16-JUN-2015

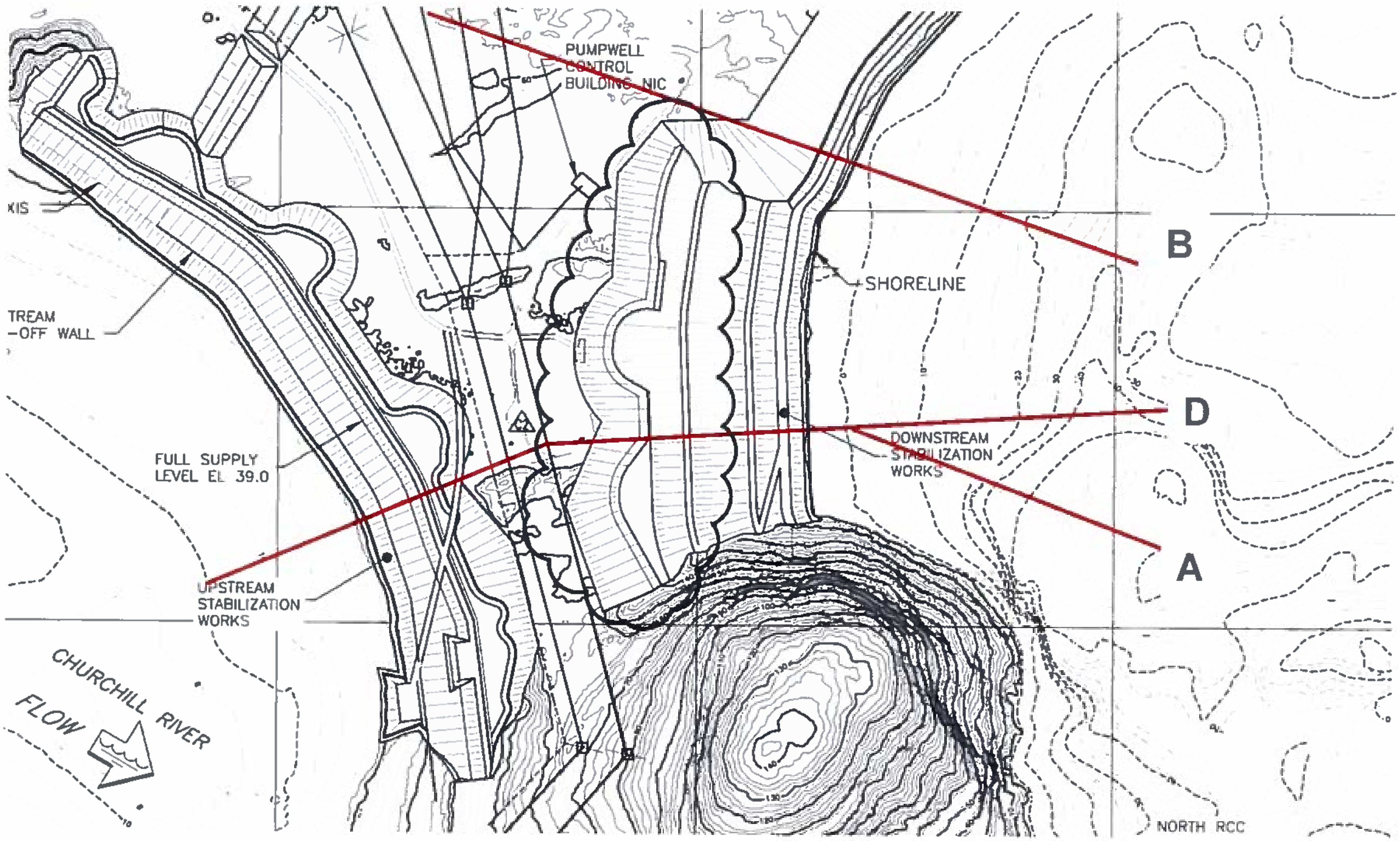

SNC·LAVALIN	NORTH SPUR STABILIZATION WORKS - Progressive Failure Study		Revision
	Nalcor Doc. No. MFA-SN-CD-2800-GT-RP-0001 Rev. A1	SLI Doc. No. 505573-3281-4GER-0001-PB	Date
	Figure C-3	SECTION B-B - REFERENCE NORTH SECTION – STRATIGRAPHY	16-JUN-2015

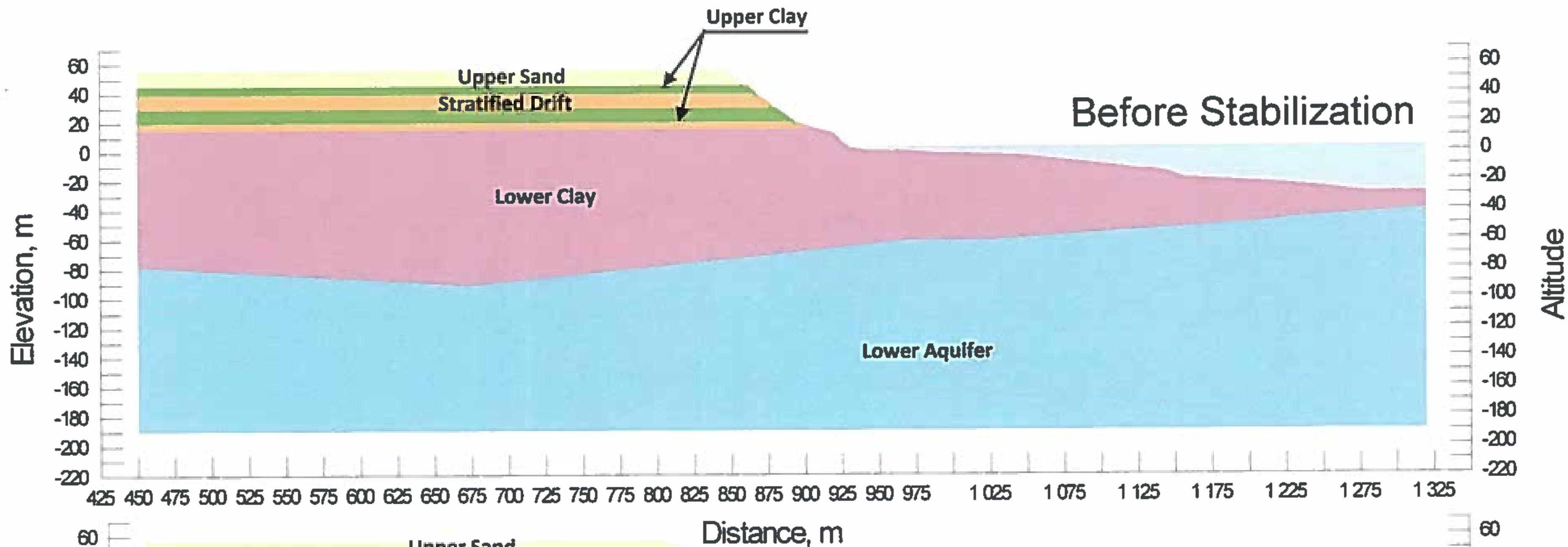

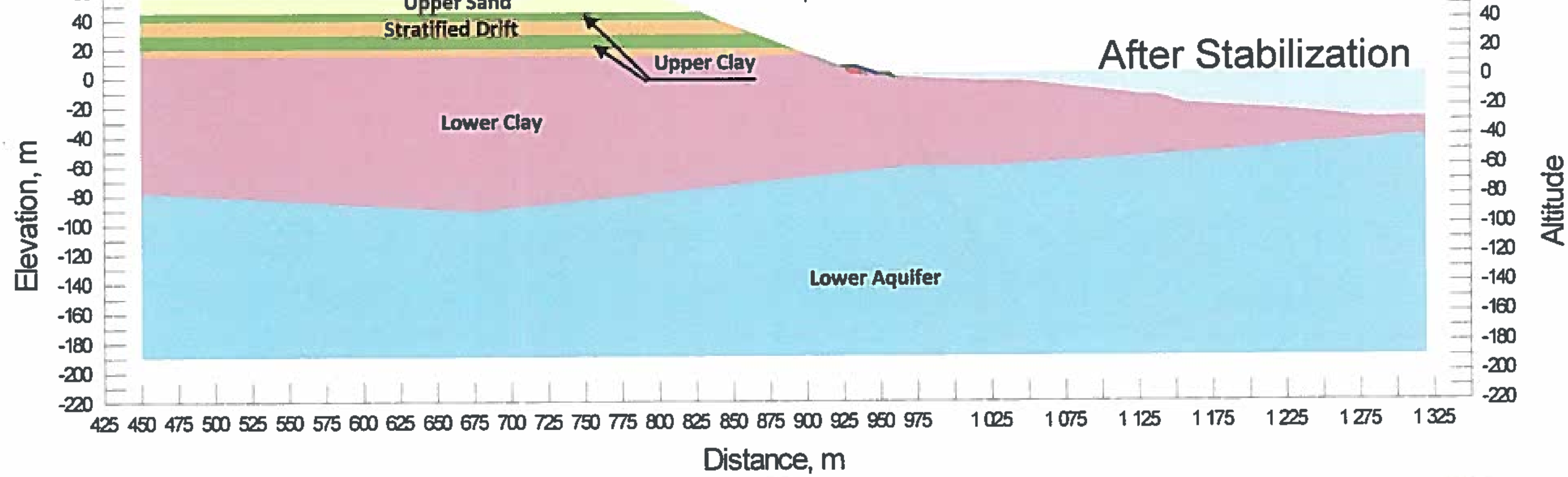

SNC·LAVALIN	NORTH SPUR STABILIZATION WORKS - Progressive Failure Study		Revision
	Nalcor Doc. No. MFA-SN-CD-2800-GT-RP-0001 Rev. A1	SLI Doc. No. 505573-3281-4GER-0001-PB	Date
	Figure C-4	SECTION B-B – SEEPAGE ANALYSIS FOR LOWER CLAY – BOUNDARY CONDITIONS AND RESULTS	16-JUN-2015

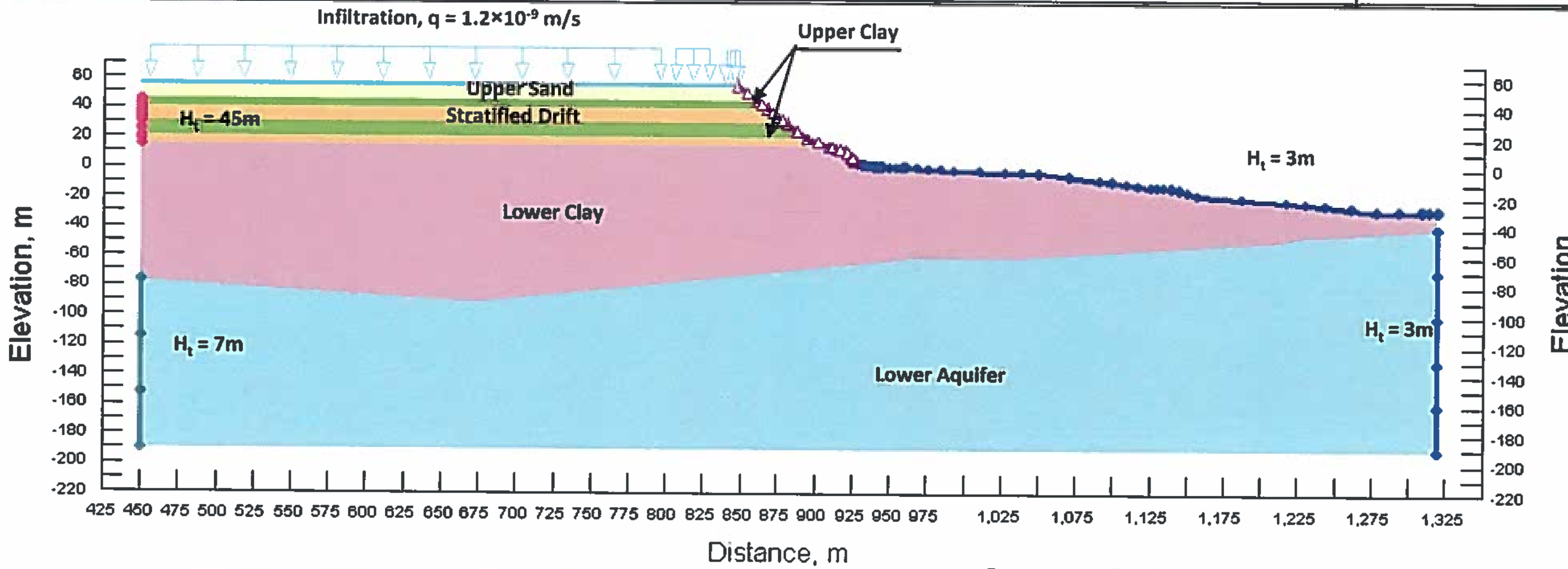

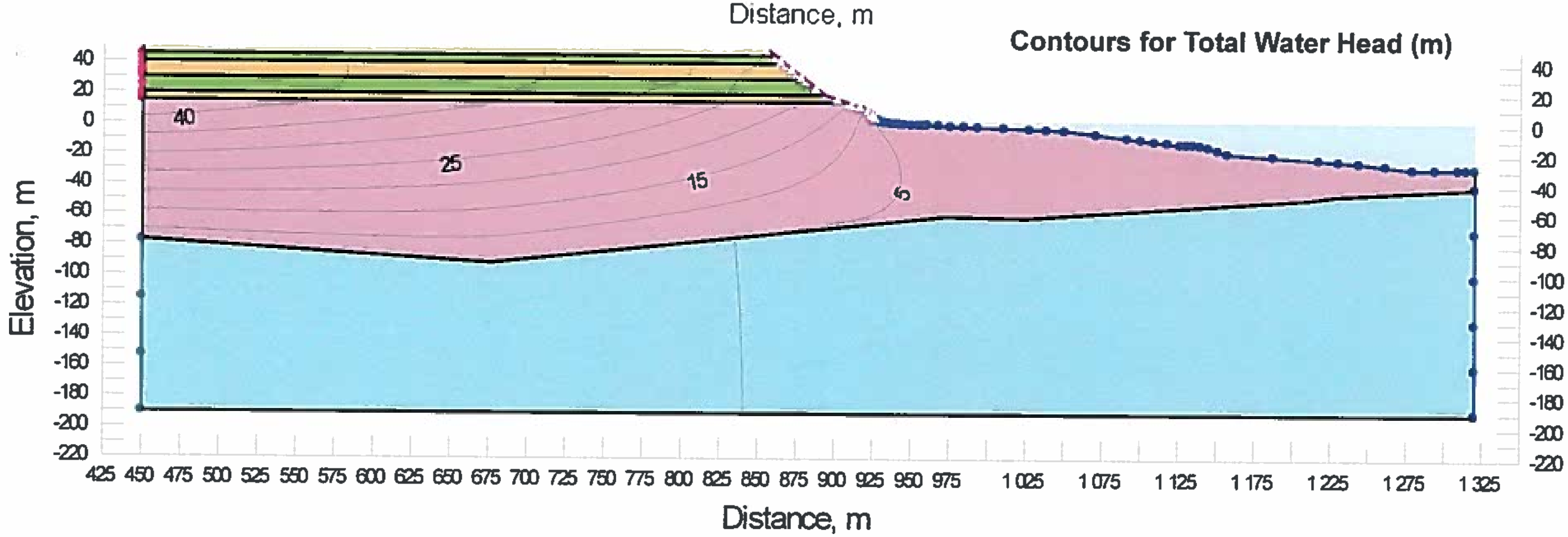

SNC·LAVALIN	NORTH SPUR STABILIZATION WORKS - Progressive Failure Study		Revision
	Nalcor Doc. No. MFA-SN-CD-2800-GT-RP-0001 Rev. A1	SLI Doc. No. 505573-3281-4GER-0001-PB	Date
	Figure C-5	SECTION B-B – SEEPAGE ANALYSIS FOR LOWER CLAY – COMPARISON WITH PIEZOMETRIC DATA	16-JUN-2015

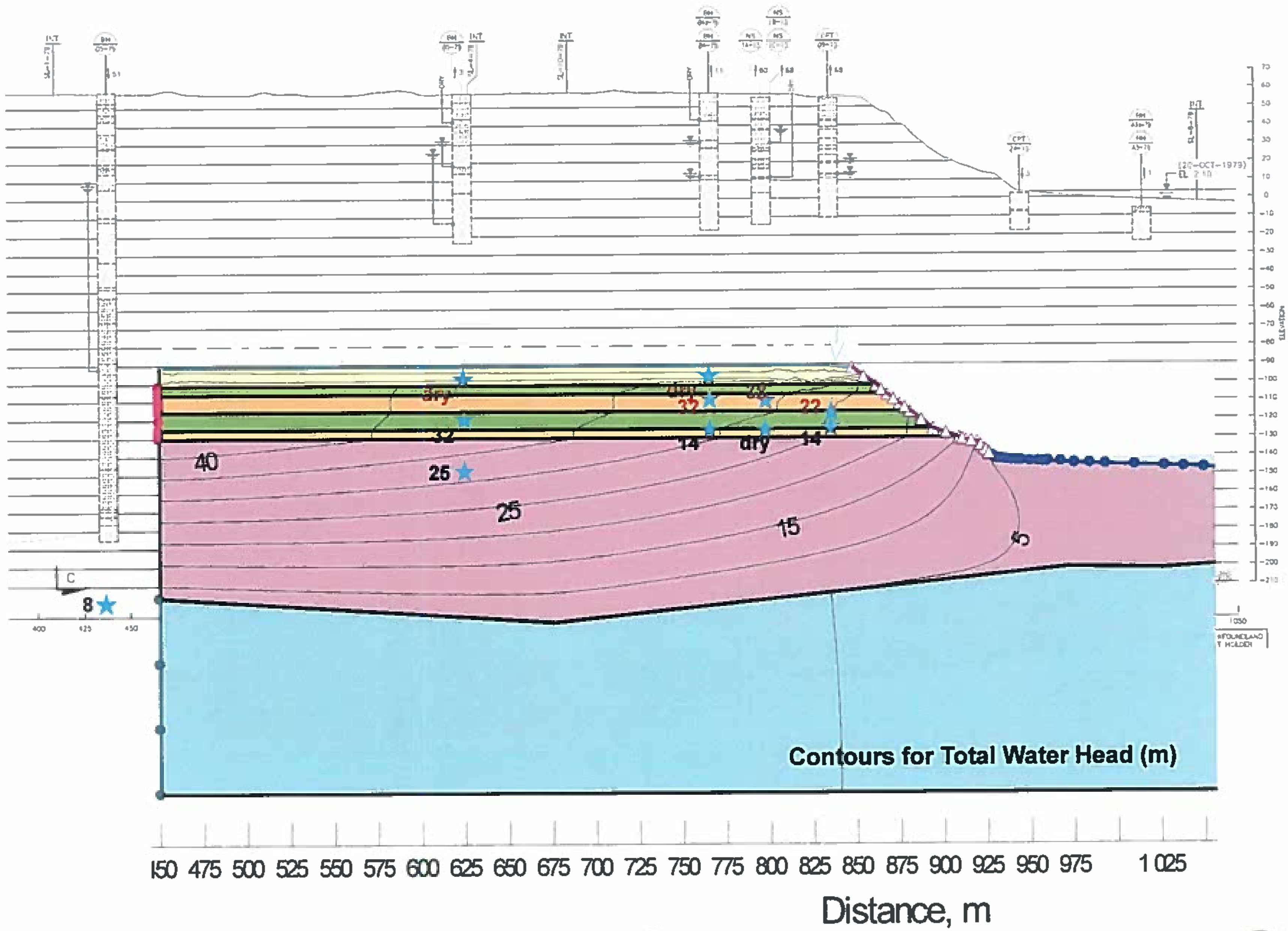

SNC·LAVALIN	NORTH SPUR STABILIZATION WORKS - Progressive Failure Study			Revision
	Nalcor Doc. No. MFA-SN-CD-2800-GT-RP-0001 Rev. A1		SLI Doc. No. 505573-3281-4GER-0001-PB	Date
	Figure C-6	SECTION B-B – UPPER CLAY PIEZOMETRIC CONDITIONS		16-JUN-2015

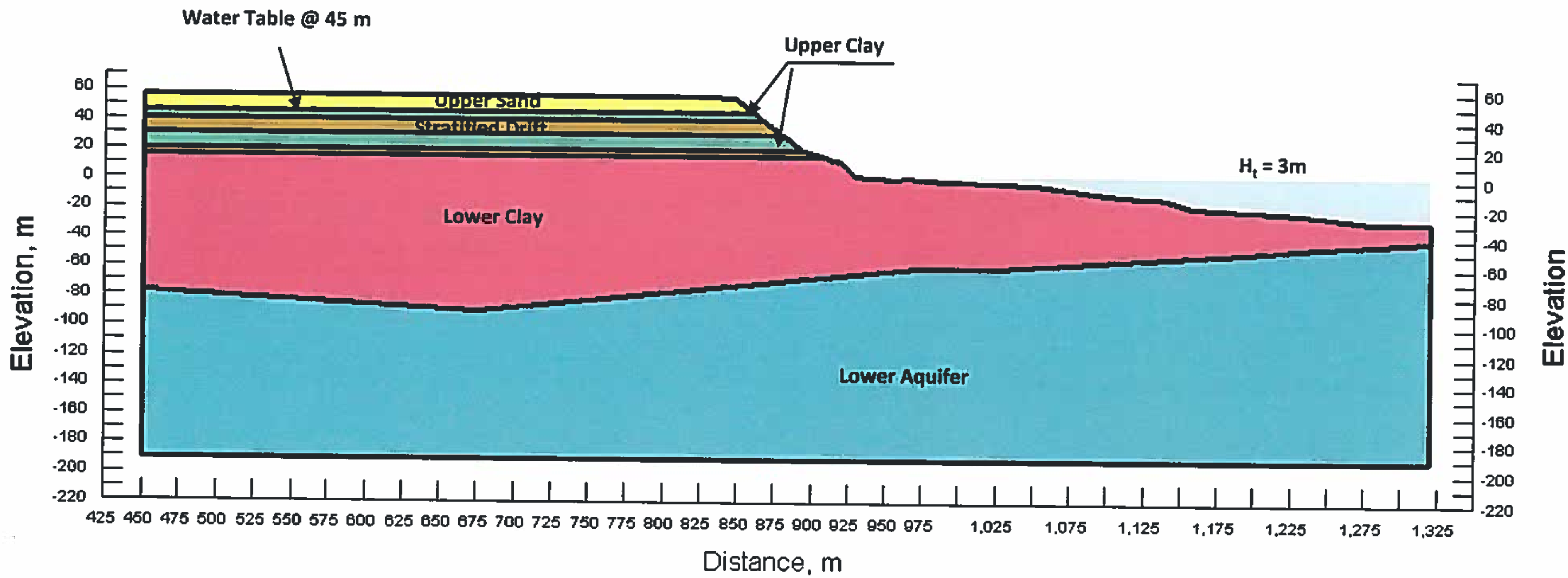

- **Perched water table observed at Upper Clay surface simulated using a hydrostatic water table at Elevation 45 m**

SNC·LAVALIN	NORTH SPUR STABILIZATION WORKS - Progressive Failure Study		Revision
	Nalcor Doc. No. MFA-SN-CD-2800-GT-RP-0001 Rev. A1	SLI Doc. No. 505573-3281-4GER-0001-PB	Date
	Figure C-7	SECTION B-B – SEEPAGE CONDITIONS FOR UPPER CLAY – COMPARISON WITH PIEZOMETRIC DATA	16-JUN-2015

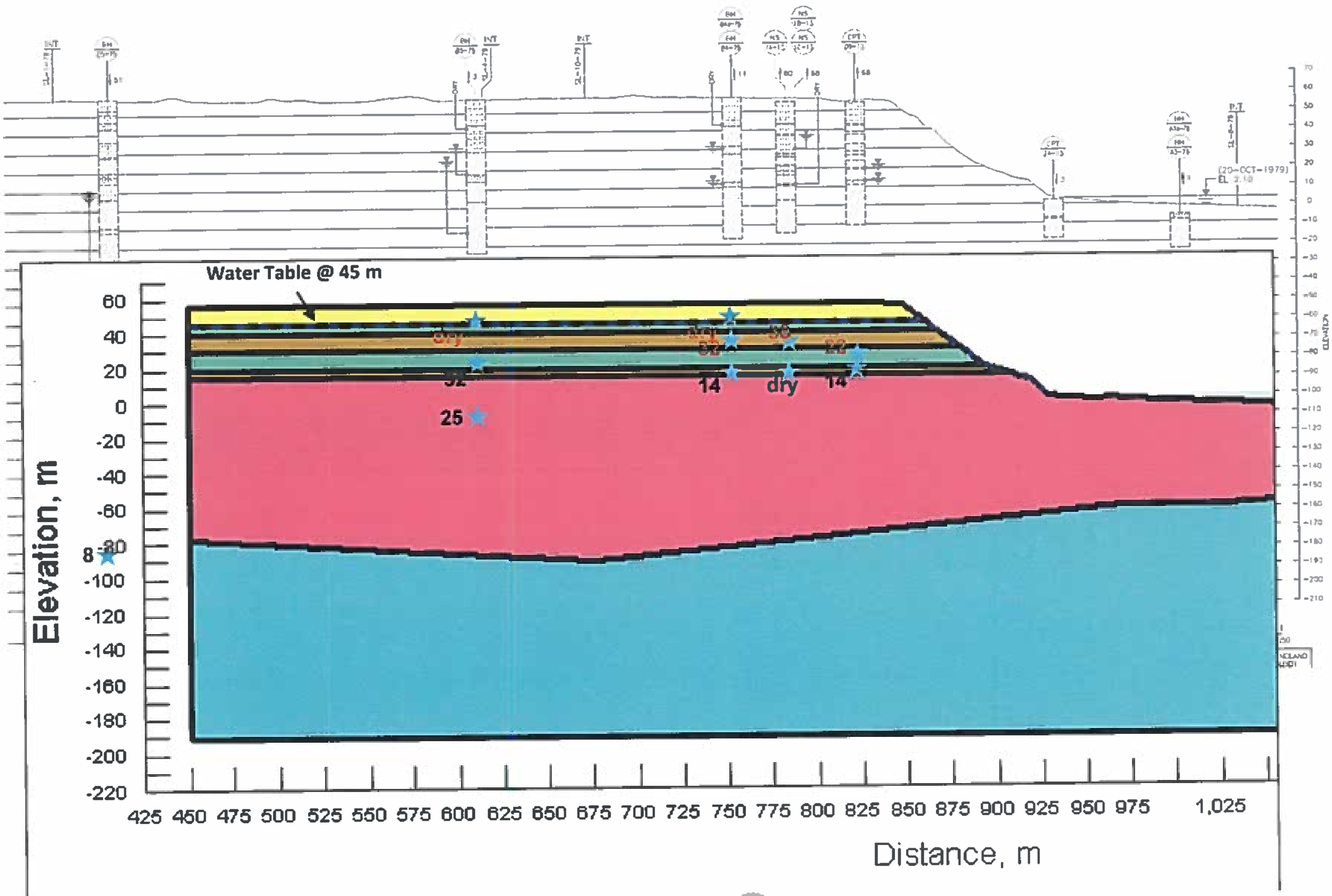

SNC·LAVALIN	NORTH SPUR STABILIZATION WORKS - Progressive Failure Study		Revision
	Nalcor Doc. No. MFA-SN-CD-2800-GT-RP-0001 Rev. A1	SLI Doc. No. 505573-3281-4GER-0001-PB	Date
	Figure C-8	SECTION B-B - IN SITU TESTS FOR SHEAR STRENGTH OF CLAY	16-JUN-2015

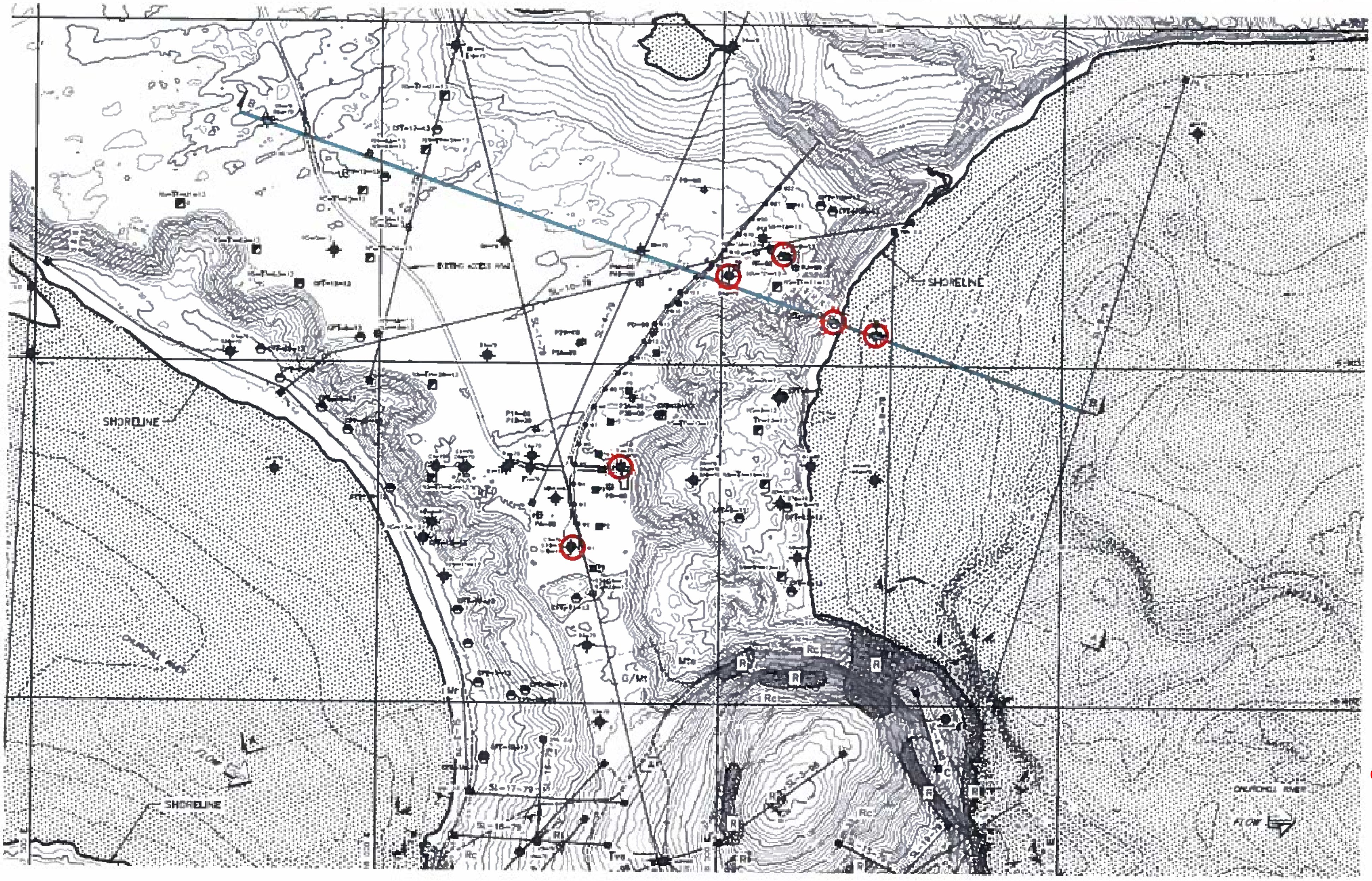

SNC·LAVALIN	NORTH SPUR STABILIZATION WORKS - Progressive Failure Study		Revision
	Nalcor Doc. No. MFA-SN-CD-2800-GT-RP-0001 Rev. A1	SLI Doc. No. 505573-3281-4GER-0001-PB	Date
	Figure C-9	SHEAR STRENGTH PROFILE OF LOWER AND UPPER CLAY LAYERS	16-JUN-2015

Upper and Lower Clay
Selected Representative
Shear Strength Profile

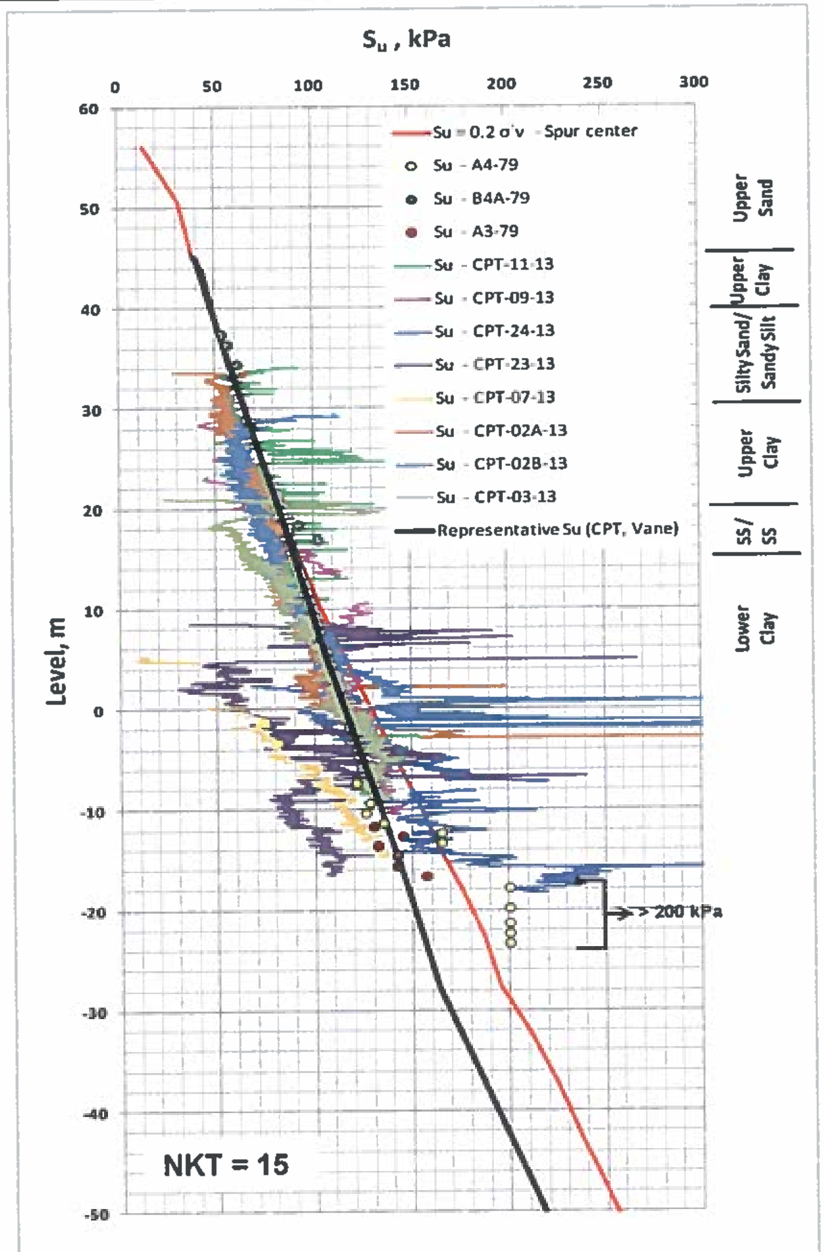

SNC·LAVALIN	NORTH SPUR STABILIZATION WORKS - Progressive Failure Study		Revision
	Nalcor Doc. No. MFA-SN-CD-2800-GT-RP-0001 Rev. A1	SLI Doc. No. 505573-3281-4GER-0001-PB	Date
	Figure C-10	SECTION B–B - VERTICAL STRESS PROFILES AND HORIZONTAL LINES	16-JUN-2015

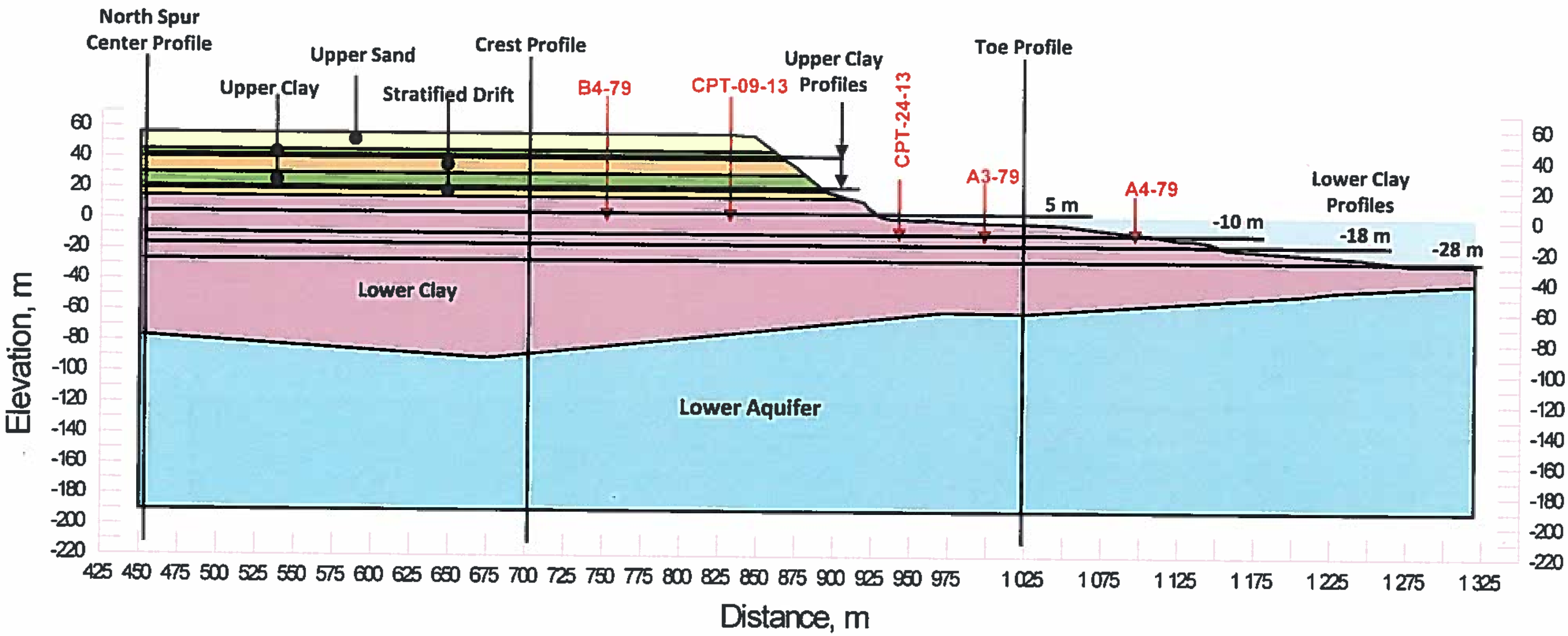

- 3 Vertical Profiles
- 2 Upper Clay Horizontal Profiles
- 4 Lower Clay Horizontal Profiles

SNC·LAVALIN	NORTH SPUR STABILIZATION WORKS - Progressive Failure Study		Revision
	Nalcor Doc. No. MFA-SN-CD-2800-GT-RP-0001 Rev. A1	SLI Doc. No. 505573-3281-4GER-0001-PB	Date
	Figure C-11	SECTION B-B - SHEAR STRESSES AND SHEAR STRENGTH ON LINES +20M AND -10M	16-JUN-2015

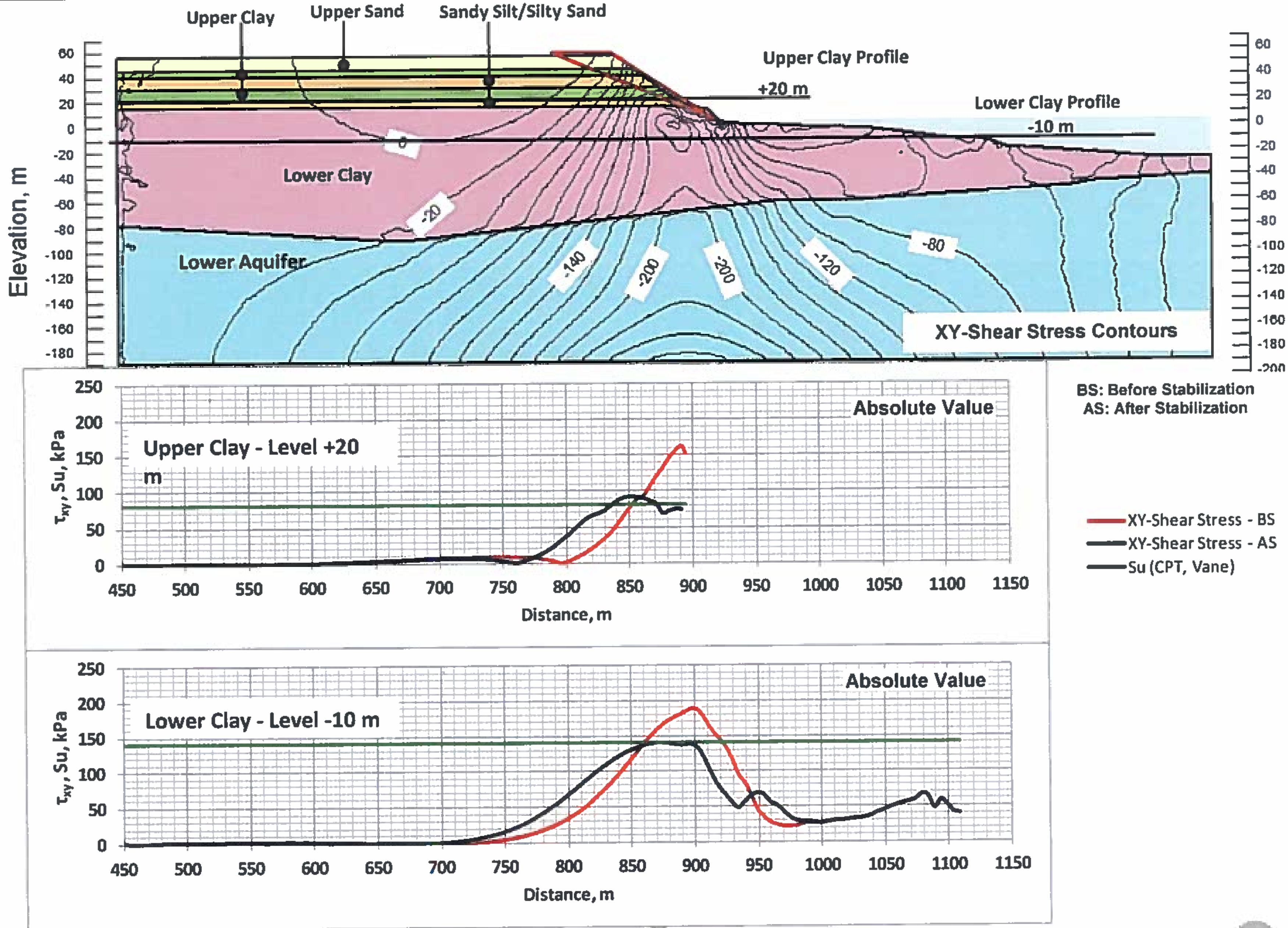

SNC·LAVALIN	NORTH SPUR STABILIZATION WORKS - Progressive Failure Study		Revision
	Nalcor Doc. No. MFA-SN-CD-2800-GT-RP-0001 Rev. A1	SLI Doc. No. 505573-3281-4GER-0001-PB	Date
	Figure C-12	SECTION B-B - SHEAR STRESSES AND SHEAR STRENGTH ON LINES +20M AND -10M	16-JUN-2015

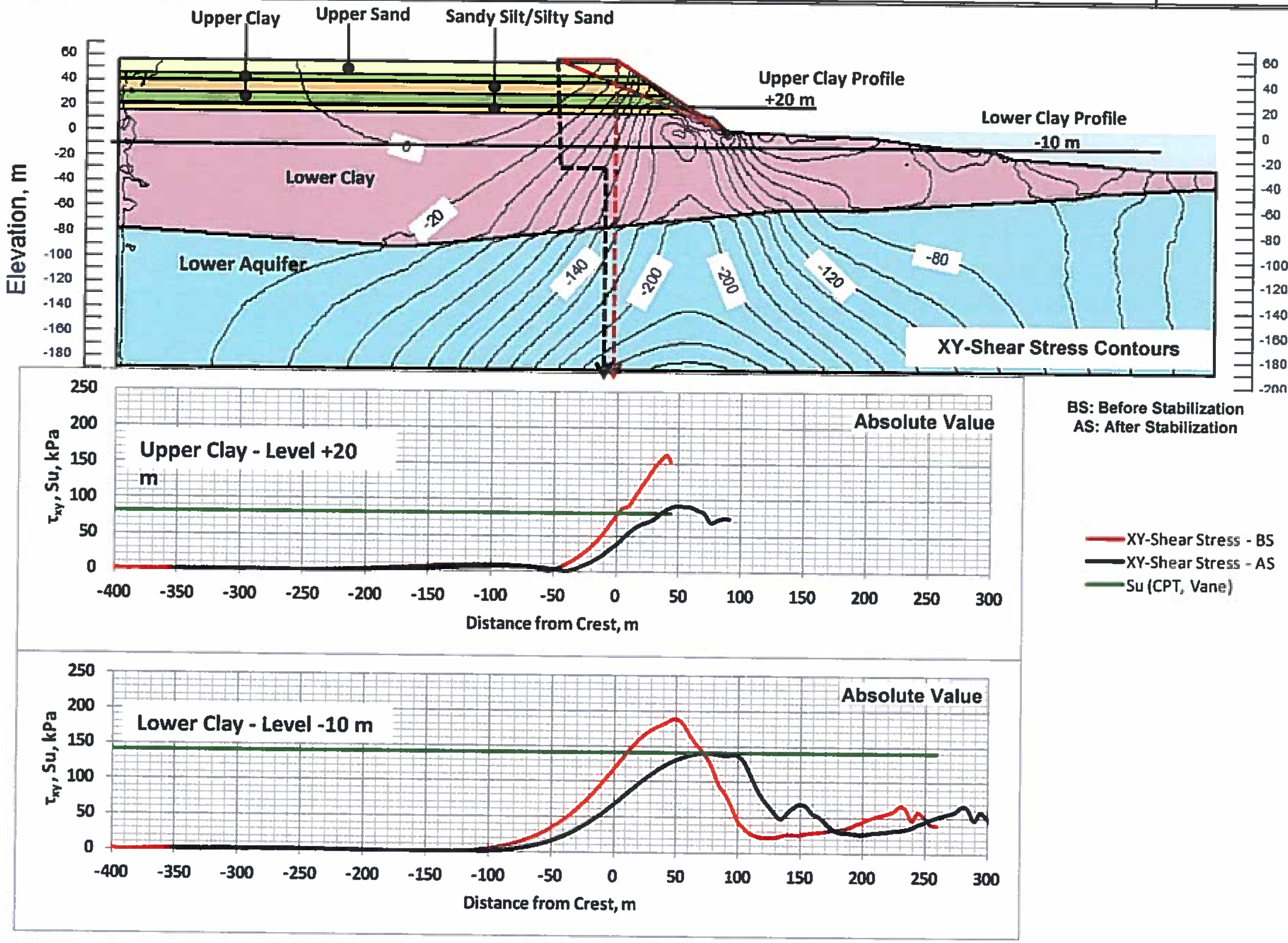

SNC·LAVALIN	NORTH SPUR STABILIZATION WORKS - Progressive Failure Study		Revision
	Nalcor Doc. No. MFA-SN-CD-2800-GT-RP-0001 Rev. A1	SLI Doc. No. 505573-3281-4GER-0001-PB	Date
	Figure C-13	SECTION B-B – UPPER CLAY MODEL - SHEAR STRESSES AND STRENGTH ON LINE 40M	16-JUN-2015

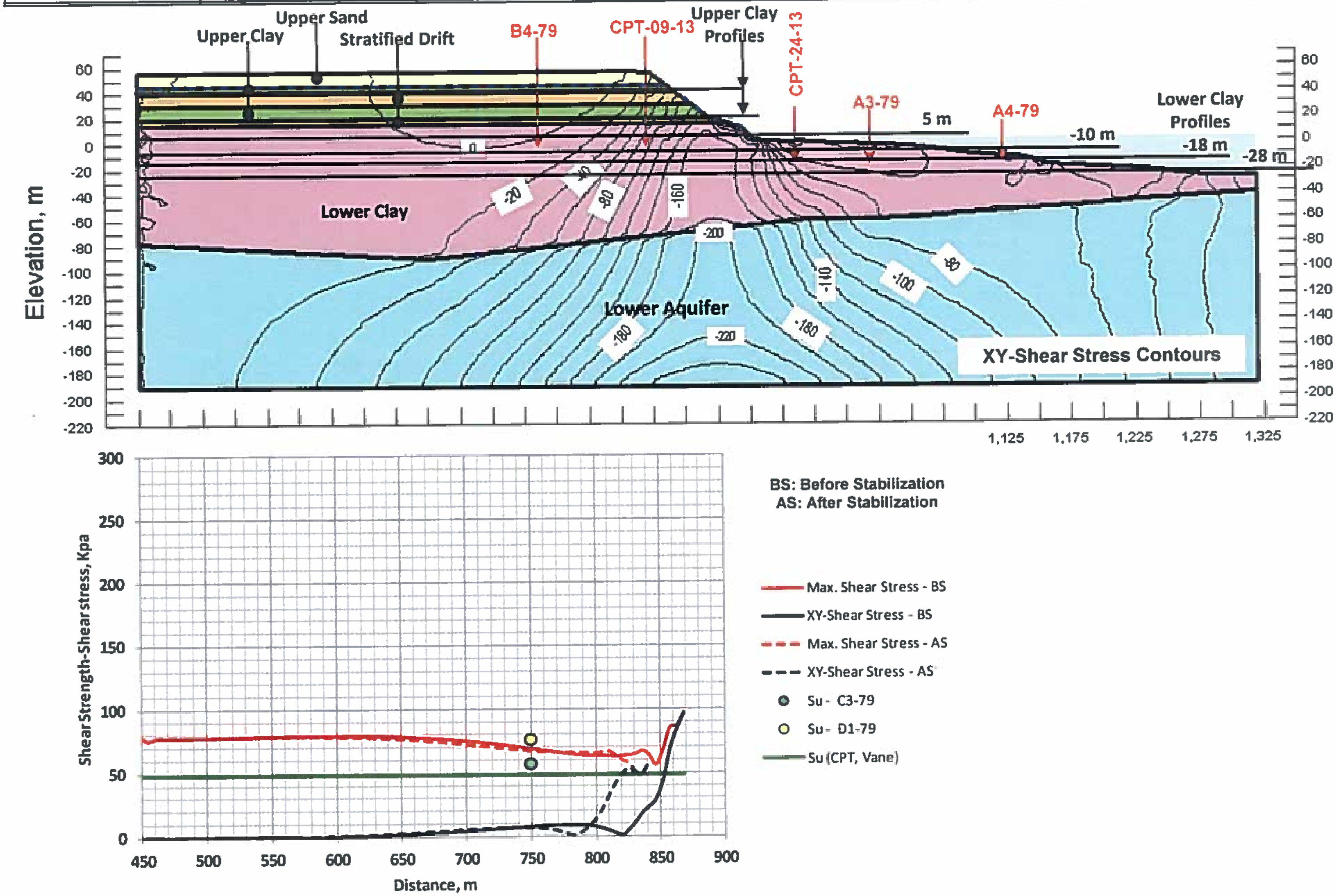

SNC·LAVALIN	NORTH SPUR STABILIZATION WORKS - Progressive Failure Study		Revision
	Nalcor Doc. No. MFA-SN-CD-2800-GT-RP-0001 Rev. A1	SLI Doc. No. 505573-3281-4GER-0001-PB	Date
	Figure C-14	SECTION B-B – UPPER CLAY MODEL - SHEAR STRESSES AND STRENGTH ON LINE 20M	16-JUN-2015

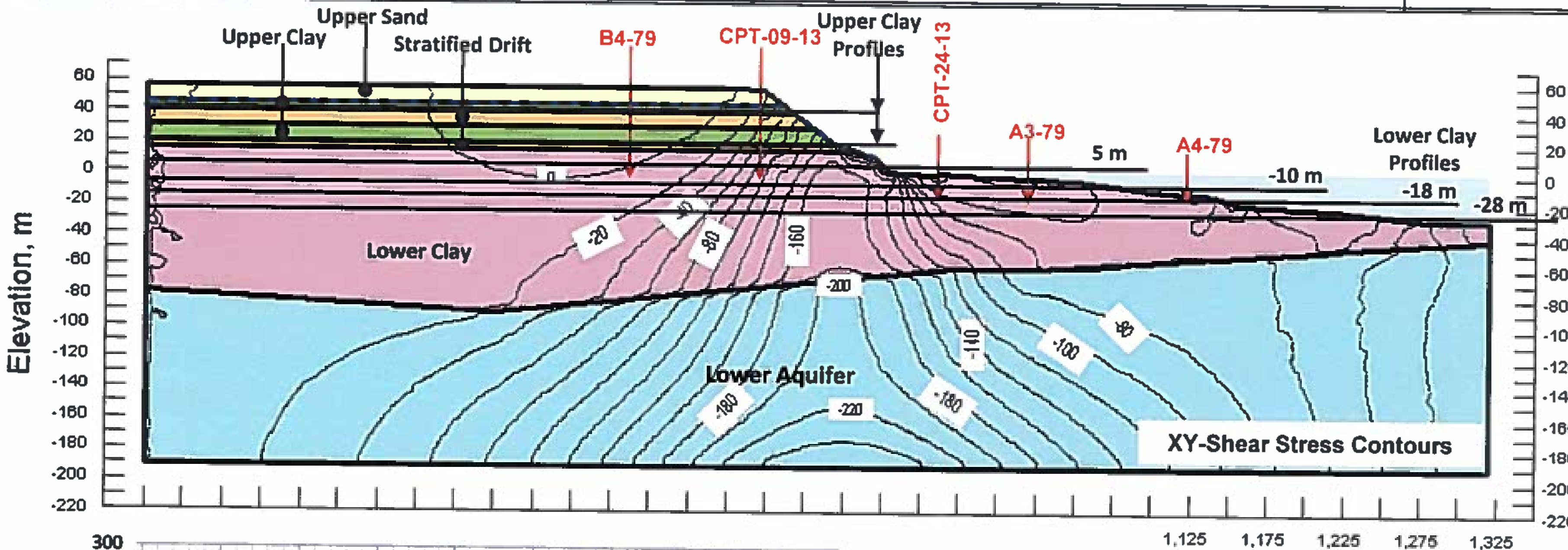

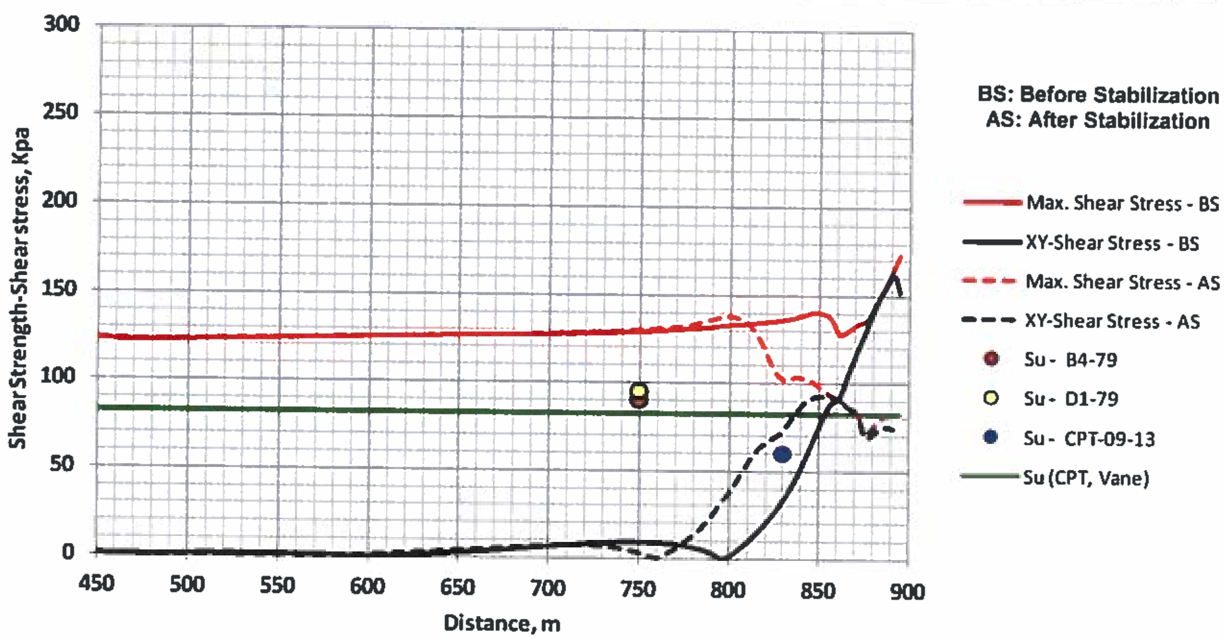

SNC·LAVALIN	NORTH SPUR STABILIZATION WORKS - Progressive Failure Study		Revision
	Nalcor Doc. No. MFA-SN-CD-2800-GT-RP-0001 Rev. A1	SLI Doc. No. 505573-3281-4GER-0001-PB	Date
	Figure C-15	SECTION B-B – UPPER CLAY MODEL - SHEAR STRESSES AND STRENGTH RELATIVE TO CREST	16-JUN-2015

Upper Clay – Level 40 m

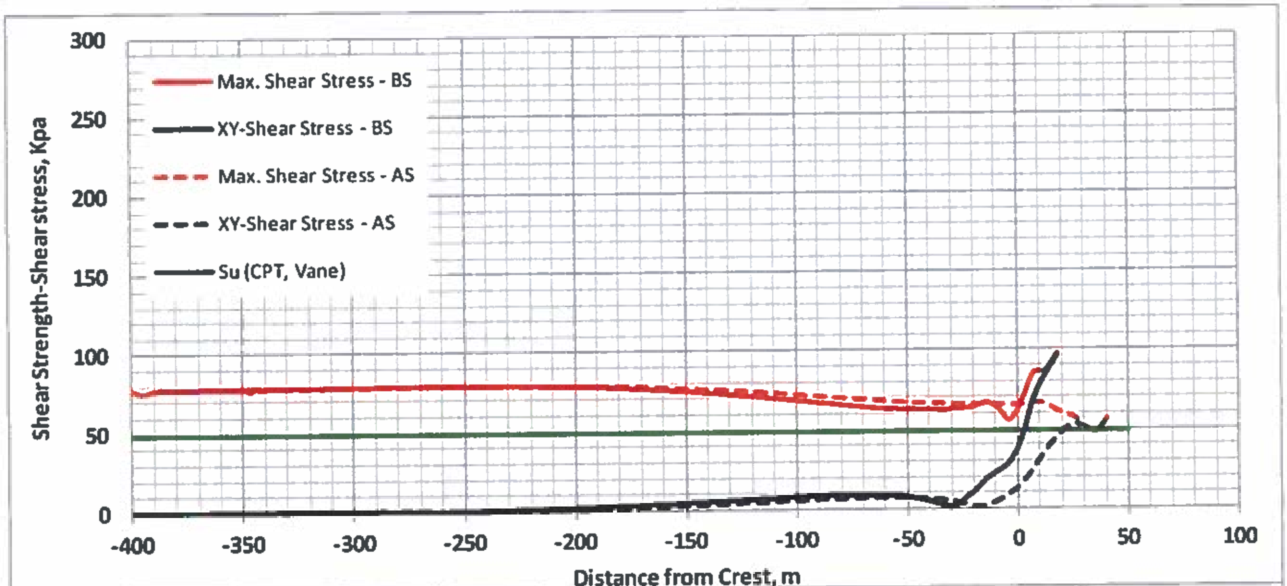

Upper Clay – Level 20 m

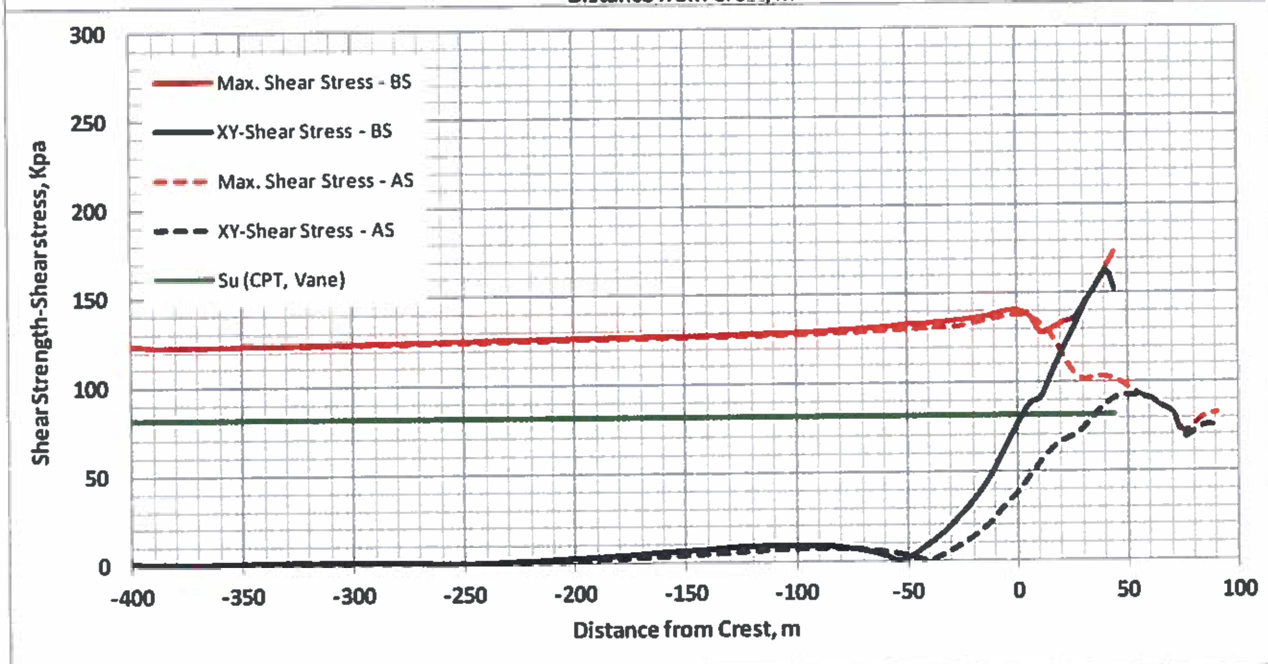

SNC·LAVALIN	NORTH SPUR STABILIZATION WORKS - Progressive Failure Study		Revision
	Nalcor Doc. No. MFA-SN-CD-2800-GT-RP-0001 Rev. A1	SLI Doc. No. 505573-3281-4GER-0001-PB	Date
	Figure C-16	SECTION B-B – LOWER CLAY MODEL - SHEAR STRESSES AND STRENGTH ON LINE -5M	16-JUN-2015

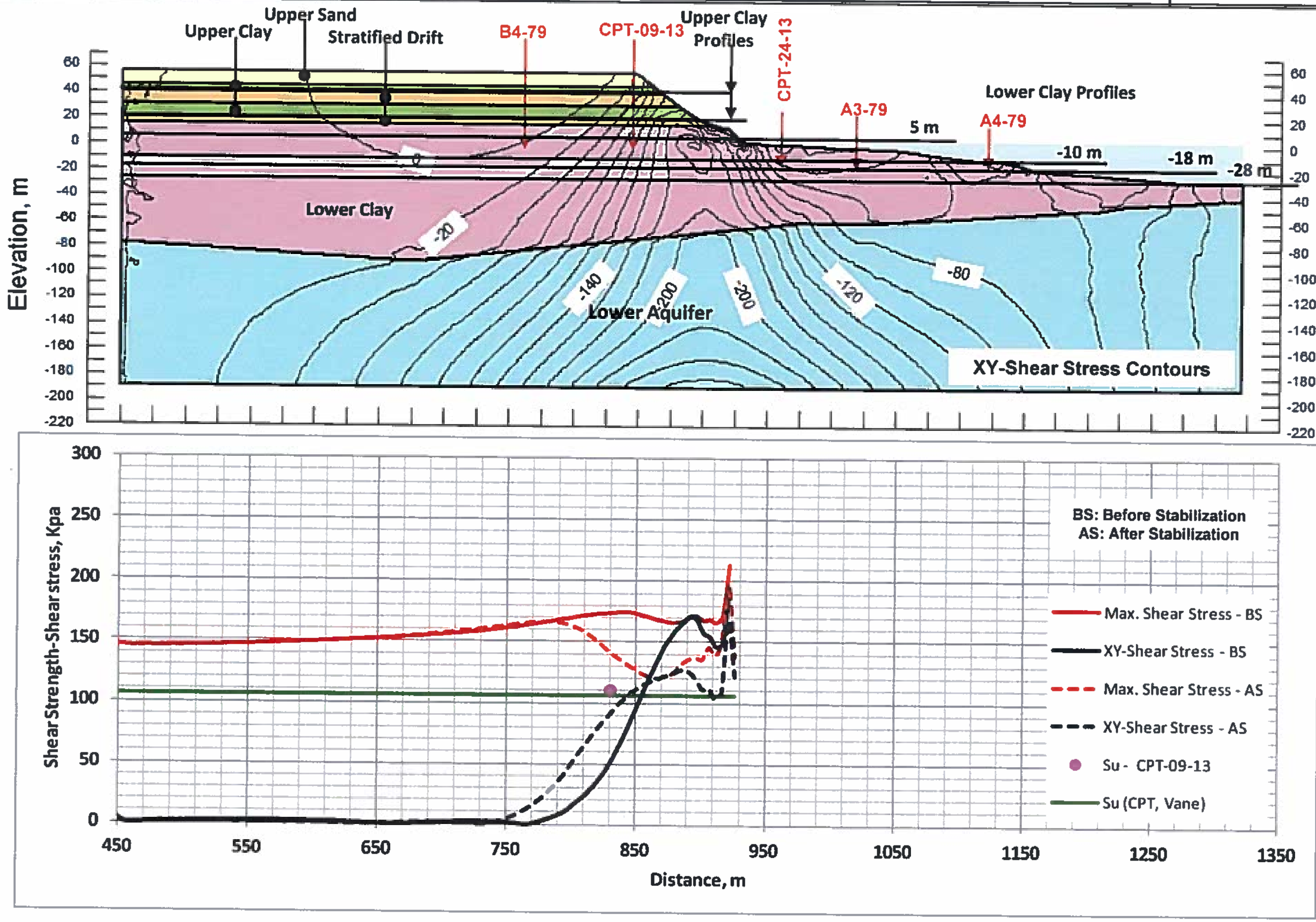

SNC·LAVALIN	NORTH SPUR STABILIZATION WORKS - Progressive Failure Study		Revision
	Nalcor Doc. No. MFA-SN-CD-2800-GT-RP-0001 Rev. A1	SLI Doc. No. 505573-3281-4GER-0001-PB	Date
	Figure C-17	SECTION B-B – LOWER CLAY MODEL - SHEAR STRESSES AND STRENGTH ON LINE -10M	16-JUN-2015

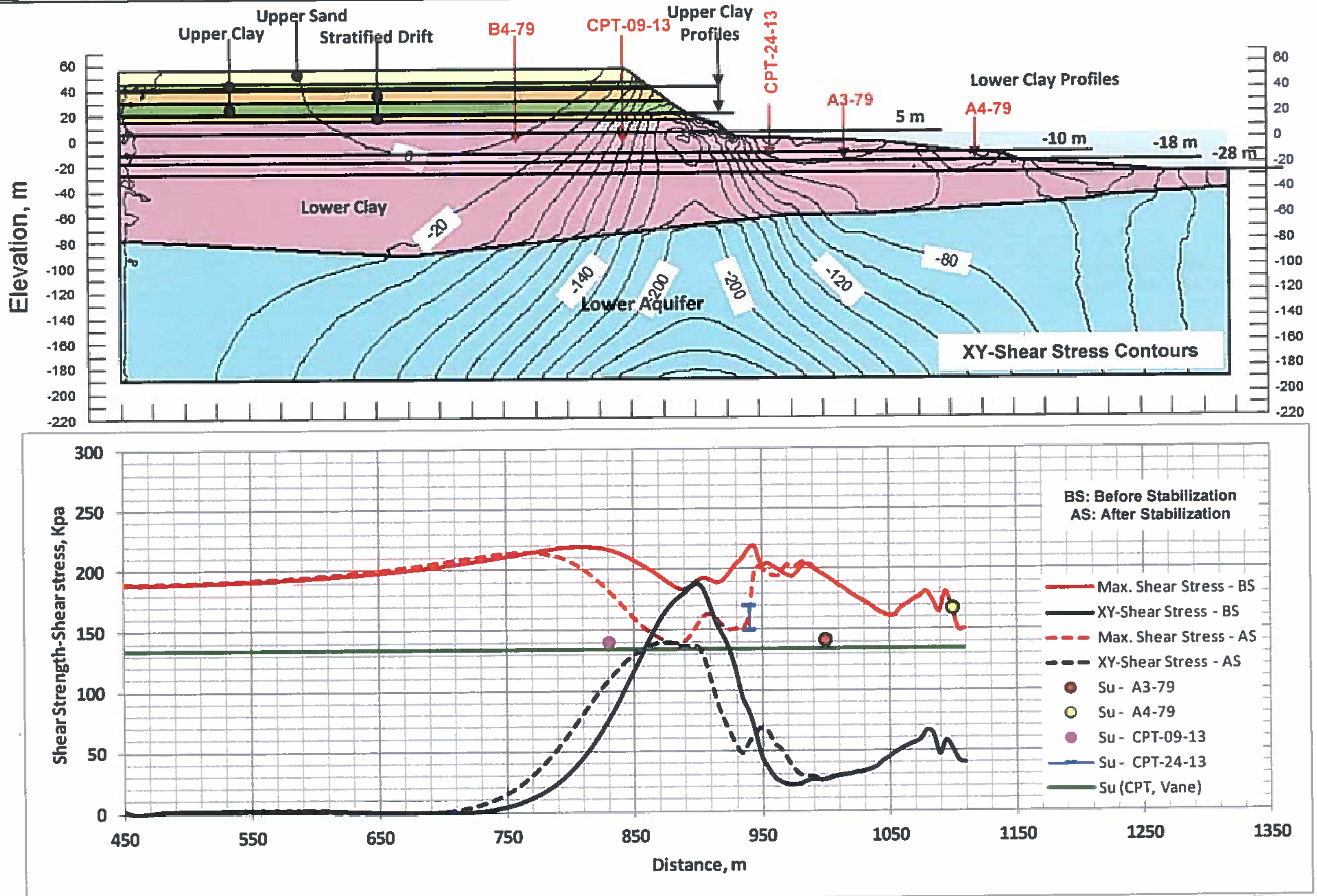

SNC·LAVALIN	NORTH SPUR STABILIZATION WORKS - Progressive Failure Study		Revision
	Nalcor Doc. No. MFA-SN-CD-2800-GT-RP-0001 Rev. A1	SLI Doc. No. 505573-3281-4GER-0001-PB	Date
	Figure C-18	SECTION B-B – LOWER CLAY MODEL - SHEAR STRESSES AND STRENGTH ON LINE -18M	16-JUN-2015

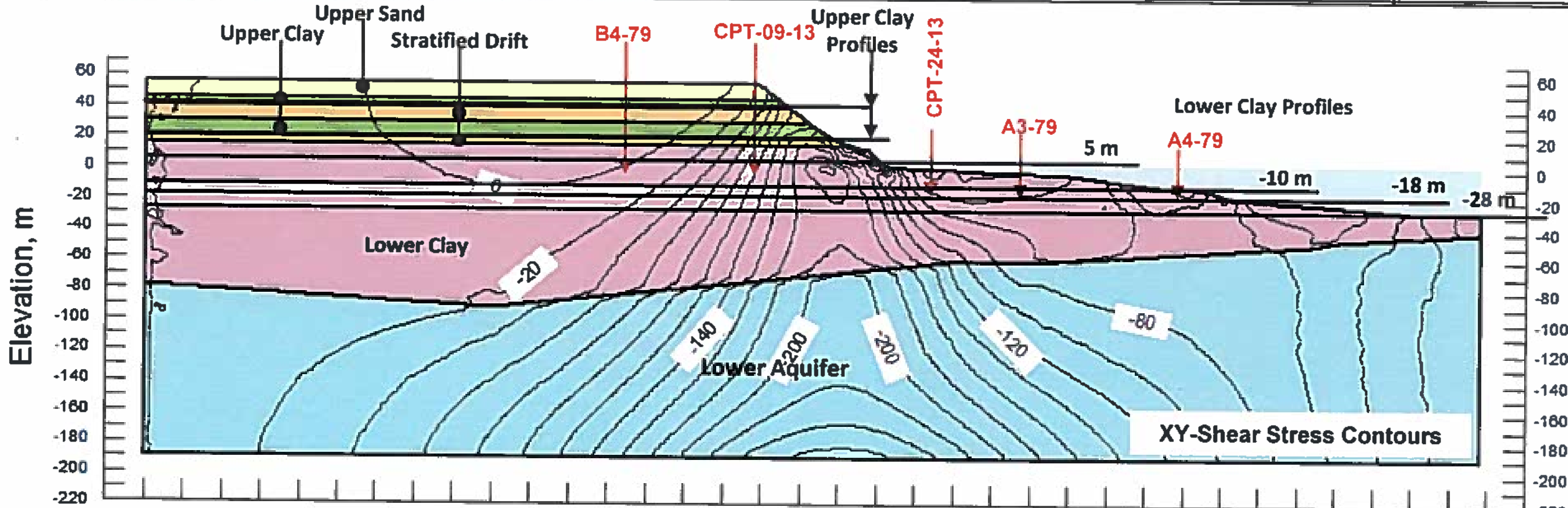

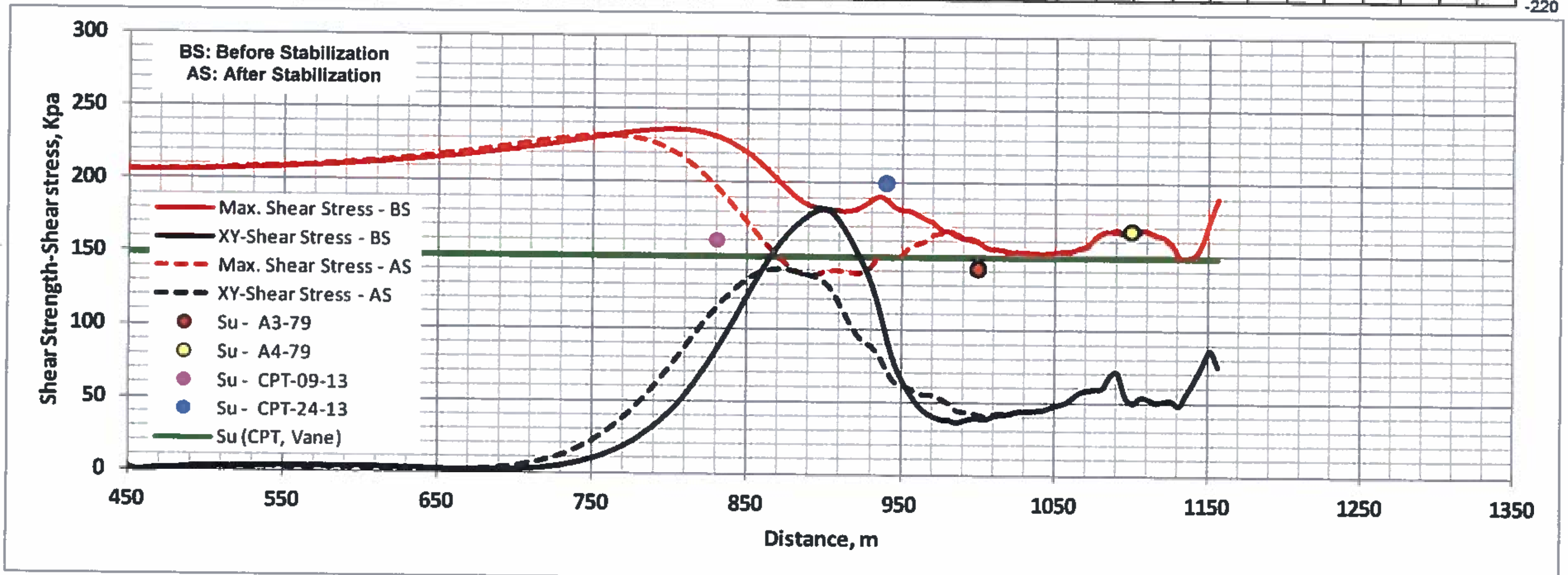

SNC·LAVALIN	NORTH SPUR STABILIZATION WORKS - Progressive Failure Study		Revision
	Nalcor Doc. No. MFA-SN-CD-2800-GT-RP-0001 Rev. A1	SLI Doc. No. 505573-3281-4GER-0001-PB	Date
	Figure C-19	SECTION B-B – LOWER CLAY MODEL - SHEAR STRESSES AND STRENGTH ON LINE -28M	16-JUN-2015

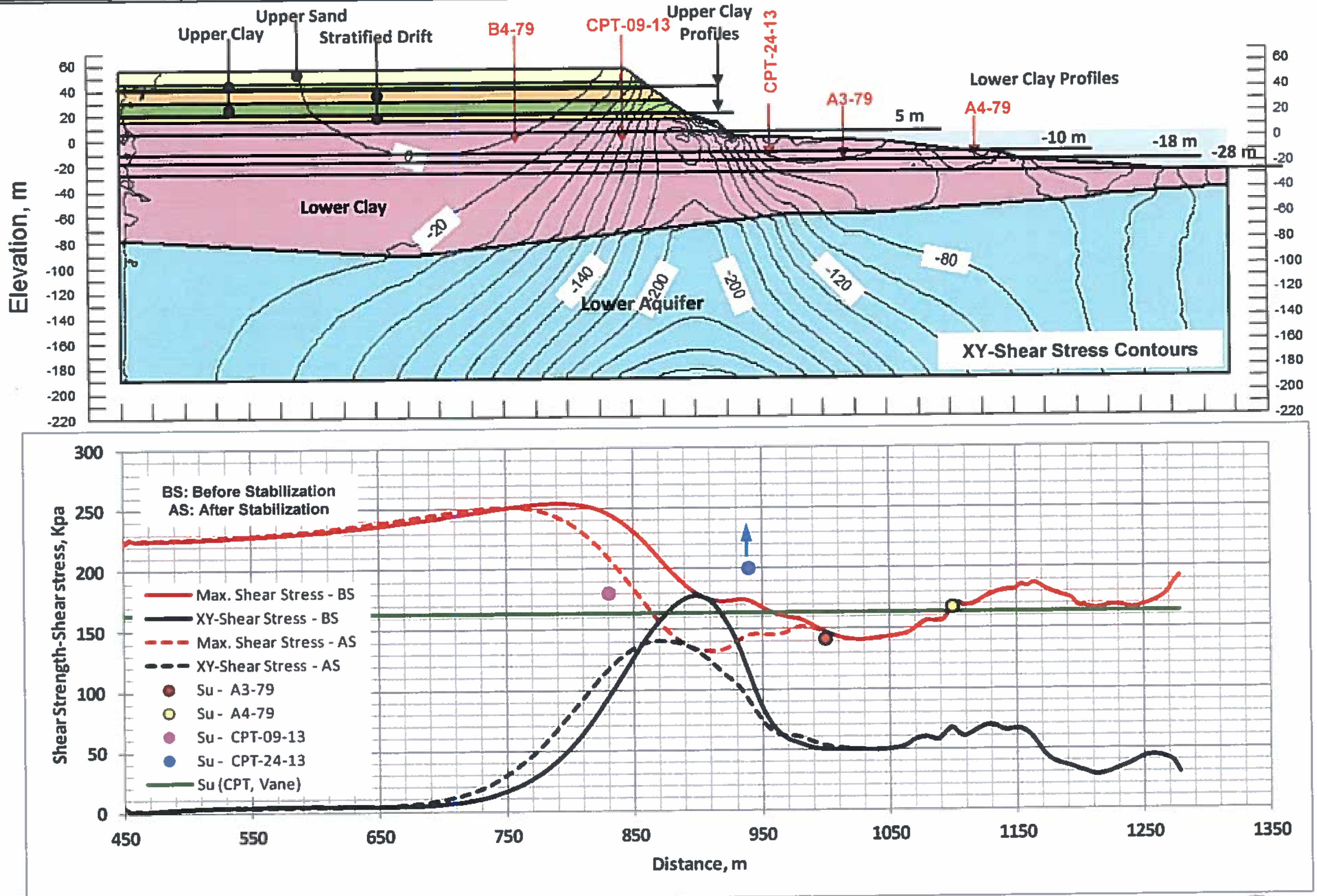

SNC·LAVALIN	NORTH SPUR STABILIZATION WORKS - Progressive Failure Study		Revision
	Nalcor Doc. No. MFA-SN-CD-2800-GT-RP-0001 Rev. A1	SLI Doc. No. 505573-3281-4GER-0001-PB	Date
	Figure C-20	MOHR CIRCLES AND LAMBE REPRESENTATION ON HORIZONTAL PLAN AT ELEV. -10 M	16-JUN-2015

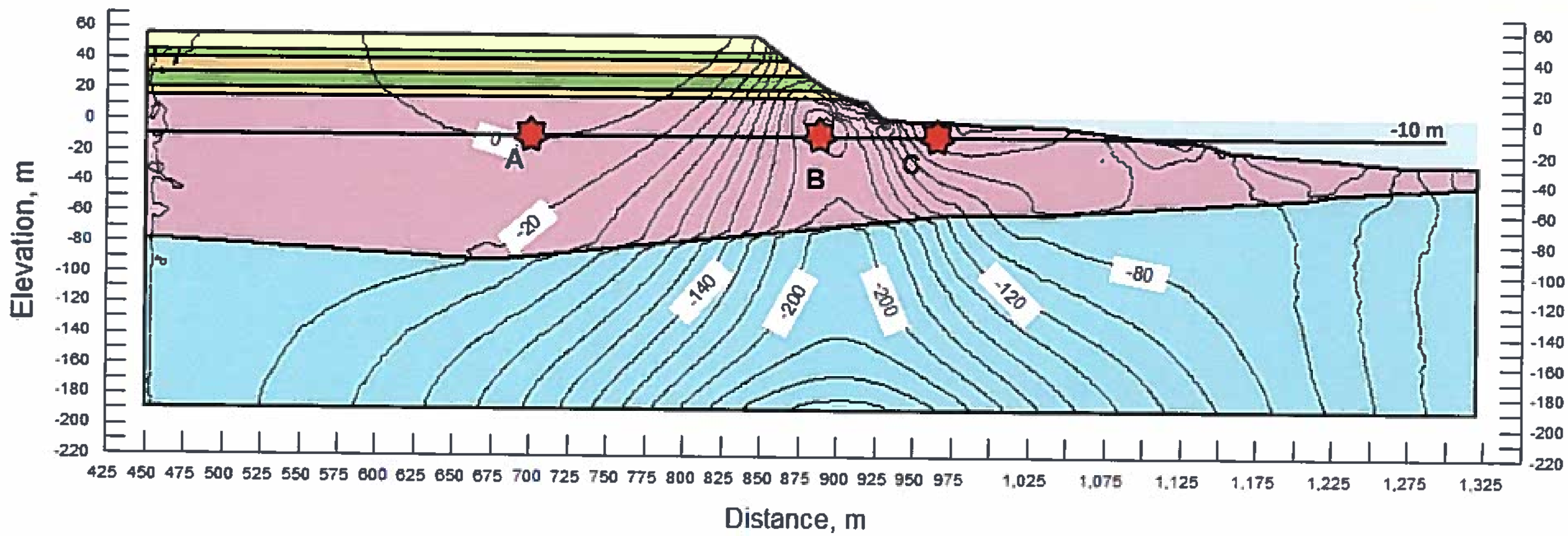

Mohr Circles and Lambe Representation on Horizontal Plan at Elev. -10 m

SNC·LAVALIN	NORTH SPUR STABILIZATION WORKS - Progressive Failure Study		Revision
	Nalcor Doc. No. MFA-SN-CD-2800-GT-RP-0001 Rev. A1	SLI Doc. No. 505573-3281-4GER-0001-PB	Date
	Figure C-21	MOHR CIRCLES AFTER STABILIZATION - POINTS A, B AND C AT ELEV. -10 M	16-JUN-2015

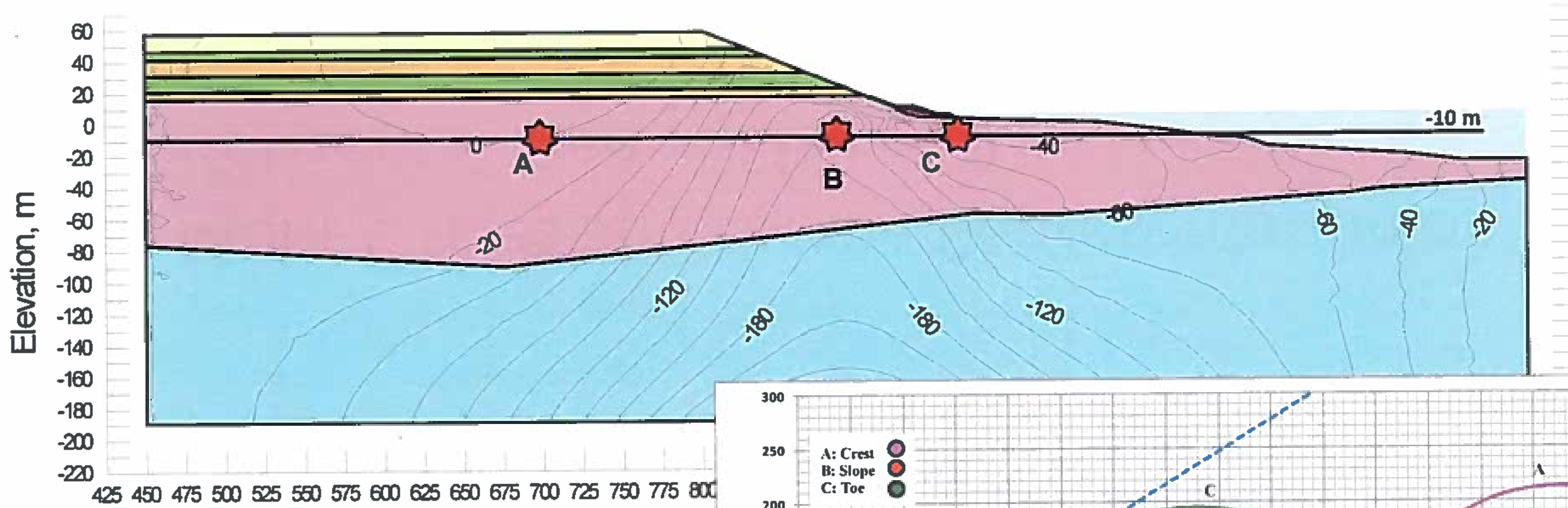

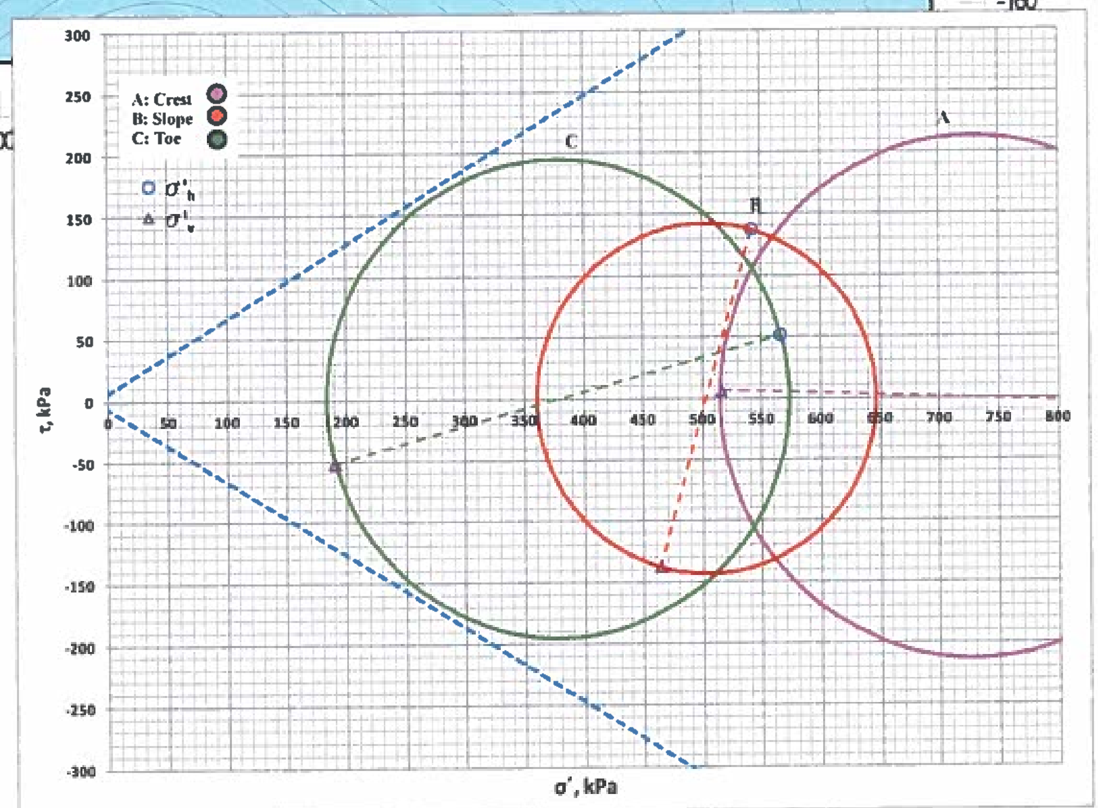

SNC·LAVALIN	NORTH SPUR STABILIZATION WORKS - Progressive Failure Study		Revision
	Nalcor Doc. No. MFA-SN-CD-2800-GT-RP-0001 Rev. A1	SLI Doc. No. 505573-3281-4GER-0001-PB	Date
	Figure C-22	SECTION B-B – LOWER CLAY MODEL – STRESSES ON LINE -10M – POINT A	16-JUN-2015

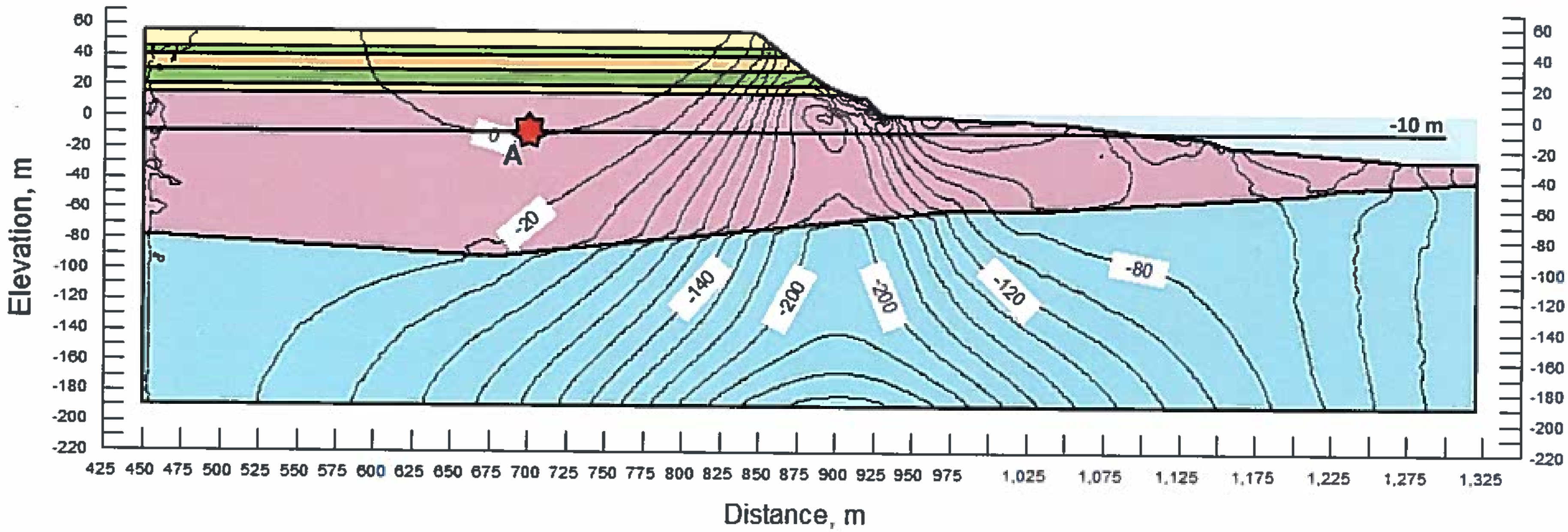

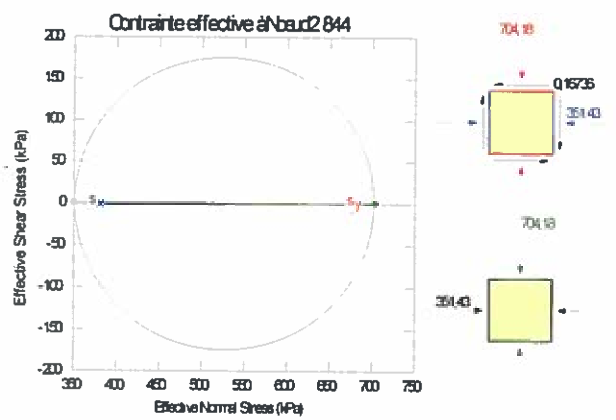

Initial State

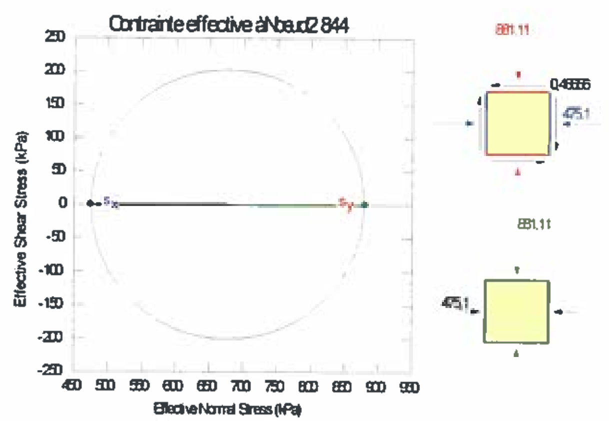

Before Stabilization

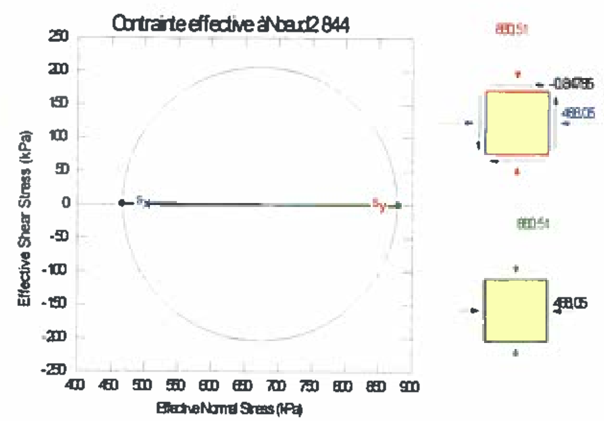

After Stabilization

SNC·LAVALIN	NORTH SPUR STABILIZATION WORKS - Progressive Failure Study		Revision
	Nalcor Doc. No. MFA-SN-CD-2800-GT-RP-0001 Rev. A1	SLI Doc. No. 505573-3281-4GER-0001-PB	Date
	Figure C-23	SECTION B-B – LOWER CLAY MODEL – STRESS PATH ON LINE -10M – POINT A	16-JUN-2015

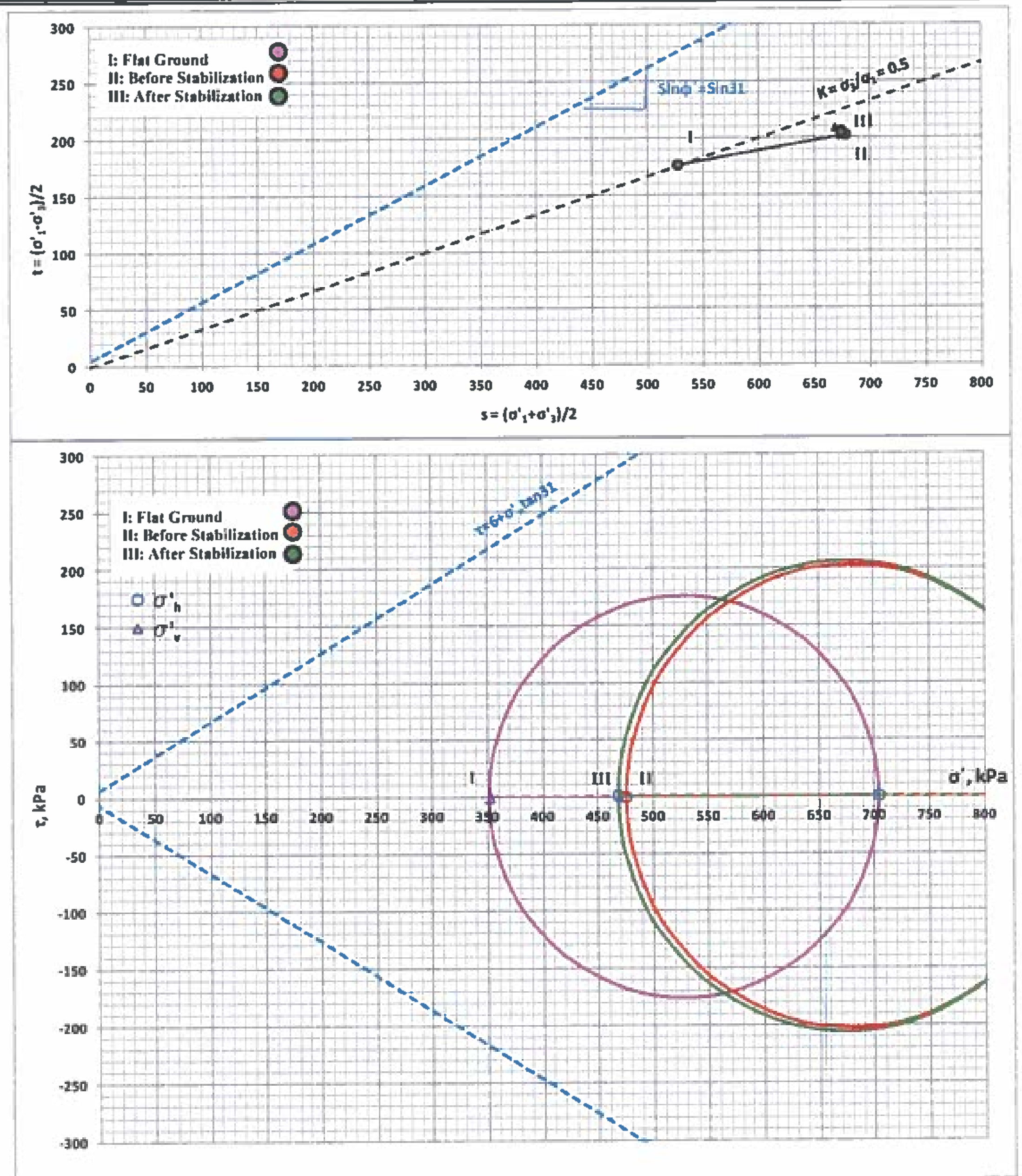

SNC•LAVALIN	NORTH SPUR STABILIZATION WORKS - Progressive Failure Study		Revision
	Nalcor Doc. No. MFA-SN-CD-2800-GT-RP-0001 Rev. A1	SLI Doc. No. 505573-3281-4GER-0001-PB	Date
	Figure C-24	SECTION B-B – LOWER CLAY MODEL – STRESSES ON LINE -10M – POINT B	16-JUN-2015

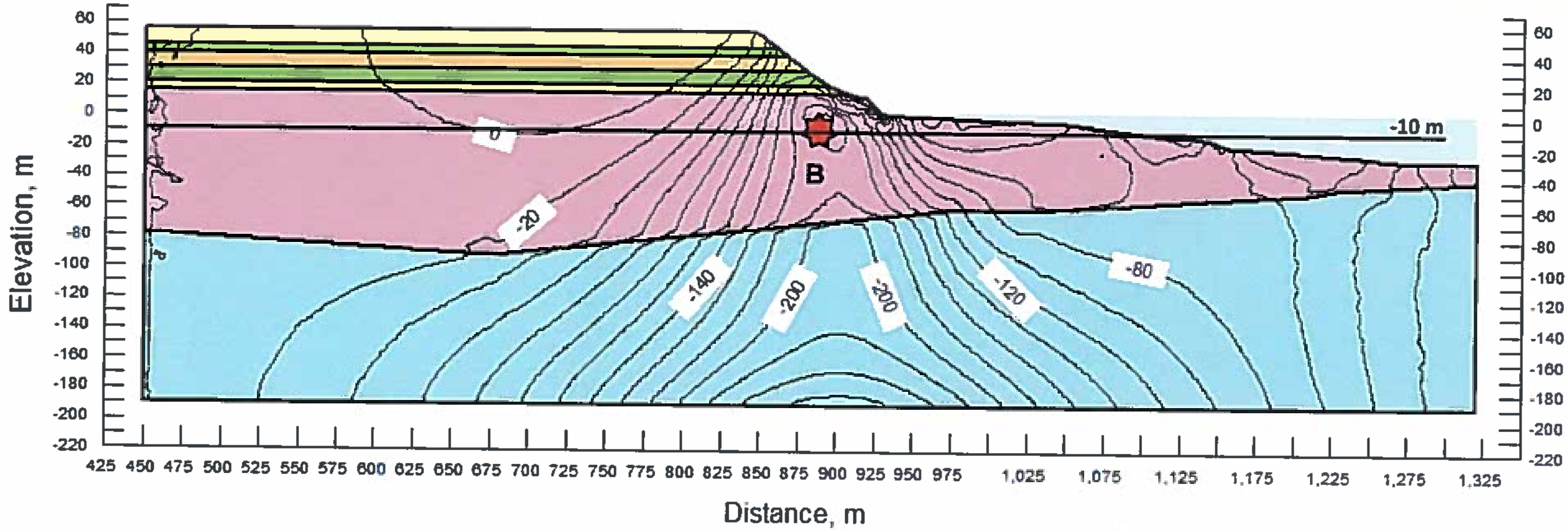

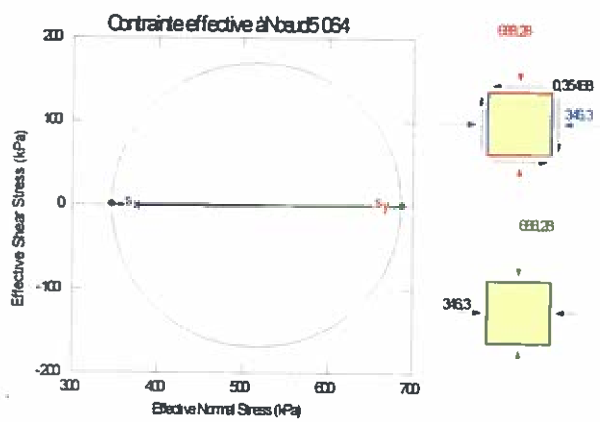

Initial State

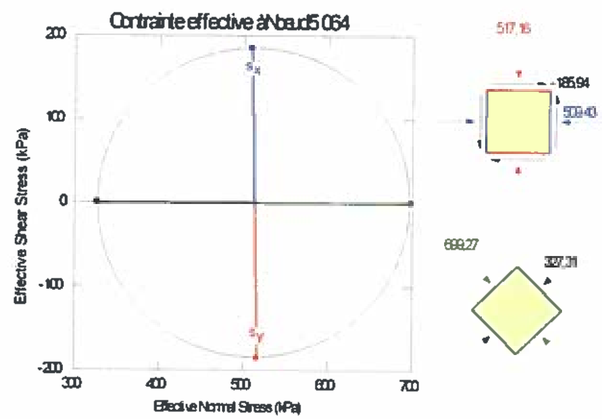

Before Stabilization

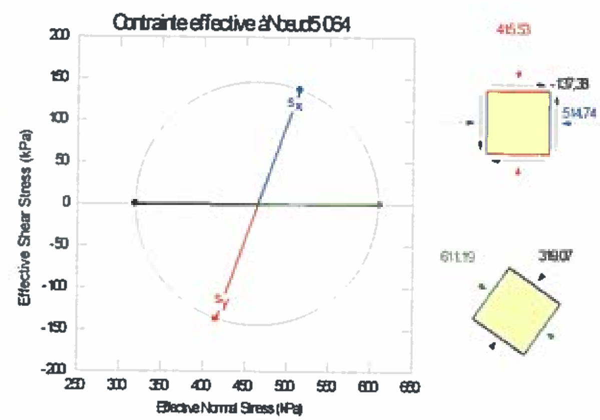

After Stabilization

SNC·LAVALIN	NORTH SPUR STABILIZATION WORKS - Progressive Failure Study		Revision
	Nalcor Doc. No. MFA-SN-CD-2800-GT-RP-0001 Rev. A1	SLI Doc. No. 505573-3281-4GER-0001-PB	Date
	Figure C-25	SECTION B-B – LOWER CLAY MODEL – STRESS PATH ON LINE -10M – POINT B	16-JUN-2015

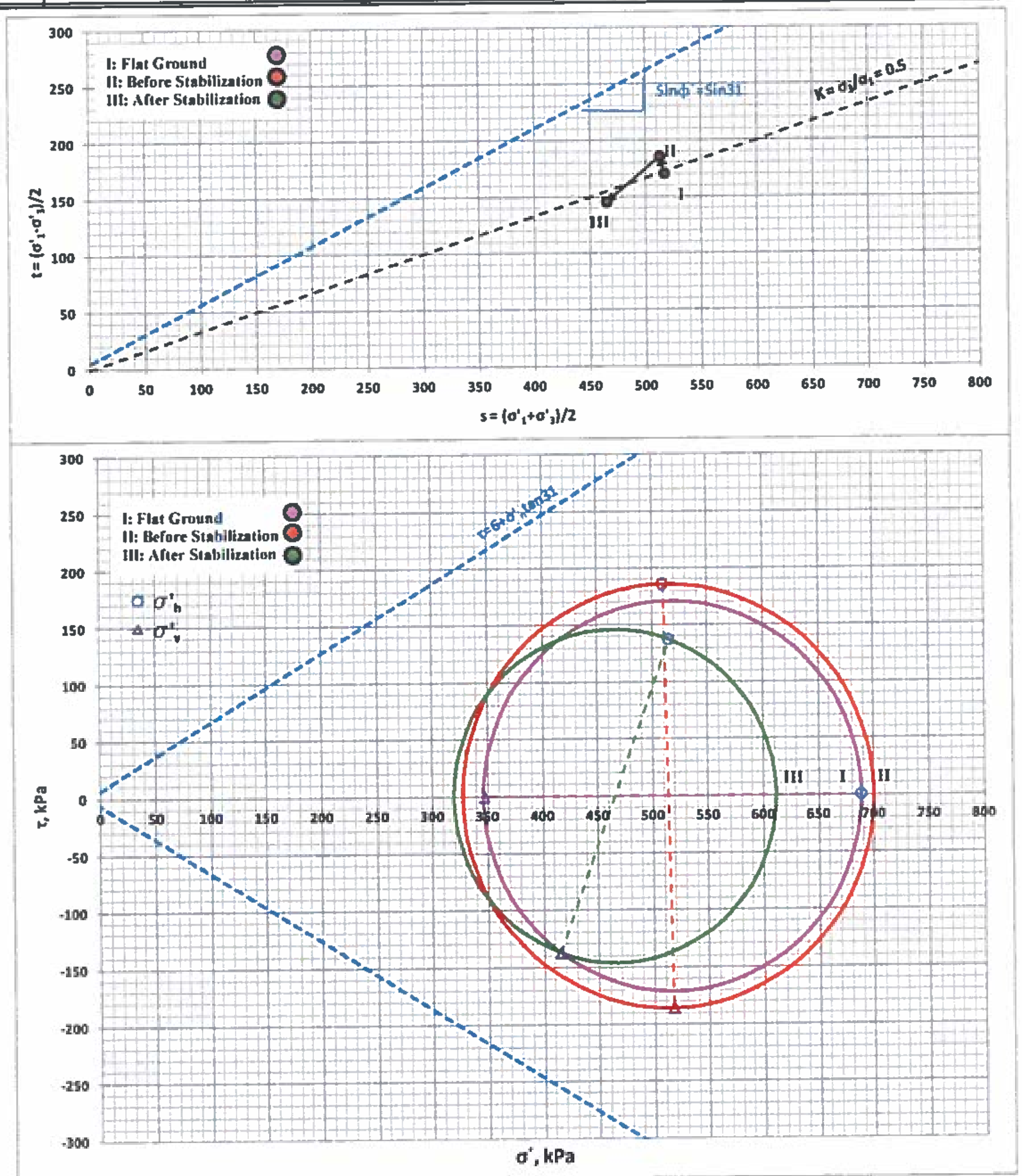

SNC·LAVALIN	NORTH SPUR STABILIZATION WORKS - Progressive Failure Study		Revision
	Nalcor Doc. No. MFA-SN-CD-2800-GT-RP-0001 Rev. A1	SLI Doc. No. 505573-3281-4GER-0001-PB	Date
	Figure C-26	SECTION B-B – LOWER CLAY MODEL – STRESSES ON LINE -10M – POINT C	16-JUN-2015

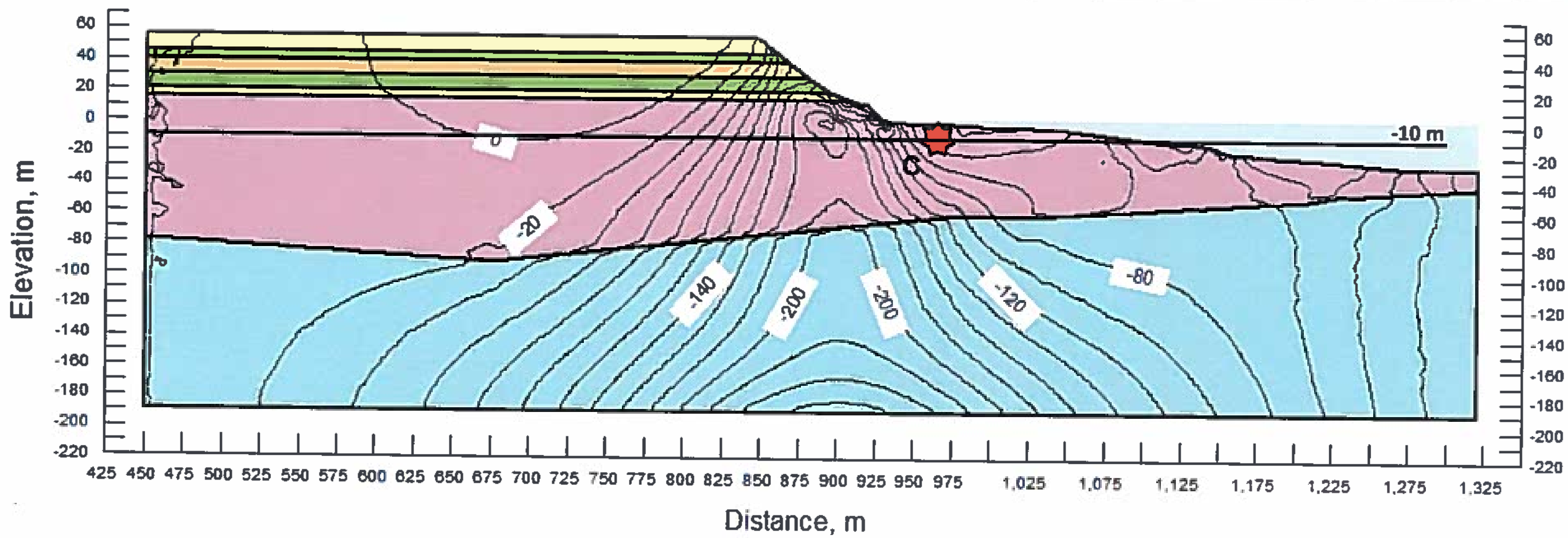

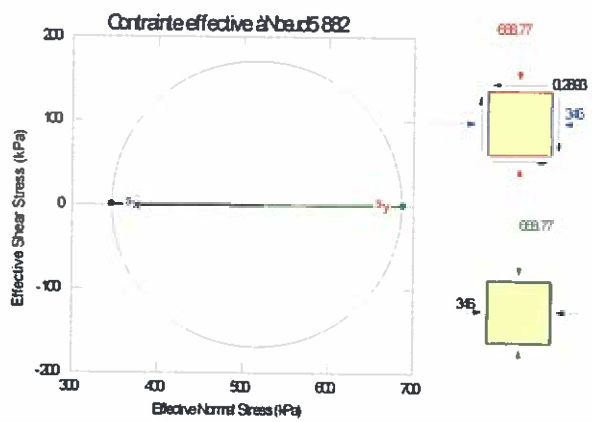

Initial State

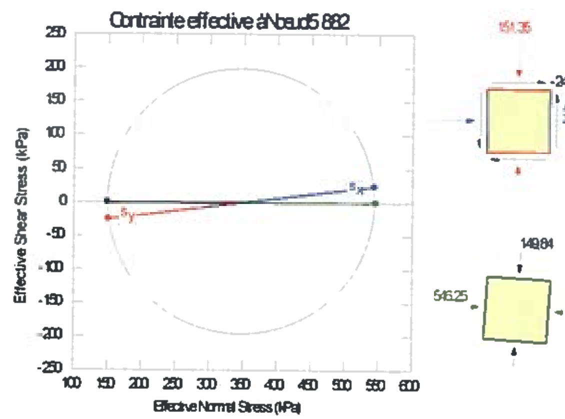

Before Stabilization

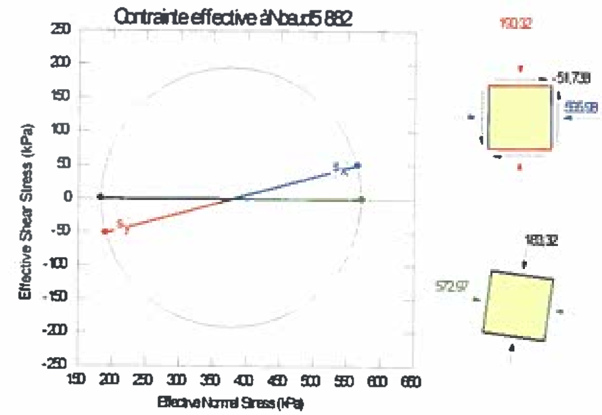

After Stabilization

SNC·LAVALIN	NORTH SPUR STABILIZATION WORKS - Progressive Failure Study		Revision
	Nalcor Doc. No. MFA-SN-CD-2800-GT-RP-0001 Rev. A1	SLI Doc. No. 505573-3281-4GER-0001-PB	Date
	Figure C-27	SECTION B-B – LOWER CLAY MODEL – STRESS PATH ON LINE -10M – POINT C	16-JUN-2015

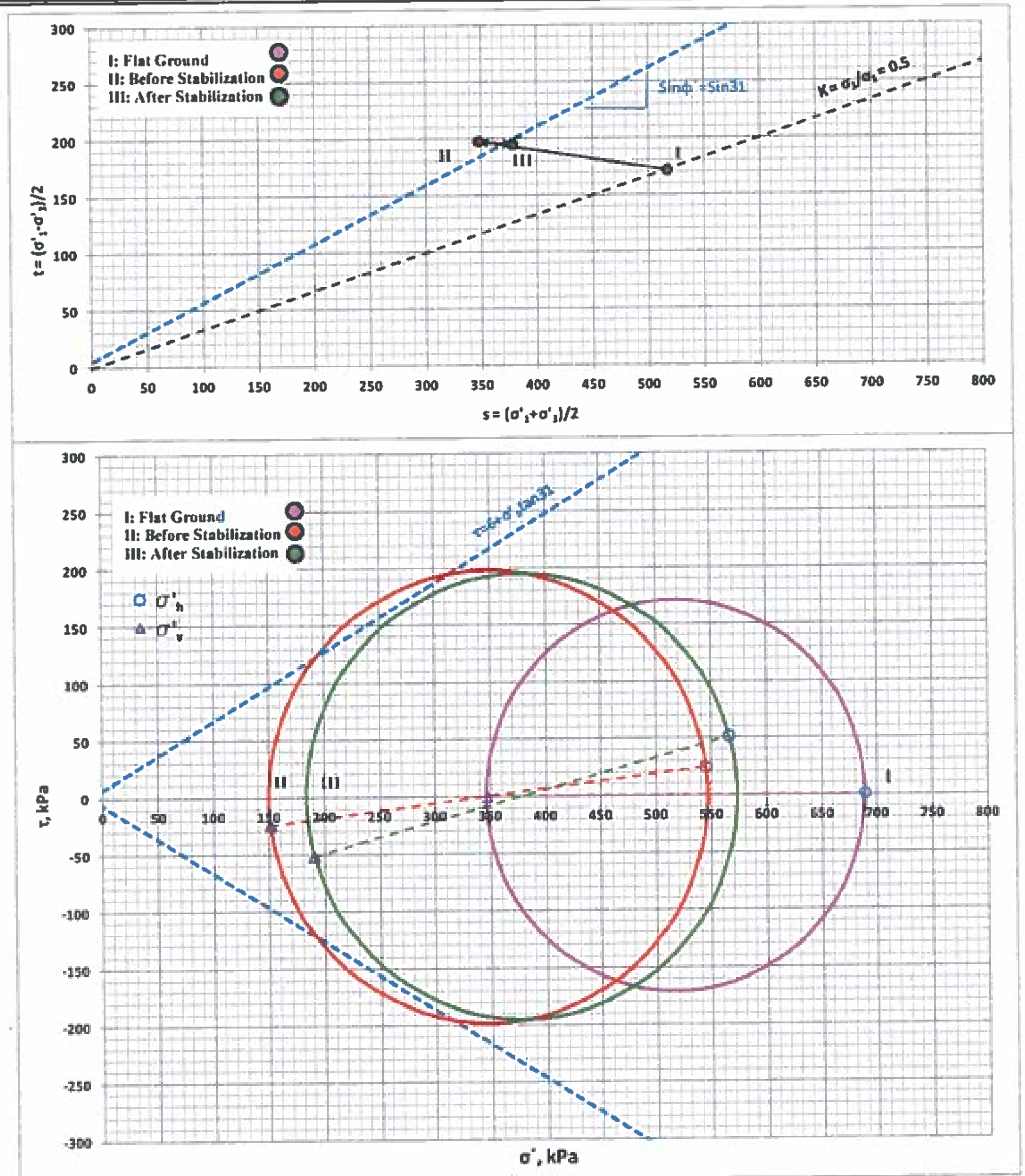

SNC·LAVALIN	NORTH SPUR STABILIZATION WORKS - Progressive Failure Study		Revision
	Nalcor Doc. No. MFA-SN-CD-2800-GT-RP-0001 Rev. A1	SLI Doc. No. 505573-3281-4GER-0001-PB	Date
	Figure C-28	MOHR CIRCLES AND LAMBE REPRESENTATION ON HORIZONTAL PLAN AT ELEV. -18 M	16-JUN-2015

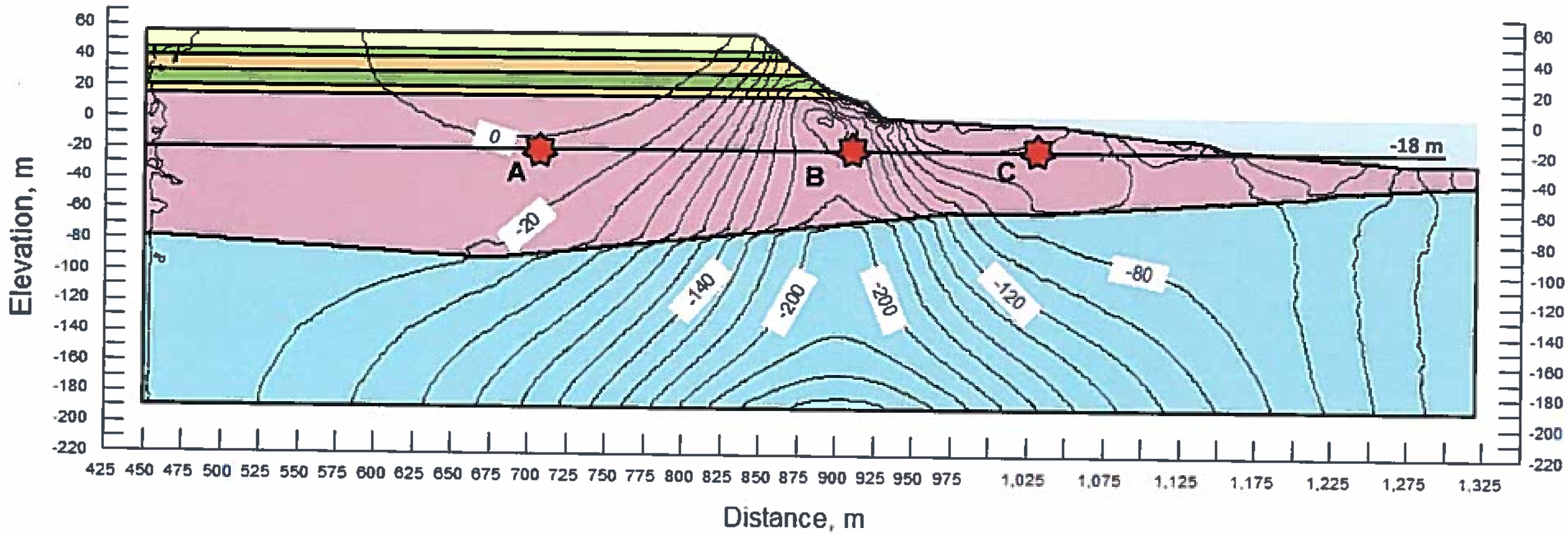

Mohr Circles and Lambe Representation on Horizontal Plan at Elev. -18 m

SNC·LAVALIN	NORTH SPUR STABILIZATION WORKS - Progressive Failure Study		Revision
	Nalcor Doc. No. MFA-SN-CD-2800-GT-RP-0001 Rev. A1	SLI Doc. No. 505573-3281-4GER-0001-PB	Date
	Figure C-29	MOHR CIRCLES AFTER STABILIZATION - POINTS A, B AND C AT ELEV. -18 M	16-JUN-2015

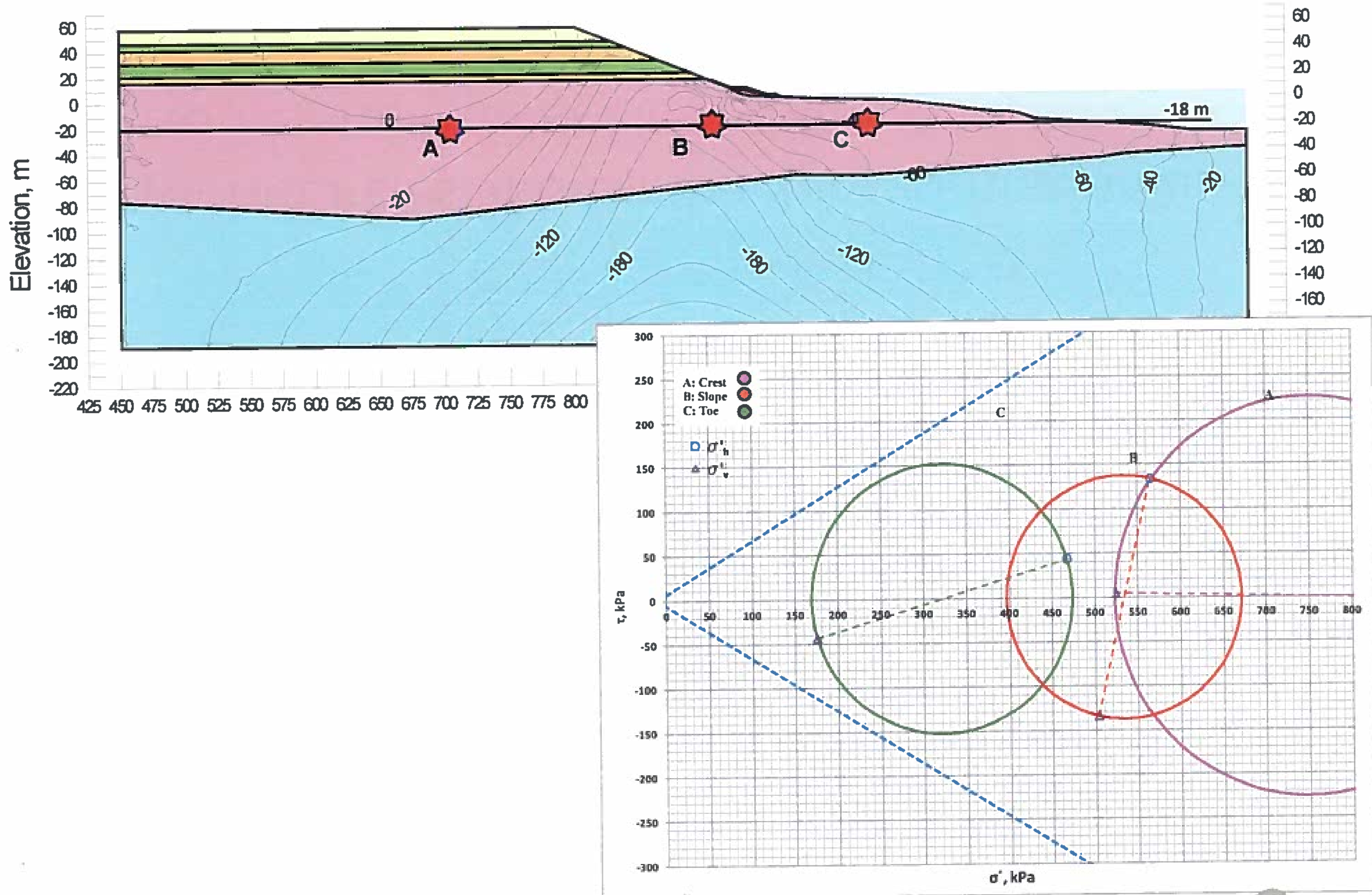

SNC·LAVALIN	NORTH SPUR STABILIZATION WORKS - Progressive Failure Study		Revision
	Nalcor Doc. No. MFA-SN-CD-2800-GT-RP-0001 Rev. A1	SLI Doc. No. 505573-3281-4GER-0001-PB	Date
	Figure C-30	SECTION B-B – LOWER CLAY MODEL – STRESSES ON LINE -18M – POINT A	16-JUN-2015

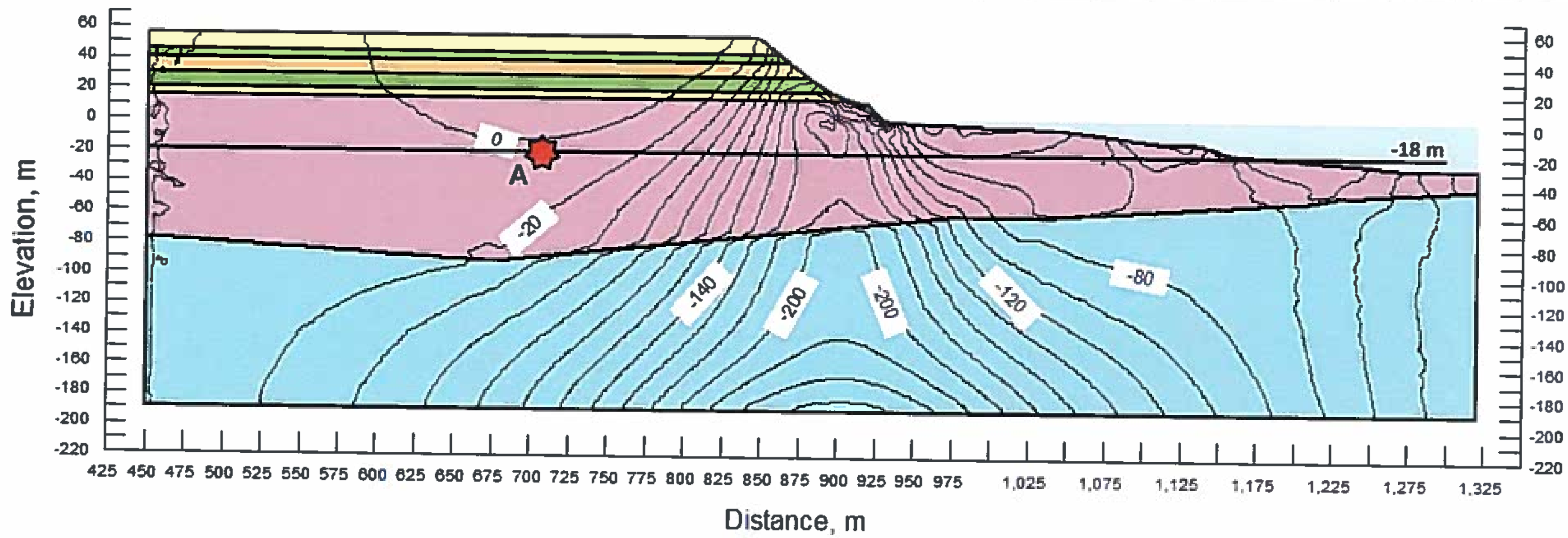

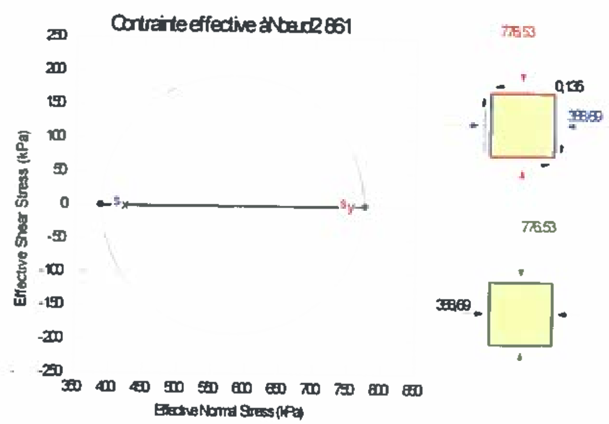

Initial State

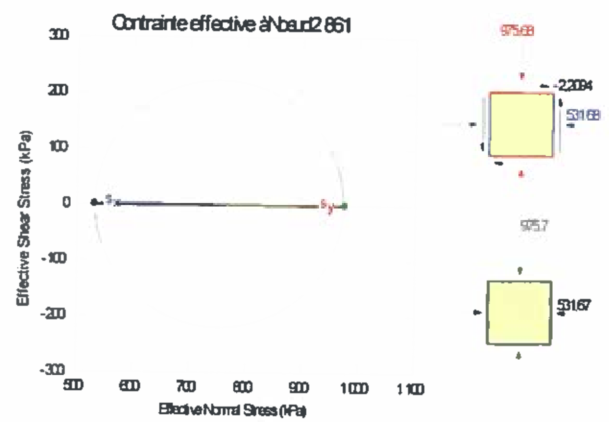

Before Stabilization

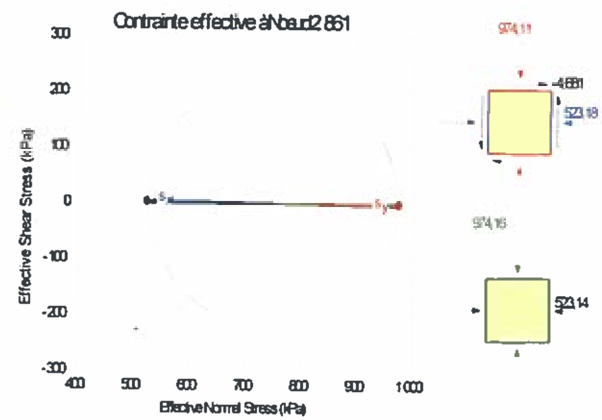

After Stabilization

SNC·LAVALIN	NORTH SPUR STABILIZATION WORKS - Progressive Failure Study		Revision
	Nalcor Doc. No. MFA-SN-CD-2800-GT-RP-0001 Rev. A1	SLI Doc. No. 505573-3281-4GER-0001-PB	Date
	Figure C-31	SECTION B-B – LOWER CLAY MODEL – STRESS PATH ON LINE -18M – POINT A	16-JUN-2015

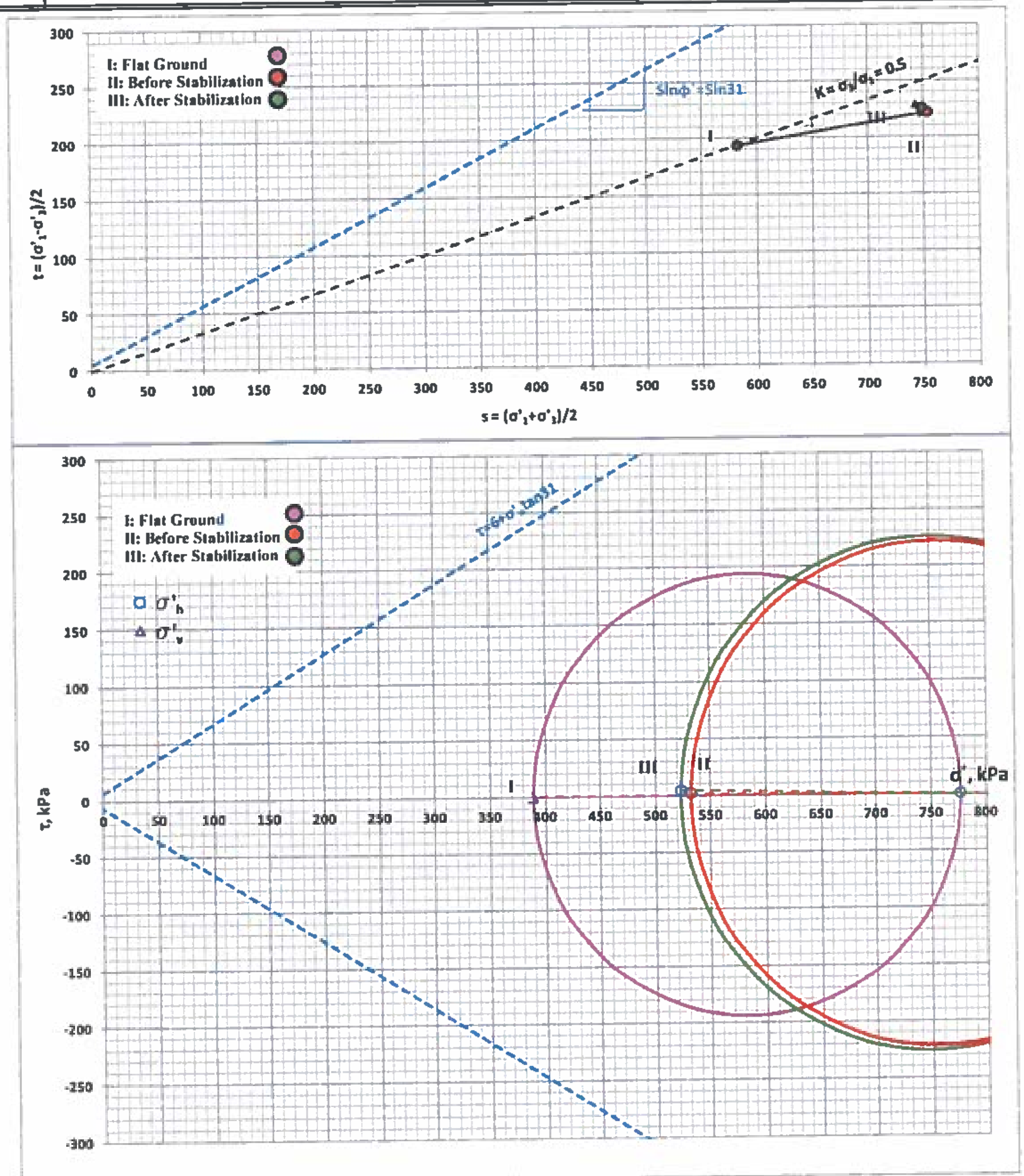

SNC·LAVALIN	NORTH SPUR STABILIZATION WORKS - Progressive Failure Study		Revision
	Nalcor Doc. No. MFA-SN-CD-2800-GT-RP-0001 Rev. A1	SLI Doc. No. 505573-3281-4GER-0001-PB	Date
	Figure C-32	SECTION B-B – LOWER CLAY MODEL – STRESSES ON LINE -18M – POINT B	16-JUN-2015

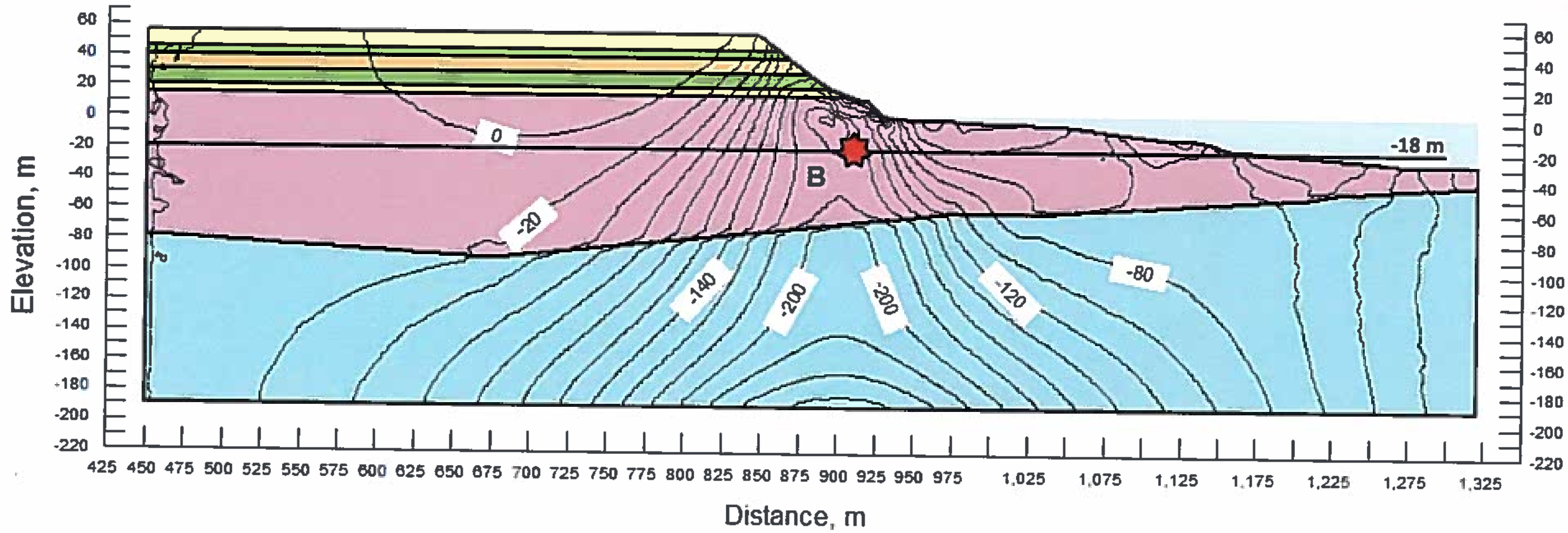

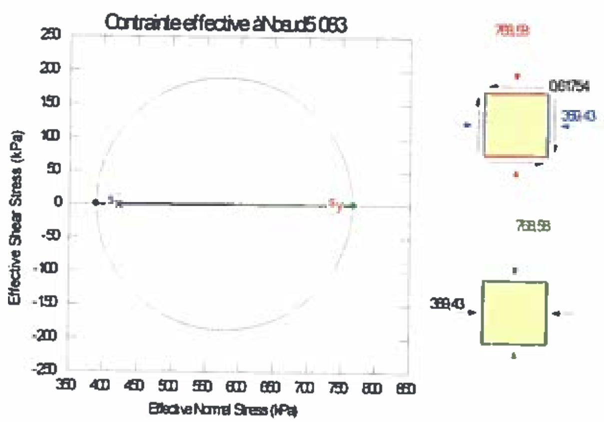

Initial State

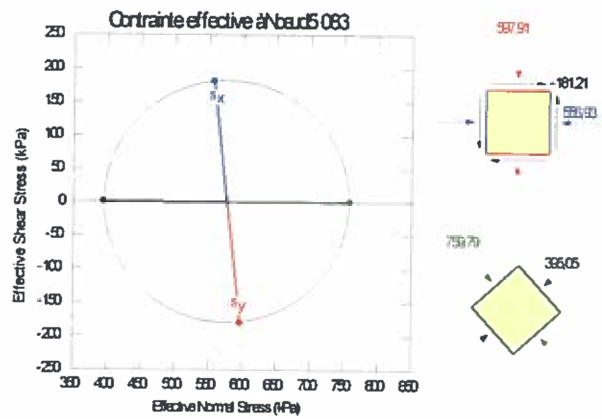

Before Stabilization

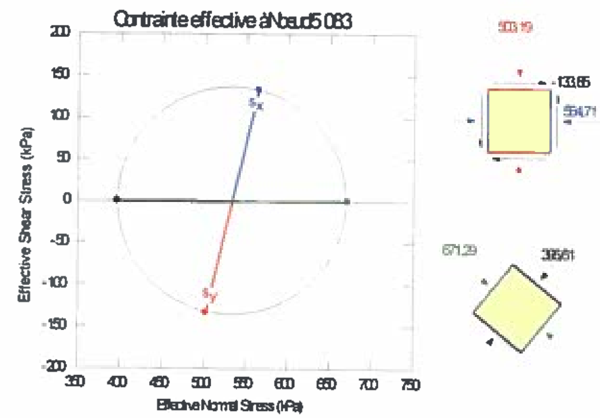

After Stabilization

SNC·LAVALIN	NORTH SPUR STABILIZATION WORKS - Progressive Failure Study		Revision
	Nalcor Doc. No. MFA-SN-CD-2800-GT-RP-0001 Rev. A1	SLI Doc. No. 505573-3281-4GER-0001-PB	Date
	Figure C-33	SECTION B-B – LOWER CLAY MODEL – STRESS PATH ON LINE -18M – POINT B	16-JUN-2015

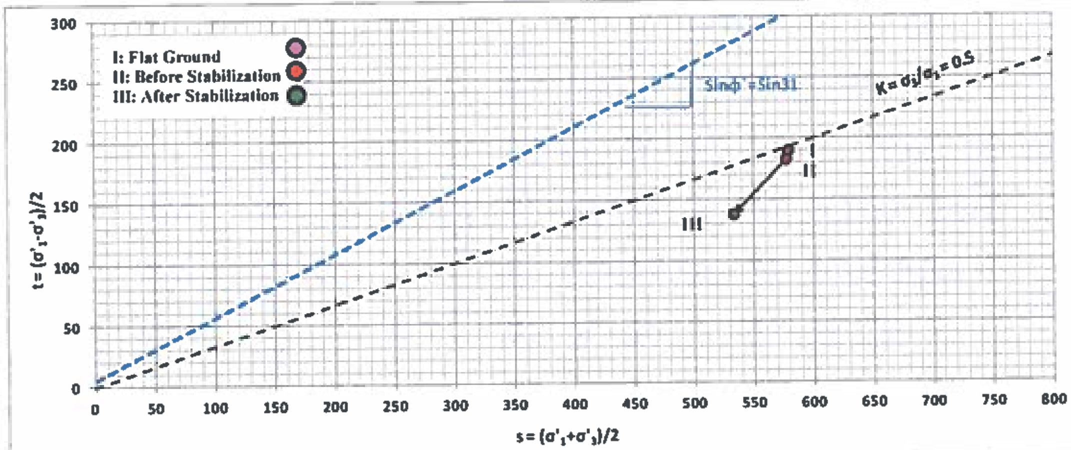

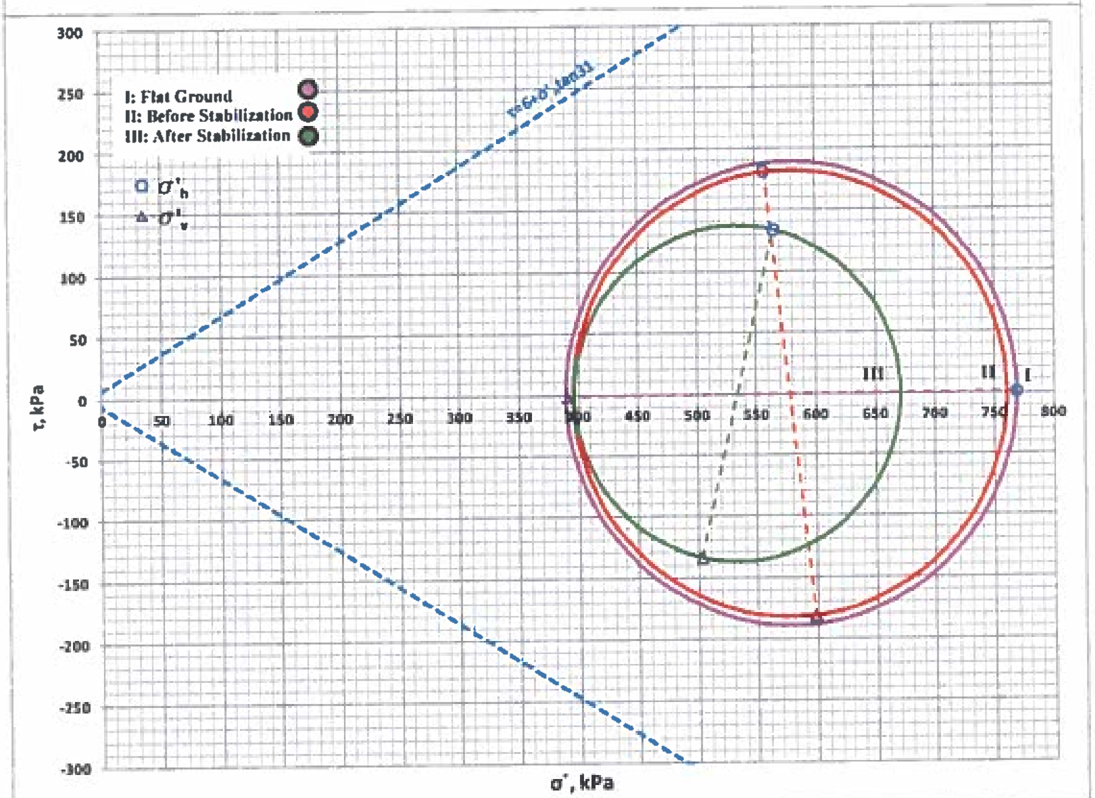

SNC·LAVALIN	NORTH SPUR STABILIZATION WORKS - Progressive Failure Study		Revision
	Nalcor Doc. No. MFA-SN-CD-2800-GT-RP-0001 Rev. A1	SLI Doc. No. 505573-3281-4GER-0001-PB	Date
	Figure C-34	SECTION B-B – LOWER CLAY MODEL – STRESSES ON LINE -18M – POINT C	16-JUN-2015

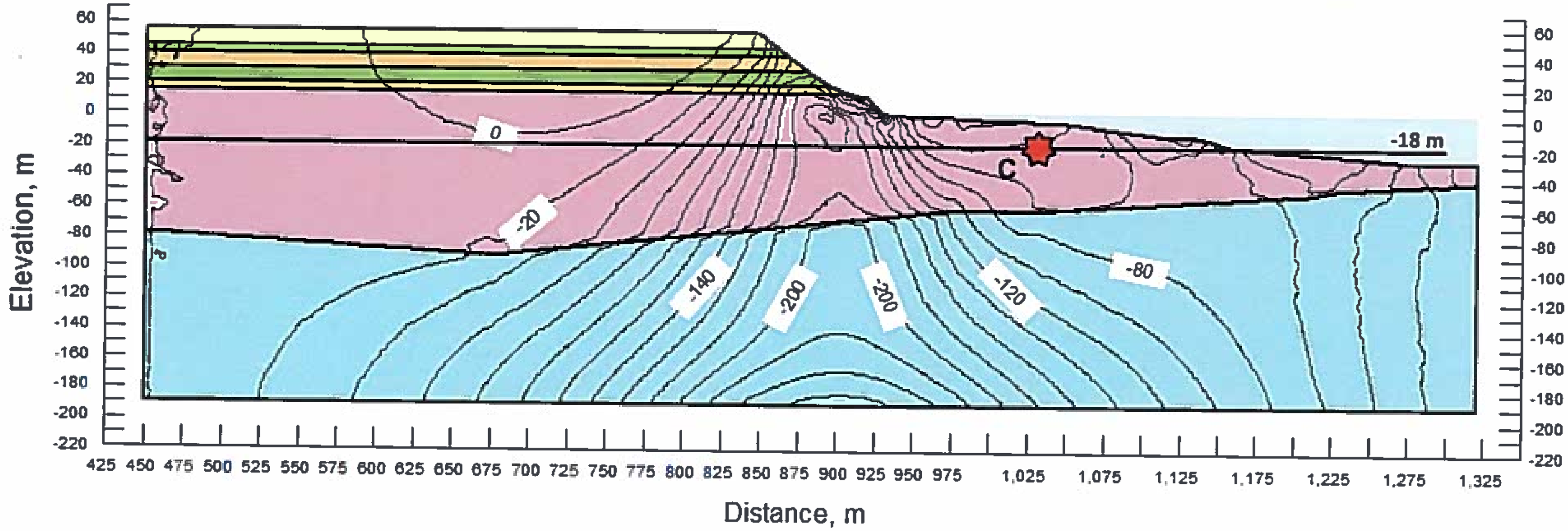

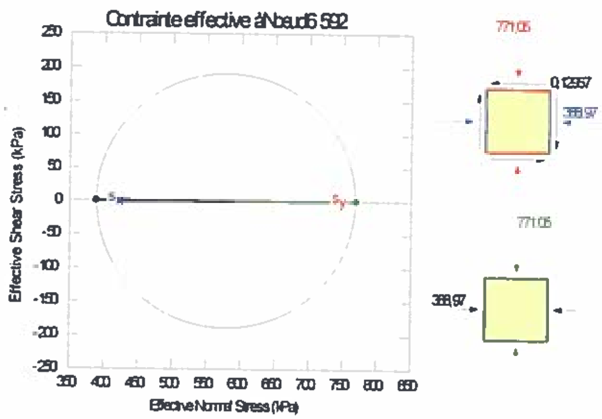

Initial State

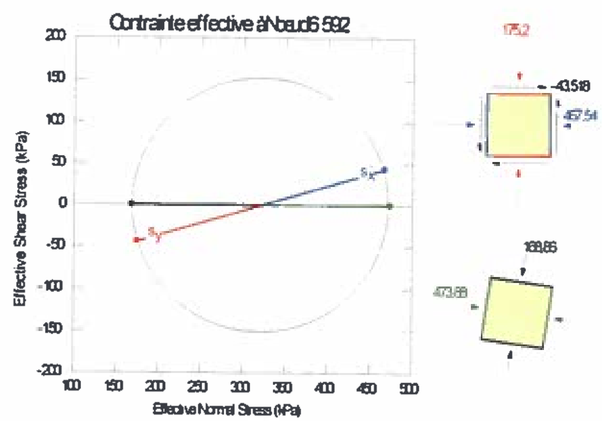

Before Stabilization

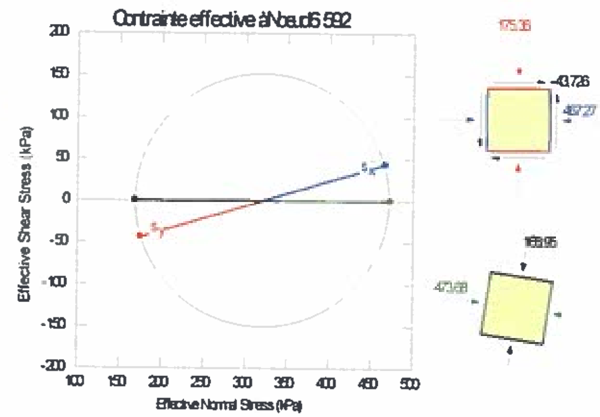

After Stabilization

SNC·LAVALIN	NORTH SPUR STABILIZATION WORKS - Progressive Failure Study		Revision
	Nalcor Doc. No. MFA-SN-CD-2800-GT-RP-0001 Rev. A1	SLI Doc. No. 505573-3281-4GER-0001-PB	Date
	Figure C-35	SECTION B-B – LOWER CLAY MODEL – STRESS PATH ON LINE -18M – POINT C	16-JUN-2015

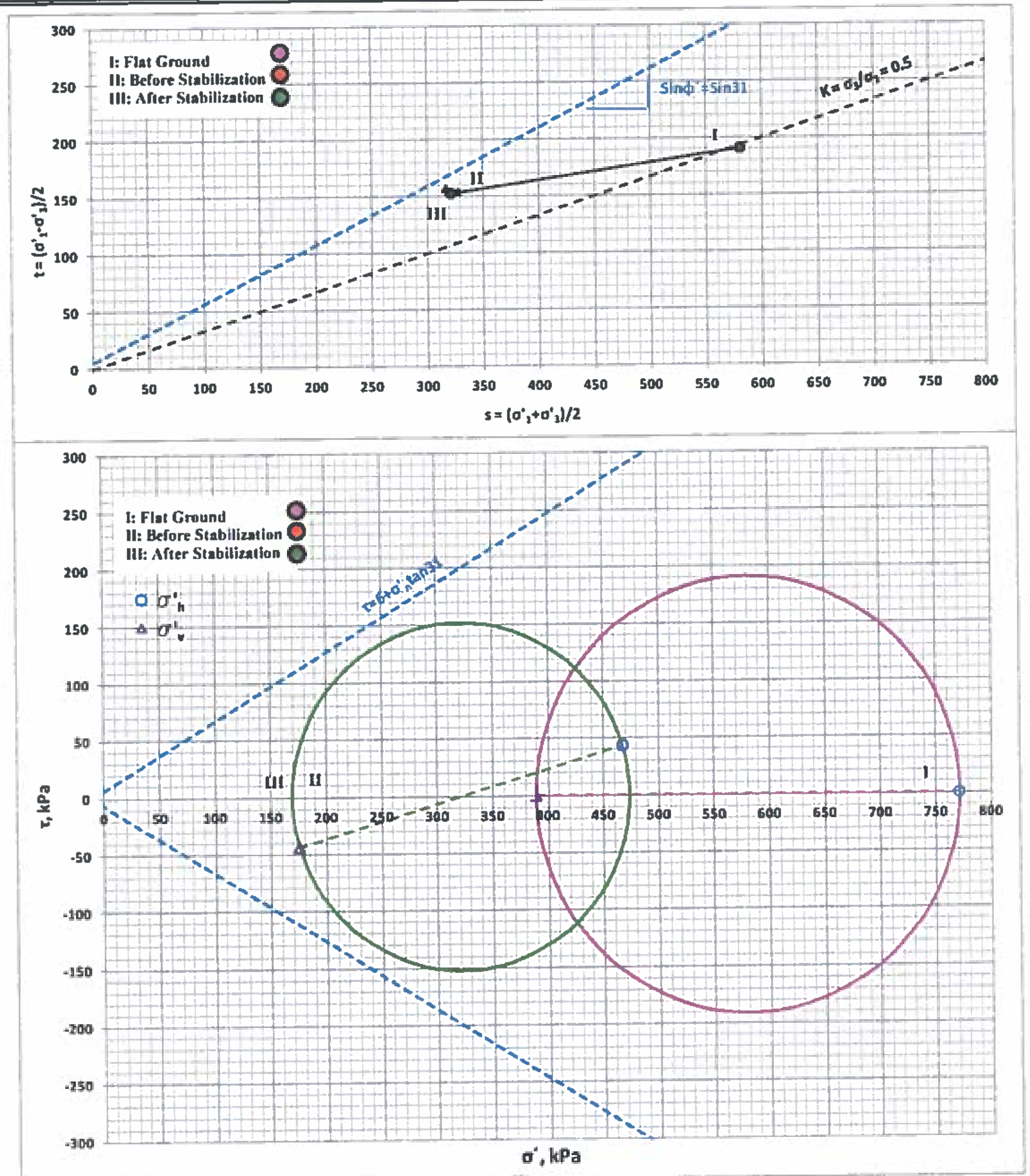

SNC·LAVALIN	NORTH SPUR STABILIZATION WORKS - Progressive Failure Study		Revision
	Nalcor Doc. No. MFA-SN-CD-2800-GT-RP-0001 Rev. A1	SLI Doc. No. 505573-3281-4GER-0001-PB	Date
	Figure C-36	SECTION D-D - LOWER CLAY MODEL – VERTICAL STRESS PROFILE AND HORIZONTAL LINES	16-JUN-2015

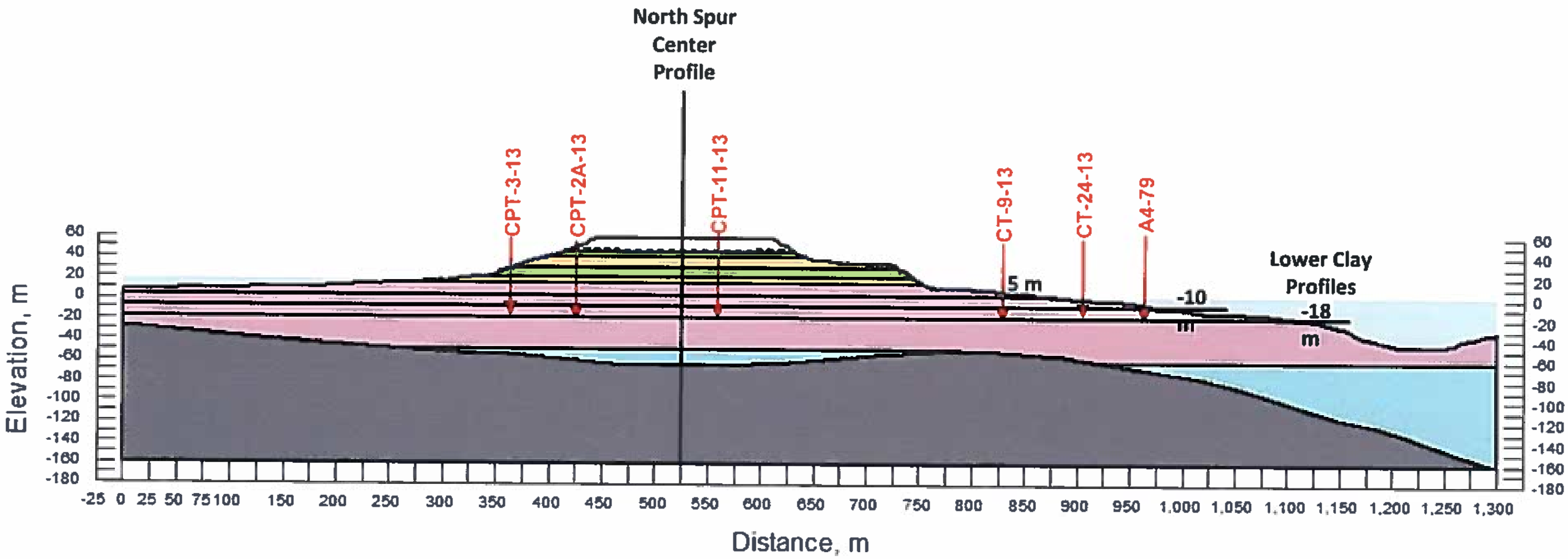

SNC·LAVALIN	NORTH SPUR STABILIZATION WORKS - Progressive Failure Study		Revision
	Nalcor Doc. No. MFA-SN-CD-2800-GT-RP-0001 Rev. A1	SLI Doc. No. 505573-3281-4GER-0001-PB	Date
	Figure C-37	SECTION D-D - LOWER CLAY MODEL – STRESSES AND STRENGTH ON LINE 5M	16-JUN-2015

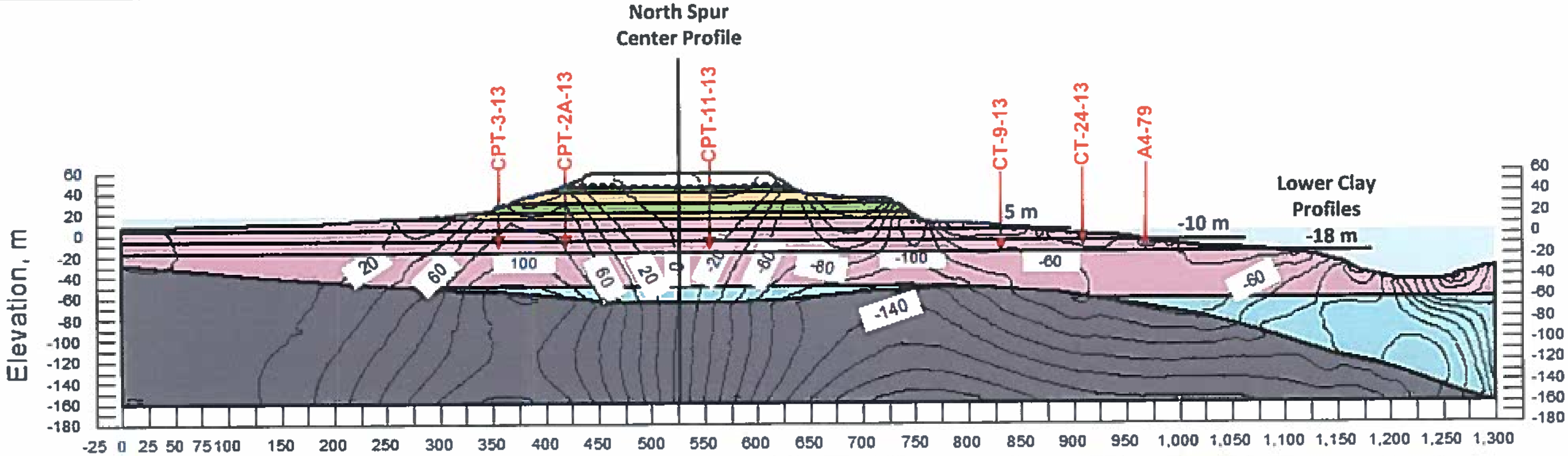

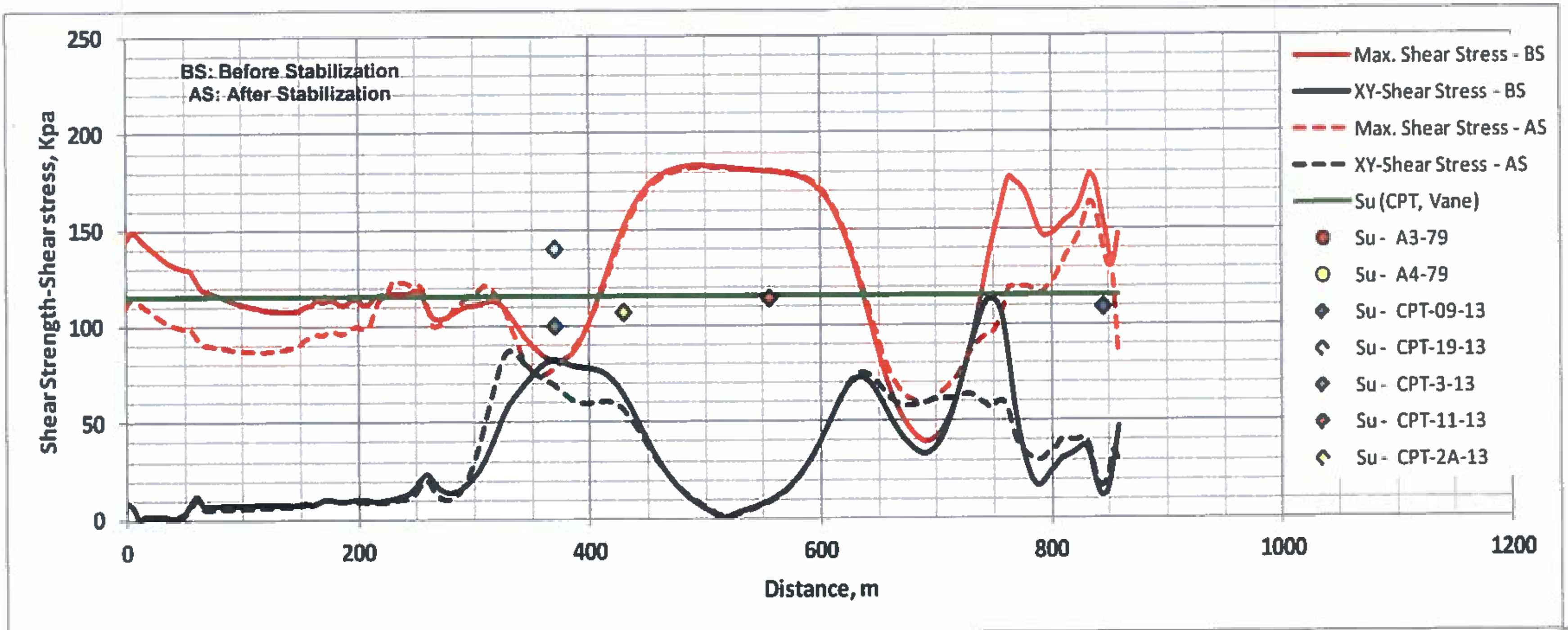

SNC·LAVALIN	NORTH SPUR STABILIZATION WORKS - Progressive Failure Study		Revision
	Nalcor Doc. No. MFA-SN-CD-2800-GT-RP-0001 Rev. A1	SLI Doc. No. 505573-3281-4GER-0001-PB	Date
	Figure C-38	SECTION D-D - LOWER CLAY MODEL – STRESSES AND STRENGTH ON LINE -10M	16-JUN-2015

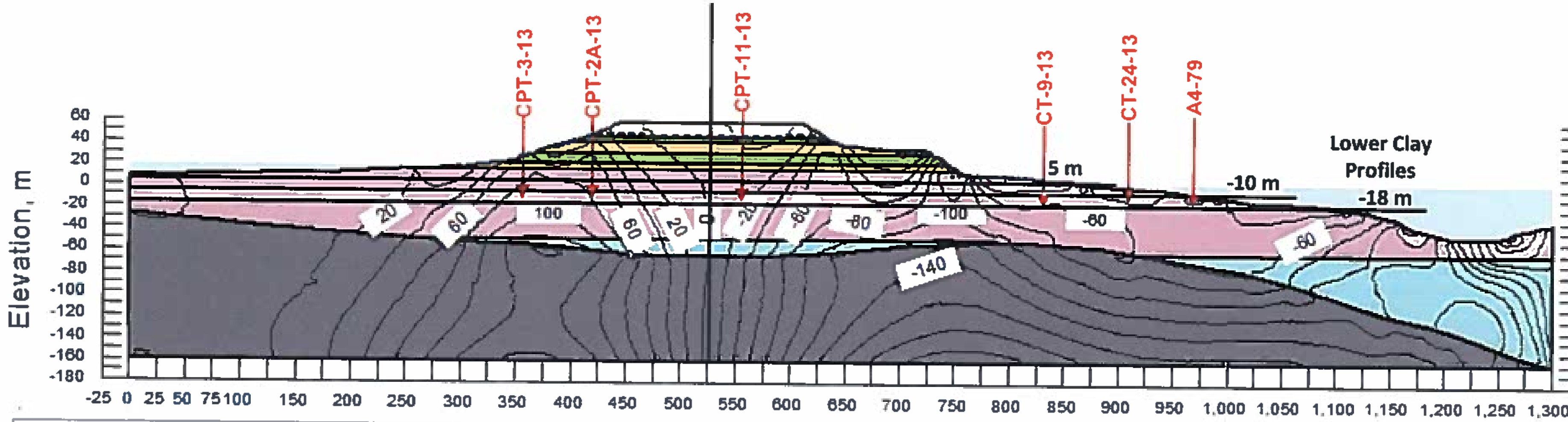

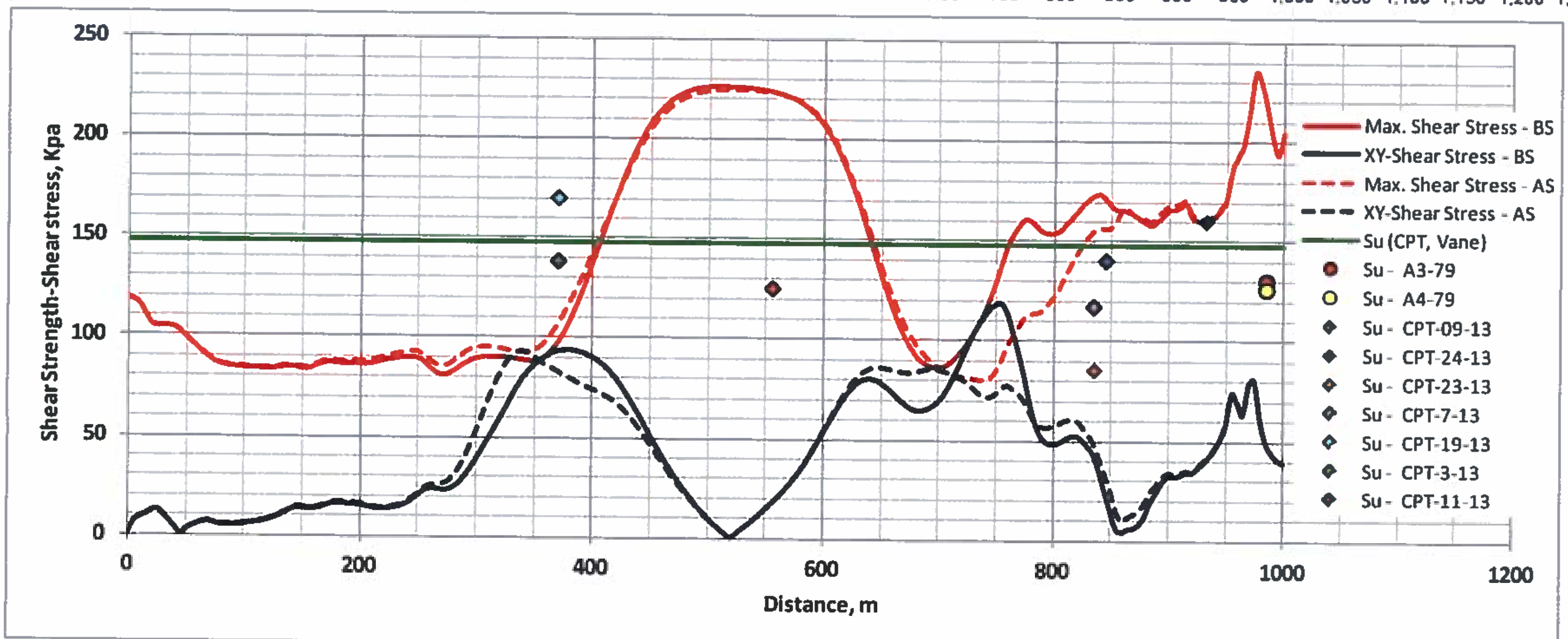

SNC·LAVALIN	NORTH SPUR STABILIZATION WORKS - Progressive Failure Study		Revision
	Nalcor Doc. No. MFA-SN-CD-2800-GT-RP-0001 Rev. A1	SLI Doc. No. 505573-3281-4GER-0001-PB	Date
	Figure C-39	SECTION D-D - LOWER CLAY MODEL – STRESSES AND STRENGTH ON LINE -18M	16-JUN-2015

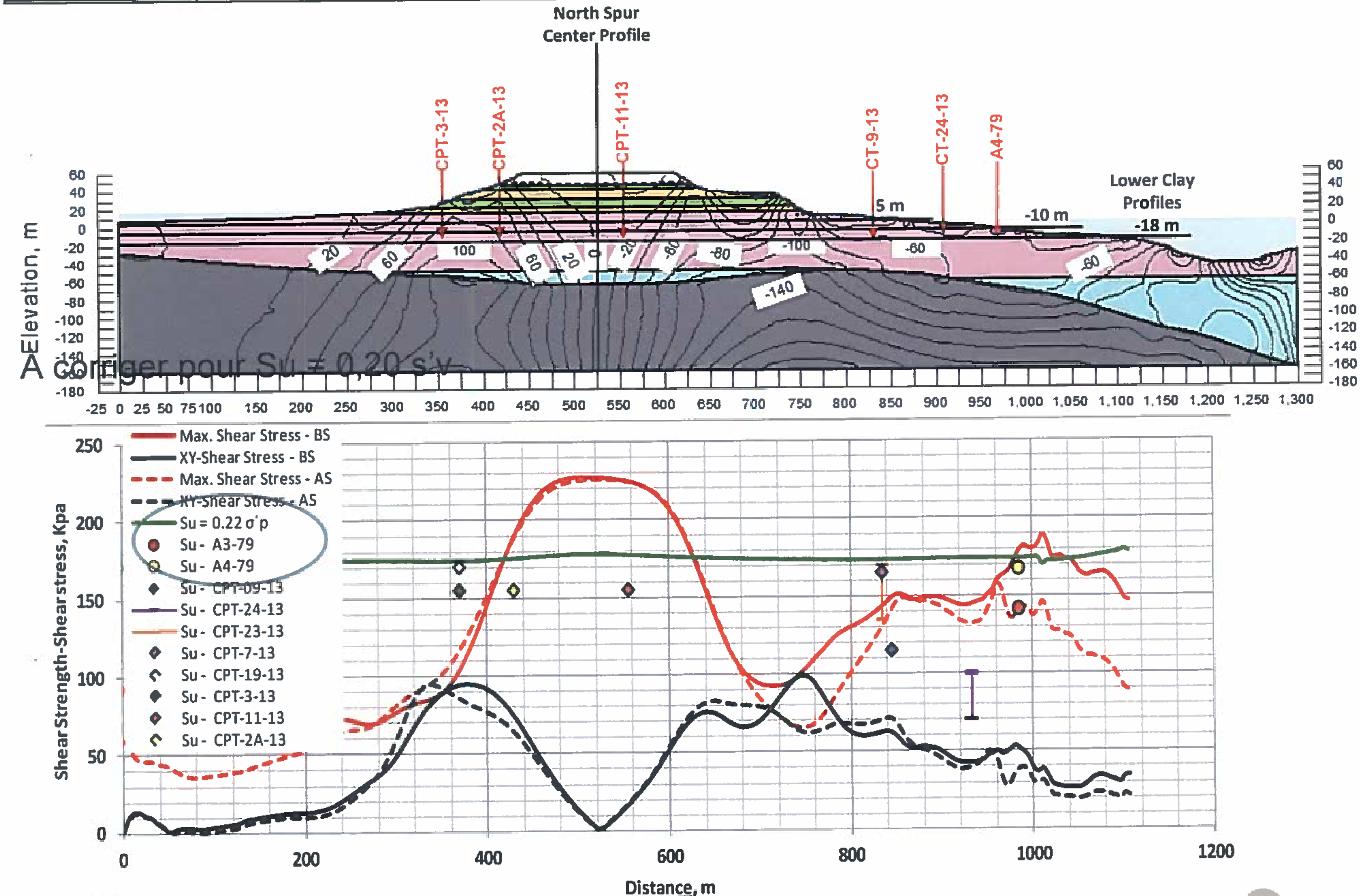

SNC·LAVALIN	NORTH SPUR STABILIZATION WORKS - Progressive Failure Study		Revision
	Nalcor Doc. No. MFA-SN-CD-2800-GT-RP-0001 Rev. A1	SLI Doc. No. 505573-3281-4GER-0001-PB	Date
	Figure C-40	SECTION D-D - STRESSES AND STRENGTH ON LINES +20M AND -10M	16-JUN-2015

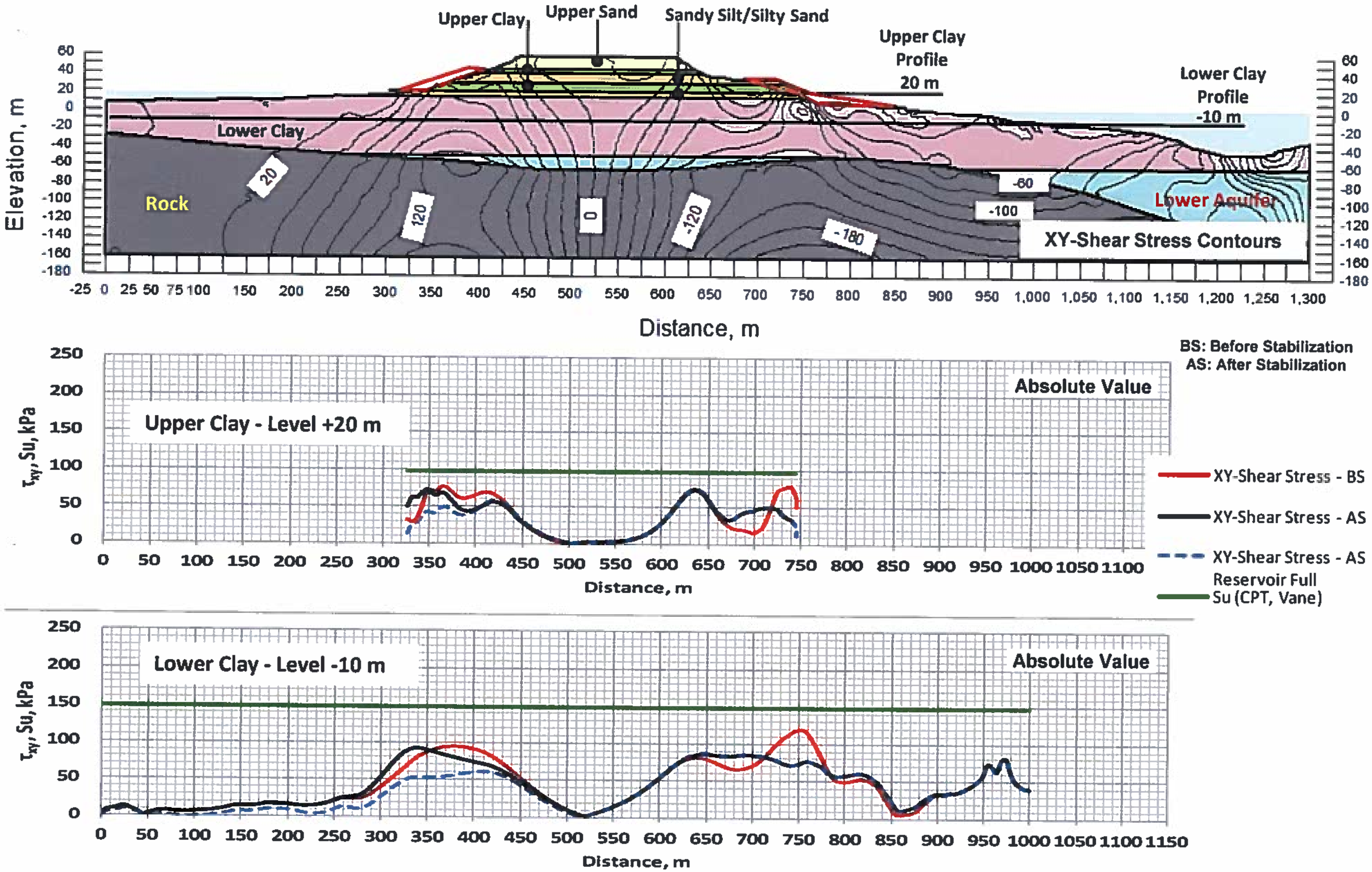

SNC·LAVALIN	NORTH SPUR STABILIZATION WORKS - Progressive Failure Study		Revision
	Nalcor Doc. No. MFA-SN-CD-2800-GT-RP-0001 Rev. A1	SLI Doc. No. 505573-3281-4GER-0001-PB	Date
	Figure C-41	SECTION D-D – RESERVOIR EFFECT IN UPPER CLAY ON LINE +20M	16-JUN-2015

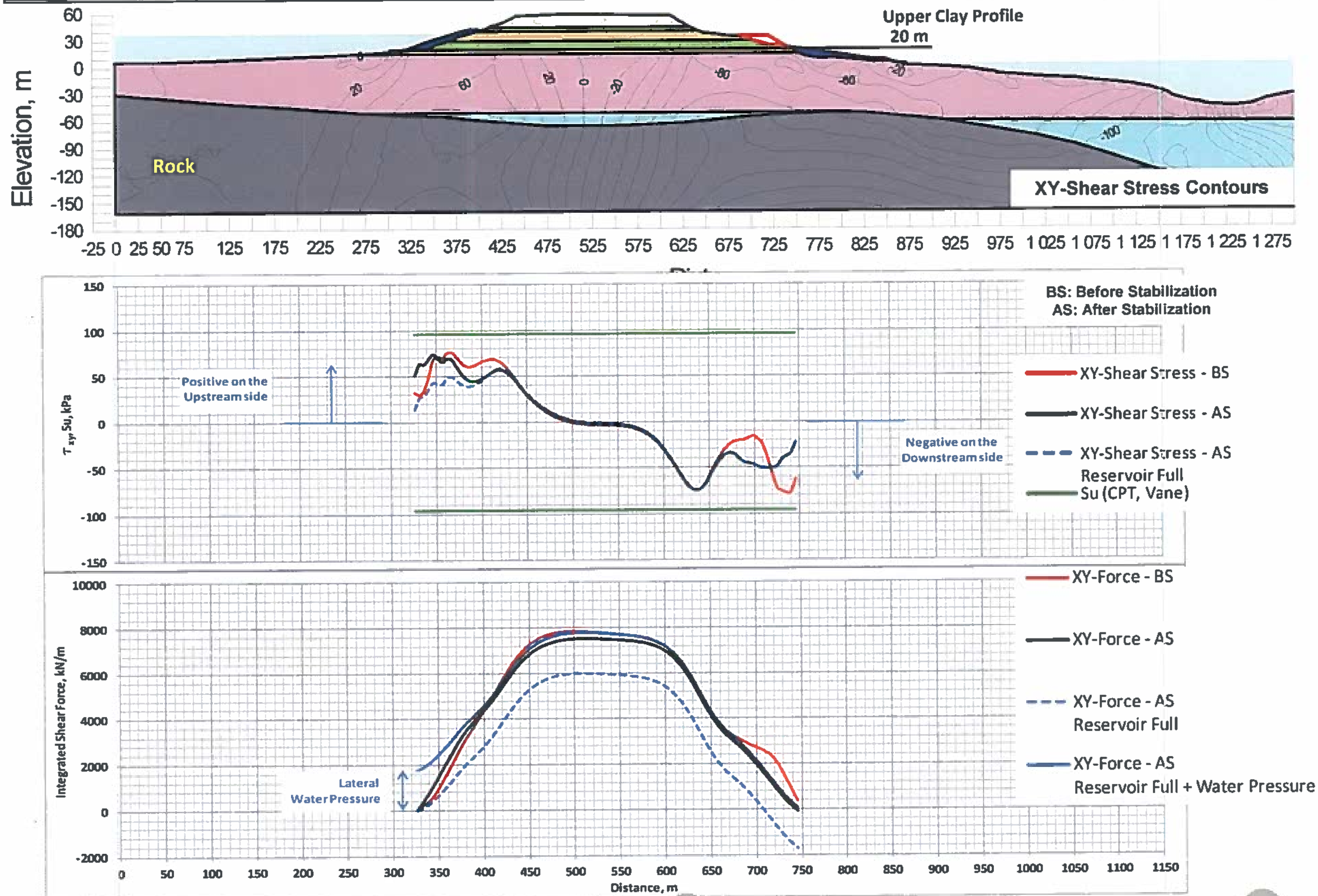

SNC·LAVALIN	NORTH SPUR STABILIZATION WORKS - Progressive Failure Study		Revision
	Nalcor Doc. No. MFA-SN-CD-2800-GT-RP-0001 Rev. A1	SLI Doc. No. 505573-3281-4GER-0001-PB	Date
	Figure C-42	SECTIONS B-B AND D-D – SHEAR STRESS COMPARISON ON LINES +20M AND -10 M	16-JUN-2015

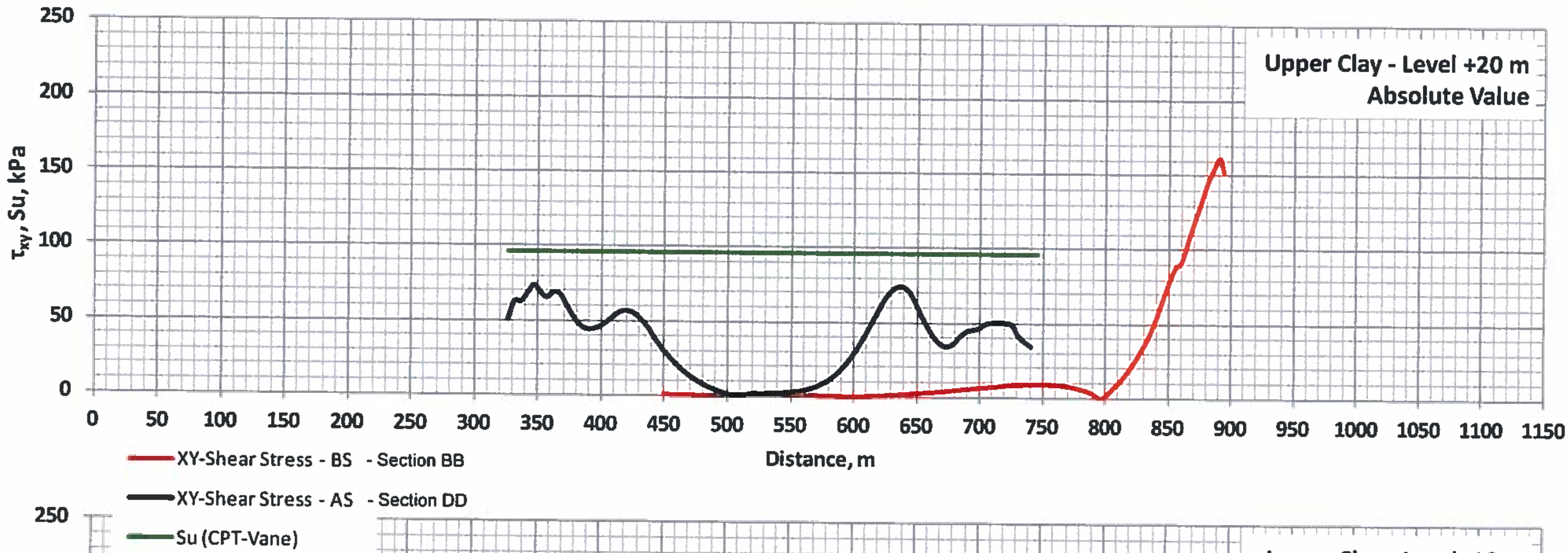

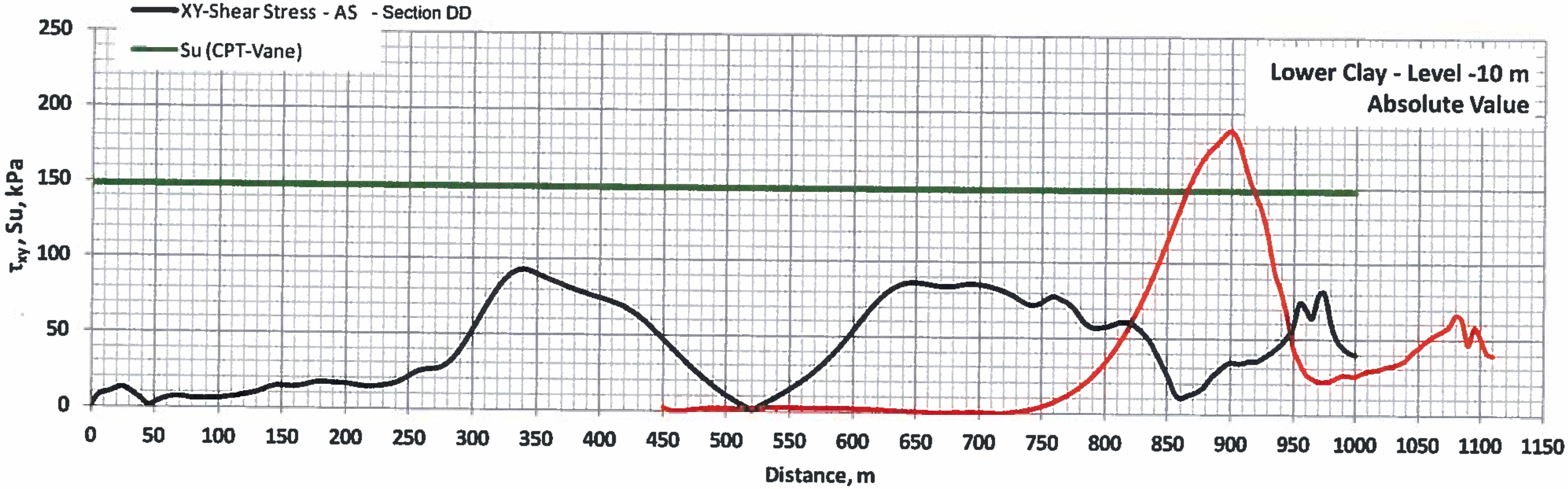

SNC·LAVALIN	NORTH SPUR STABILIZATION WORKS - Progressive Failure Study		Revision
	Nalcor Doc. No. MFA-SN-CD-2800-GT-RP-0001 Rev. A1	SLI Doc. No. 505573-3281-4GER-0001-PB	Date
	Figure C-43	LOWER CLAY MODEL – SECTIONS B-B, C-C AND D-D - COMPARISON	16-JUN-2015

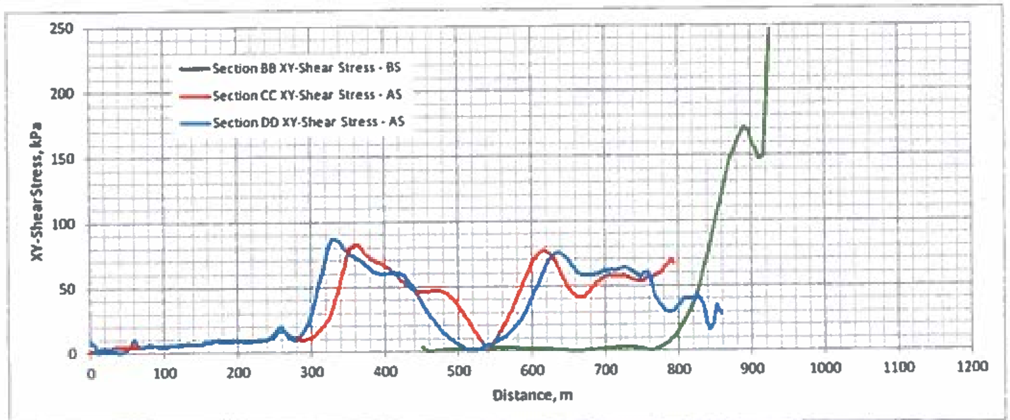

Line +5 m

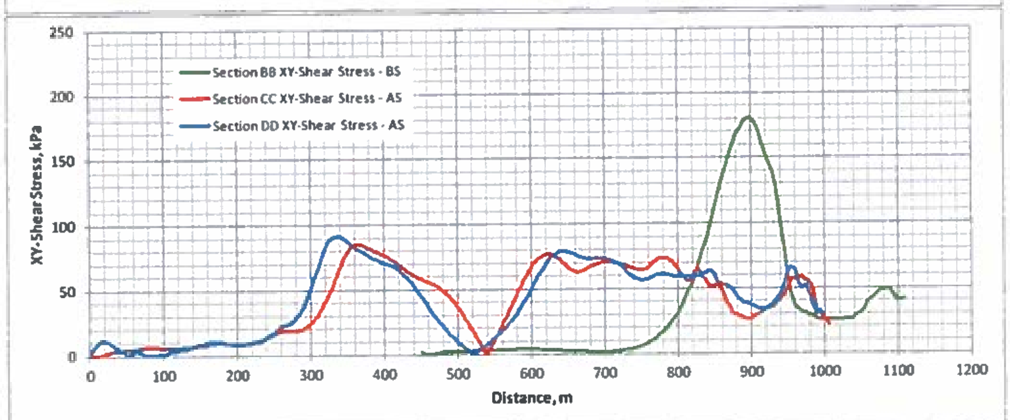

Line -10 m

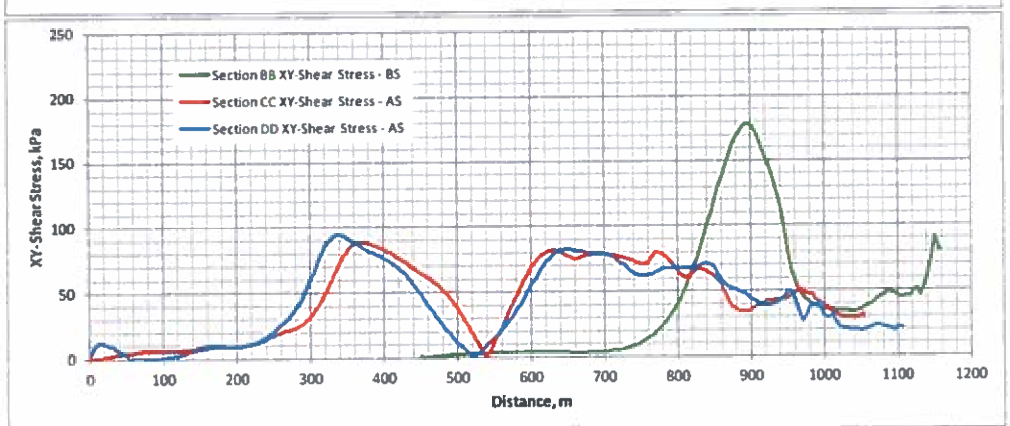

Line -18m

SNC·LAVALIN	NORTH SPUR STABILIZATION WORKS - Progressive Failure Study		Revision
	Nalcor Doc. No. MFA-SN-CD-2800-GT-RP-0001 Rev. A1	SLI Doc. No. 505573-3281-4GER-0001-PB	Date
	Figure C-44	SECTION A-A - LOWER CLAY MODEL – STRESSES AND STRENGTH ON LINE -50M – RESERVOIR AT ELEV. 39 M	16-JUN-2015

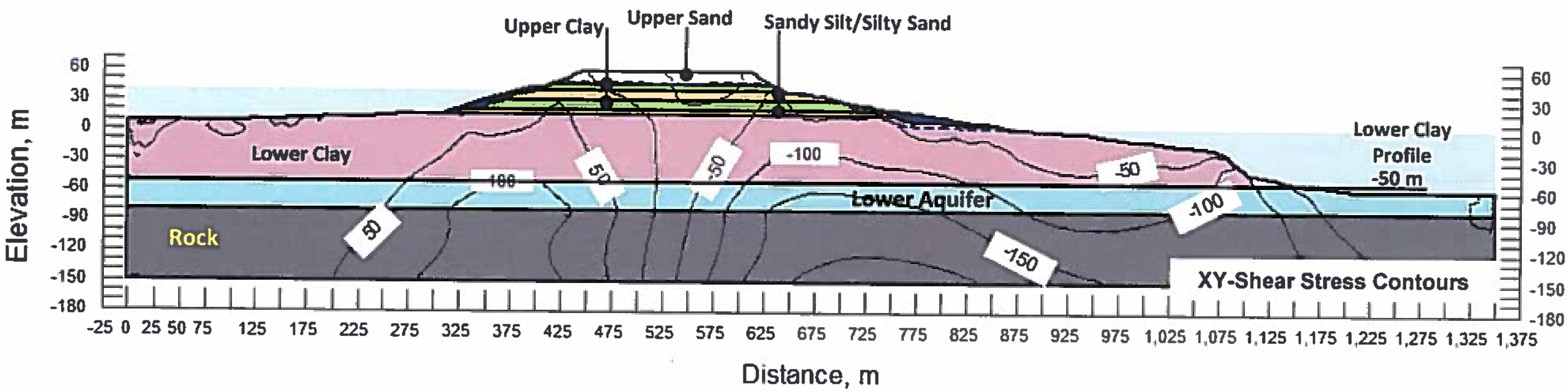

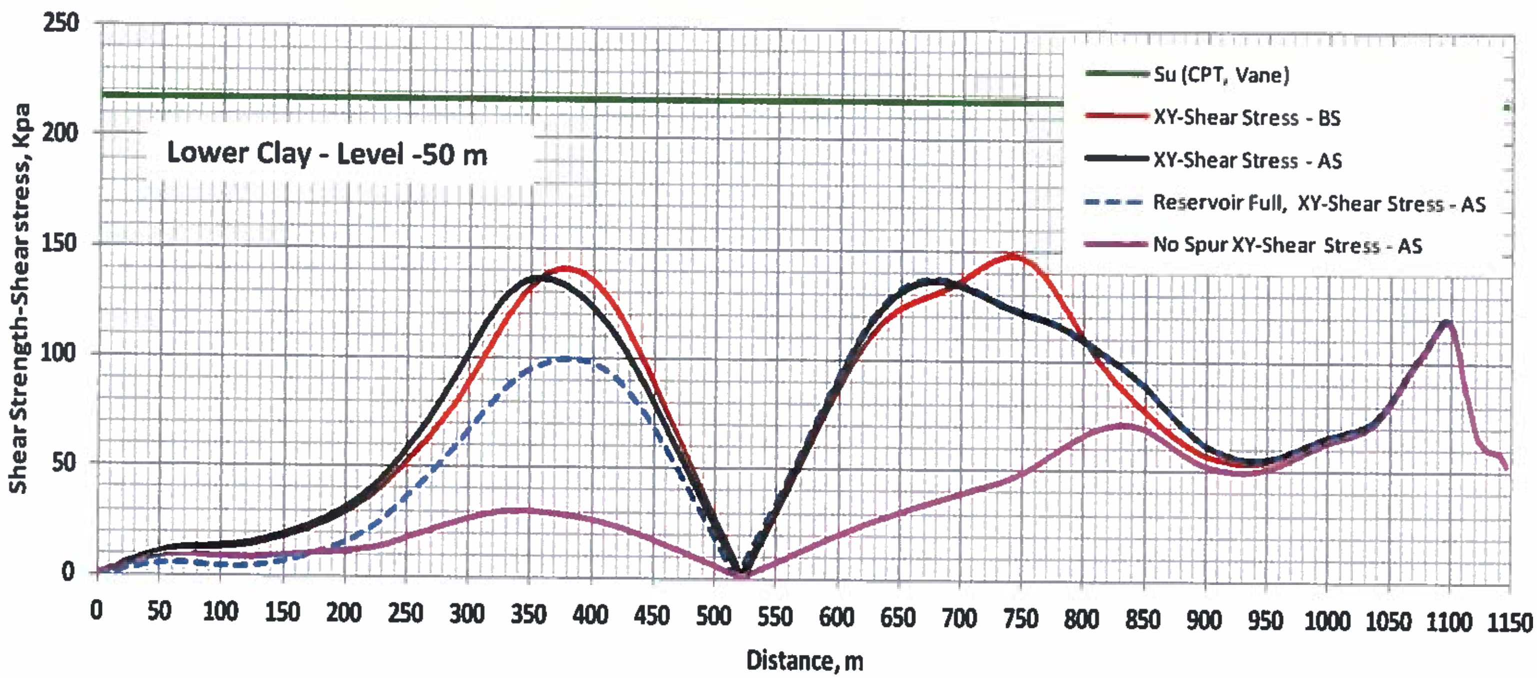

BS: Before Stabilization
AS: After Stabilization

SNC·LAVALIN	NORTH SPUR STABILIZATION WORKS - Progressive Failure Study		Revision
	Nalcor Doc. No. MFA-SN-CD-2800-GT-RP-0001 Rev. A1	SLI Doc. No. 505573-3281-4GER-0001-PB	Date
	Figure C-45	SECTION B-B – EFFECT OF A SURCHARGE – SHEAR STRESSES ON HORIZONTAL PLANS	16-JUN-2015

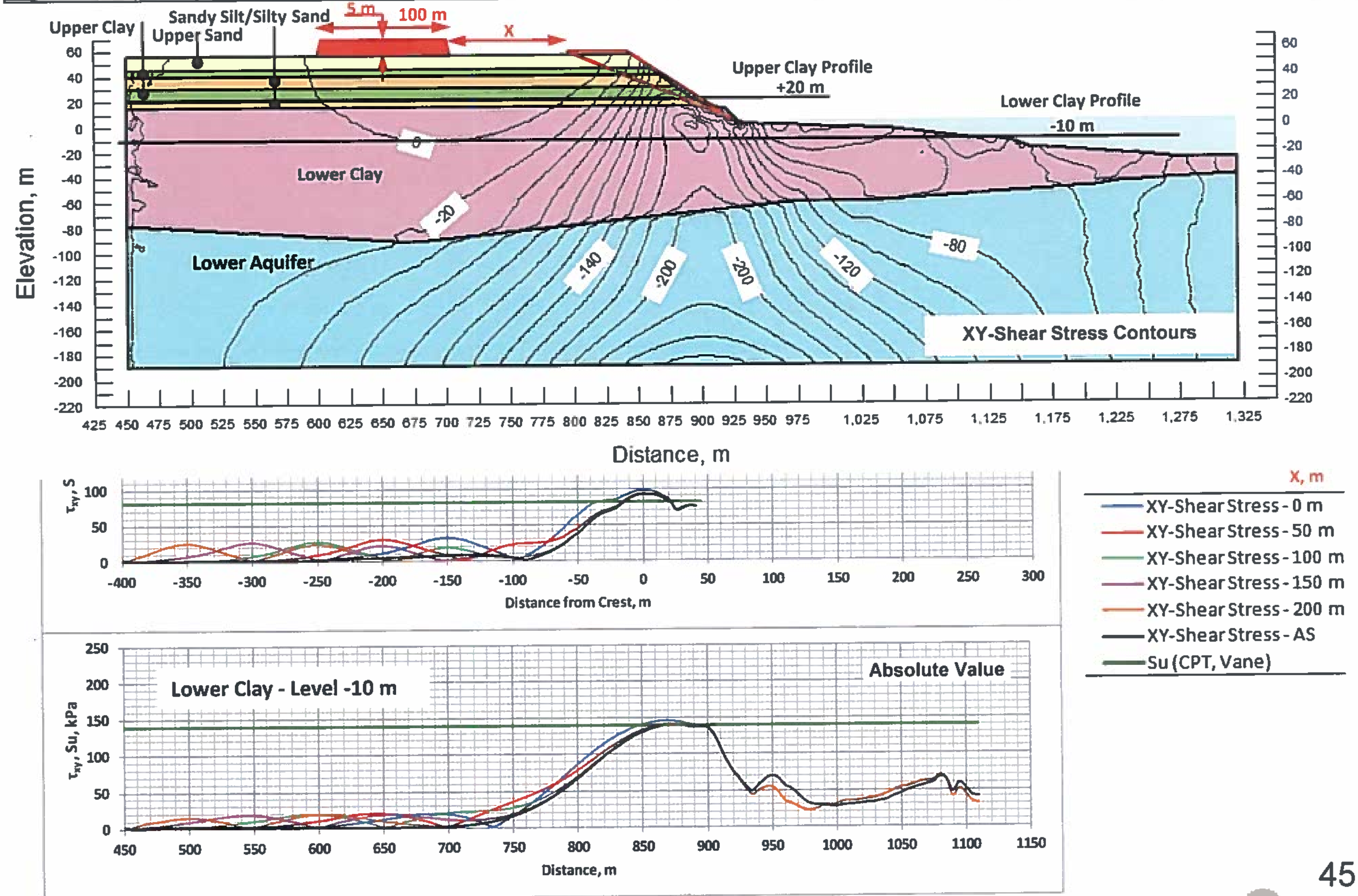

SNC·LAVALIN	NORTH SPUR STABILIZATION WORKS - Progressive Failure Study		Revision
	Nalcor Doc. No. MFA-SN-CD-2800-GT-RP-0001 Rev. A1	SLI Doc. No. 505573-3281-4GER-0001-PB	Date
	Figure C-46	SECTION B-B – EFFECT OF A SURCHARGE – SHEAR STRESSES ON HORIZONTAL PLANS	16-JUN-2015

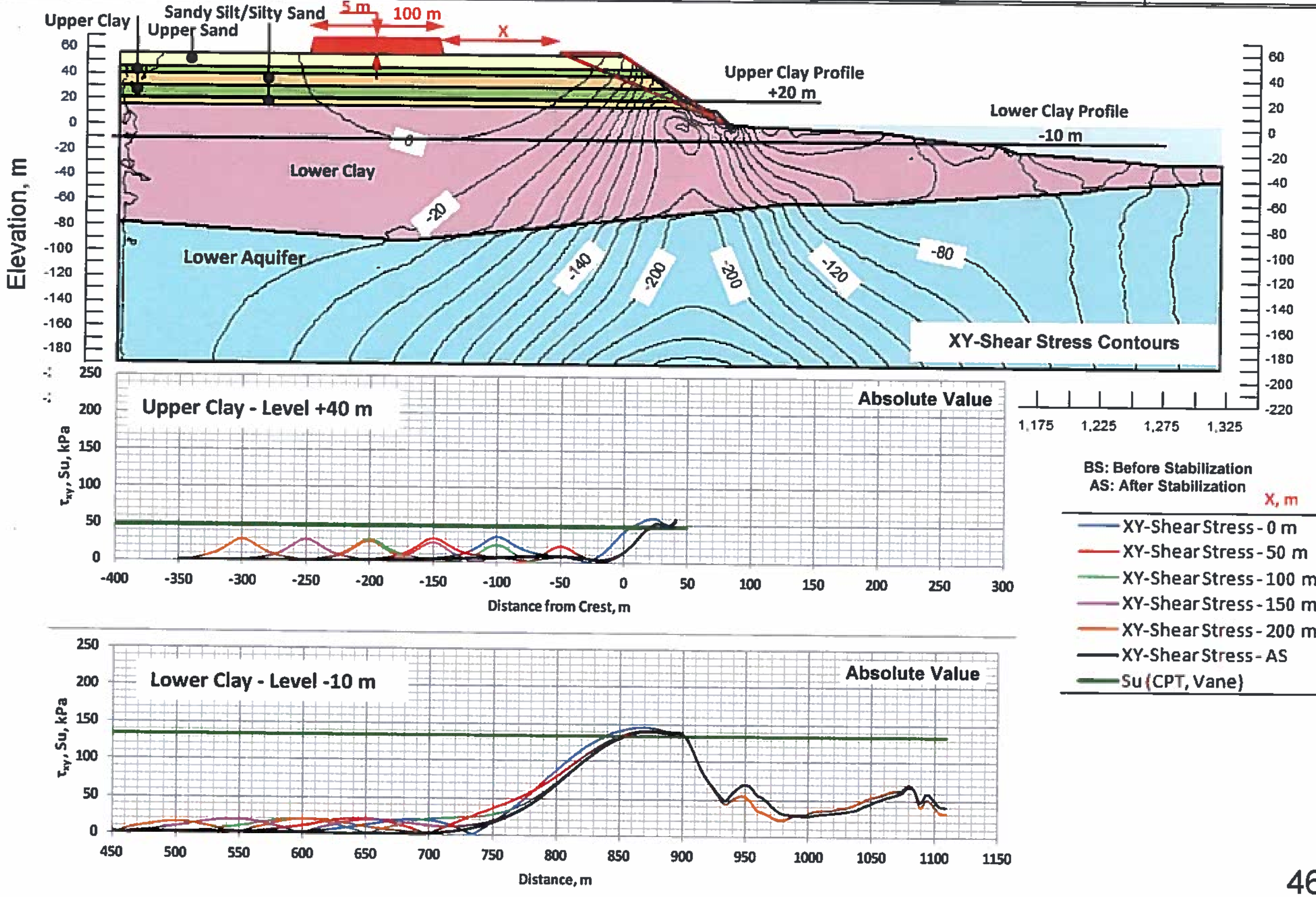

SNC·LAVALIN	NORTH SPUR STABILIZATION WORKS - Progressive Failure Study		Revision
	Nalcor Doc. No. MFA-SN-CD-2800-GT-RP-0001 Rev. A1	SLI Doc. No. 505573-3281-4GER-0001-PB	Date
	Figure C-47	SECTION B-B - EFFECT OF A SURCHARGE – STABILITY ANALYSES	16-JUN-2015